Tectonics

Supporting Information for

Phanerozoic tectonic and sedimentation history of the Arctic: constraints from deep-time low-temperature thermochronology data of Ellesmere Island and Northwest Greenland

Cornelia Spiegel[(1)], Mohammad S. Sohi[(1)], Wolfgang Reiter[(1)], Katrin Meier[(1)], Barbara Ventura[(1)], Frank Lisker[(1)], Solveig Estrada[(2)], Karsten Piepjohn[(2)], Kai Berglar[(2)], Nikola Koglin[(2)], Andreas Klügel[(1)], Patrick Monien[(1)], Axel Gerdes[(3,4)], Ulf Linnemann[(5)]

(1) Department of Geosciences, University of Bremen, Germany
(2) Federal Institute for Geosciences and Natural Resources, Hannover, Germany
(3) Department of Geosciences, Goethe University Frankfurt, Frankfurt am Main, Germany
(4) Frankfurt Isotope and Element Research Center (FIERCE), Goethe University Frankfurt, Germany
(5) Museum for Mineralogy and Geology, Senckenberg Natural History Collections Dresden, Germany

Contents of this file

Introduction

- The supporting information provides the details on the analytical procedures of rock processing, apatite fission track, apatite (U-Th)/He, and zircon U-Pb dating, and thermal history modelling
- The figures include relationships between (U-Th)/He dates and effective U-content (Fig. S1) and illustrations of all thermal models with envelopes for good and acceptable paths and with constraint boxes including inversion points (Fig. S2).
- The Tables include a summary of input parameters for the models (S1), a summary of the model outcomes along with colour-coded quality assessment (S2), Calculations for burial and exhumation as derived from the modelled weighted mean paths (S3), the single-grain data from apatite fission track analyses (S4), documentation and detailed analytical data from apatite (U-Th)/He analysis (S5), analytical details on zircon U-Pb analysis (S6) and the age groups distinguished from the zircon U-Pb data (S7)

Supporting Information – Analytical details

Rock processing and mineral separation

All samples were crushed by screw press and jaw crusher, sieved to retrieve the fraction between 63 and 250 µm, and processed by Wilfley Table for pre-concentrating heavy minerals. All sedimentary samples were treated with 5% acetic acid to remove carbonate. Diamagnetic and paramagnetic minerals were separated using Franz magnetic separation. Finally, a two-step heavy liquid separation with LST and DIM heavy liquids was used to obtain pure apatite and zircon separates.

Apatite Fission Track Analysis

Apatites were mounted in epoxy resin, ground and polished to reveal internal surfaces. The mounts were then etched in 5 M HNO_3 for 20 s at 20°C, and attached to a low-U white mica detector. Thermal neutron irradiation was carried out at the FRM II reactor facility of the Technical University of Munich in Garching (Germany). Subsequently, the white mica detectors were etched for 30 min in 48% HF at room temperature, for revealing the induced tracks. Whenever possible, >20 apatite grains and 100 horizontal confined track lengths were measured per sample. For each horizontal confined track, the angle to the crystallographic c-axis was determined (Ketcham et al., 2007a). Dpar values were used as kinetic indicator (Donelick, 1993) and averaged from three single measurements for each analysed grain. AFT analysis was performed using the external detector method and the zeta calibration approach (Gleadow, 1981; Hurford and Green, 1983, respectively). AFT ages and statistical parameters were calculated using the Trackkey software, version 4.2.g (Dunkl, 2002). AFT ages in table 1 are given as central ages with one-sigma errors (Galbraith and Laslett, 1993). All single grain data are reported in Table S4

Apatite (U-Th-Sm)/He analysis

Apatite separates were inspected for grains suitable for (U-Th-Sm)/He analysis, which requires pristine crystals >60 µm, well-defined morphologies, and absence of mineral or fluid inclusions and cracks. Apatites which meet these criteria were handpicked, measured for dimensions, classified according to grain morphology, and photographically documented. Grains were then mounted in platinum tubes, which were previously cleaned for four hours with 50% HNO_3 (including one hour in an ultrasonic bath), and subsequently rinsed with distilled water and ethanol. Helium was extracted from apatite crystals by laser heating (5 minutes, 900°C) using a solid-state diode laser (970 nm wavelength). The extracted helium was measured by the ^{3}He isotope dilution method using a PrismaPlus QMG 220 quadrupole mass spectrometer (Pfeiffer). Analytical precision was better than 1% for most analyses. Afterwards, apatites were retrieved from the laser chamber for U, Th and Sm-analysis.

U, Th and Sm contents of apatites were determined by ICP-MS using a Thermo Element2. Single apatite grains with enclosing Pt tubes were placed in 5 mL Savillex beakers and dissolved in 100 µL double-distilled 65% HNO_3 and 100 µL internal standard solution (25 ng mL^{-1} In and Bi in 2% HNO_3) on a hot plate at 110°C. Prior to analysis solutions were diluted with ultrapure water to a final volume of 5 mL. The isotopes ^{147}Sm, ^{149}Sm, ^{232}Th, and ^{238}U were analysed at low resolution in 10 runs at 10 mass scans each. The instrument was calibrated using high-purity single element standard solutions. Precision and accuracy were monitored by analysing a model apatite solution (2% HNO_3 matrix with 40 ppm Ca, 18.32 ppm P, 50 ppb Sm, 20 ppb Th, 20 ppb U) in 100-fold dilution five to seven times during each analytical session, and by analysing replicates. Precision was mostly better than 2% and accuracy better than 5%.

Apatite (U-Th-Sm)/He ages were calculated using the ^{4}He ingrowth equations (e.g., Farley, 2002). Calculated raw ages were corrected for alpha-ejection after Farley et al. (1996), using the stopping distances of Ketcham et al. (2011). Uncertainties related to grain size measurements and alpha ejection corrections are estimated to be about 5%. Following common practice, U, Th, and Sm amounts are presented as concentrations in table 2. These were calculated by dividing the measured absolute amounts through the mass of the apatite grain, which in turn was derived from size and morphology of the analysed grain (allowing volume calculation) and the density of apatite (3.2 g/cm^{3}). Detailed measurements including measurements of grain dimensions and absolute amounts of U, Th and Sm are reported in Table S5. As additional control, repeated measurements of the Durango apatite age standard were performed during the course of analysis, yielding an average AHe age of 29.9 ± 1.9 Ma, well within the range of the published AHe reference age for Durango (31.02 ± 1.01 Ma, McDowell et al., 2005).

Thermal History modelling

Thermal history modelling was performed by the software HeFTy (Ketcham, 2005), using the annealing model of Ketcham et al. (2007b), the diffusion models of Farley (2000) and of Flowers et al. (2009), and a Monte Carlo approach with 10 000 to 500 000 time-temperature paths calculated for each model run (Tables S1 & S2). According to the fit with the data observed, thermal histories were classified as "acceptable" (goodness of fit value >0.05) or "good" (goodness of fit value >0.5). Details on input data are reported in Table S1, a summary of the results of thermal history inversions and the net burial and exhumation data calculated from the models are provided in Tables S2 and S3, respectively.

Zircon U/Pb dating

a) Analytic details of zircon U-Pb ICP-MS dating at Frankfurt:

Zircon grains were selected by hand picking under a microscope, choosing the freshest, least cracked zircon grains. The selected zircon grains were mounted in epoxy resin. The epoxy mounts were polished to half their thickness, coated with carbon and imaged by means of cathodoluminescence (CL) using a JEOL JSM 6490 instrument.

For U–Pb isotope analyses of the zircon grains a Thermo-Scientific Element II SF–ICP–Mass-Spectrometer was used, coupled to a Resolution (Resonetics) 193 nm ArF excimer laser system (CompexPro 110, Coherent) equipped with a S-155 two-volume ablation cell (Laurin Technic, Australia), which allows detection and sequential sampling of heterogeneous grains (e.g., growth zones) during the time resolved data acquisition, due to its quick response time of <1 s (time until maximum signal strength was achieved) and wash-out (<99% of previous signal) time of <3 s (Zeh & Gerdes 2012). The laser spot size was 30 µm. Laser repetition rate and energy were 5.5 Hz and ~2 J cm^{-2}, respectively, which resulted in a crater depth of ~20 µm during 20 s of ablation. A detailed description of the analytical procedure and data processing, including common lead corrections and error propagations, is given in Gerdes & Zeh (2006, 2009). The reference zircon GJ-1 was used as primary standard for all measurements (^{206}Pb/^{238}U age = 603 ± 1 Ma; GUF ID-TIMS value; Wolfgang Dörr personal communications). The accuracy of the U–Pb measurements was verified by analysis of the reference zircons Plešovice (^{207}Pb/^{206}Pb age = 337.13 ± 0.37 Ma; Sláma et al. 2008) and 91500 (^{207}Pb/^{206}Pb age = 1065.4 ± 0.3 Ma; Wiedenbeck et al. 1995), which both have been used as secondary standards. The primary standard zircon GJ-1 yielded an age of 602.7 ± 1.1 Ma (MSWD of concordance and equivalence = 0.86, probability of concordance and equivalence = 0.84, n = 49). The reference zircon Plešovice yielded an age of 338.8 ± 2.5 Ma ($MSWD_{C+E}$ = 0.78, $Prob_{C+E}$ = 0.630, n = 3) and the standard zircon 91500 an age of 1061.8 ± 4.6 Ma ($MSWD_{C+E}$ = 1.14, $Prob_{C+E}$ = 0.32, n = 8), which are identical, within error, with published data. All errors are 2σ. All Concordia plots and U–Pb age calculations were performed with the program ISOPLOT (Ludwig 2001). The software AGEDISPLAY (Sircombe 2004) was used for population density calculations.

b) Analytic details of zircon U-Pb ICP-MS dating at Dresden:

Zircon grains were selected by hand picking under a microscope, choosing the freshest, least cracked zircon grains. The selected zircon grains were mounted in epoxy resin. The epoxy mounts were polished to half their thickness. The grains were analyzed for U, Th, and Pb isotopes by LA-ICP-MS techniques using a Thermo-Scientific Element 2 XR sector field ICP-MS coupled to a New Wave UP-193 Excimer Laser System. A teardrop-shaped, low volume laser cell constructed by Ben Jähne (Dresden) and Axel Gerdes (Frankfurt/M.) was used to enable sequential sampling of heterogeneous grains (e.g., growth zones) during time resolved data acquisition. Each analysis consisted of approximately 15 s background acquisition followed by 30 s data acquisition, using a laser spot-size of 25 and 35 µm, respectively. A common-Pb correction based on the interference- and background-corrected ^{204}Pb signal and a model Pb composition (Stacey & Kramers, 1975) was carried out if necessary. The necessity of the correction is judged on whether the corrected $^{207}Pb/^{206}Pb$ lies outside of the internal errors of the measured ratios. Discordant analyses were generally interpreted with care. Raw data were corrected for background signal, common Pb, laser induced elemental fractionation, instrumental mass discrimination, and time-dependant elemental fractionation of Pb/Th and Pb/U using an Excel® spreadsheet program developed by Axel Gerdes (Institute of Geosciences, Goethe-University Frankfurt, Frankfurt/Main, Germany). Reported uncertainties were propagated by quadratic addition of the external reproducibility obtained from the standard zircon GJ-1 (~0.6% and 0.5-1% for the $^{207}Pb/^{206}Pb$ and $^{206}Pb/^{238}U$, respectively) during individual analytical sessions and the within-run precision of each analysis. Concordia diagrams (2sigma error ellipses) and concordia ages (95% confidence level) were produced using Isoplot/Ex 2.49 (Ludwig, 2001) and frequency and relative probability plots using AgeDisplay (Sircombe, 2004). The $^{207}Pb/^{206}Pb$ age was taken for interpretation for all zircons >1.0 Ga, and the $^{206}Pb/^{238}U$ ages for younger grains. For further details on analytical protocol and data processing see Gerdes & Zeh (2006).

The uncertainty in the degree of concordance of Precambrian-Palaeozoic grains dated by the LA-ICP-MS method is relatively large and results obtained from just a single analysis have to be interpreted with care. A typical uncertainty of 2-3% (2σ) in $^{207}Pb/^{206}Pb$ for a Late Neoproterozoic grain (e.g., 560 Ma) relates to an absolute error on the $^{207}Pb/^{206}Pb$ age of 45-65 Ma. Such a result gives space for interpretation of concordance or slight discordance. The latter one could be caused by episodic lead loss, fractionation, or infiltration Pb isotopes by a fluid or on micro-cracks. Thus, zircons showing a degree of concordance in the range of 90-110 % in this paper are classified as concordant because of the overlap of the error ellipse with the concordia (Linnemann et al., 2011).

Th/U ratios are obtained from the LA-ICP-MS measurements of investigated zircon grains. U and Pb content and Th/U ratio were calculated relative to the GJ-1 zircon standard and are accurate to approximately 10%. Detailed results of zircon U/Pb dating and the distributions of the U/Pb ages are provided in Tables S6 and S7, respectively.

References (cited in text and following tables & figures)

- Dawes, P., 2006. Explanatory notes to the Geological map of Greenland, 1 : 500 000, Thule, Sheet 5. Geological Survey of Denmark and Greenland Map series 2.
- Dewing, K., Hadlari, T., 2023. Franklinian composite tectono-sedimentary element, Canadian Arctic Island. *In* Sedimentary Successions of the Arctic region and their hydrocarbon prospectivity. *Edited by* Drachev, S., Brekke, H., Henriksen, E., and Moore, T. Geological Society of London Memoirs 57.
- Donelick, R., 1993. Apatite etching characteristics versus chemical composition. Nuclear tracks and Radiation Measurements 21, 604.
- Dunkl, I., 2002. Trackkey: a Windows program for calculation and graphical presentation of fission track data. Computer & Geosciences 28, 3-12.
- Embry, A., 1988. Middle-upper Devonian sedimentation in the Canadian Arctic Islands and the Ellesmerian orogeny. *In* Devonian of the World, *Edited by* N. MacMillan, A. Embry, and D. Glass. Canadian Society of Petroleum Geologists, Memoir 14, 15-28.
- Embry, A., Beauchamp, B., 2008. Sverdrup Basin, *in* Miall, A., ed. Sedimentary Basins of the World, 5. The Sedimentary Basins of the United States and Canada. Amsterdam Elsevier, 451-471.
- Farley, K., 2000. Helium diffusion from apatite: General behaviour as illustrated by Durango fluorapatite. Journal of Geophysical Research 105(B2), 2903-2914.
- Farley, K., 2002. (U-Th)/He dating: Techniques, calibrations, and applications, in: Noble Gases in Geochemistry and Cosmochemistry, Reviews in Mineralogy & Geochemistry 47, 819-844.
- Farley, K., Wolf, R., Silver, L., 1996. The effects of long alpha-stopping distances on (U-Th)/He ages. Geochimica et Cosmochimica Acta 60/21, 4223-4229.
- Flowers, R., Ketcham, R., Shuster, D., Farley, K., 2009. Apatite (U-Th)/He thermochronometry using a radiation damage accumulation and annealing model. Geochimica et Cosmochimica Acta 73, 2347-2365.
- Frisch, T., Hunt, P., 1988. U-Pb zircon and monazite ages from the Precambrian shield of Ellesmere and Devon Islands, Arctic Archipelago. Geological Survey of Canada Paper 88-2, 117-125.
- Galbraith, R.F, Laslett, G. M., 1993. Statistical models for mixed fission track ages. Nuclear Tracks and Radiation Measurements 21, 459-470.
- Gerdes, A., Zeh, A. 2006. Combined U-Pb and Hf isotope LA-(MC-) ICP-MS analysis of detrital zircons: Comparison with SHRIMP and new constraints for the provenance and age of an Armorican metasediment in Central Germany. Earth and Planetary Science Letters 249, 47-61.
- Gerdes, A., Zeh, A., 2009. Zircon formation versus zircon alteration – new insights from combined U–Pb and Lu–Hf in situ LA-ICP-MS analyses, and consequences for the interpretation of Archean zircon from the Central Zone of the Limpopo Belt. Chemical Geology 261, 230–243.
- Gilotti, J., McClelland, W., Piepjohn, K., von Gosen, W., 2018. U-Pb geochronology of Paleoproterozoic gneiss from southeastern Ellesmere Island: implications for displacement estimates on the Wegener fault. Arktos 4:12.
- Gleadow, A.J.W., 1981. Fission track dating methods: what are the real alternatives? Nuclear Tracks and Radiation Measurements 5, 3-14.
- Harrison, J., Gilbert, C., Lynds, T., Ford, A., Thorsteinsson, R., Frisch, T., de Freitas, T., Kerr, J., 2015. Geology, tectonic assemblage map of Alexandra Fiord, central Ellesmere and eastern Axel Heiberg islands, Nunavut. Geological Survey of Canada, Canadian Geoscience Map 30 (ed. preliminary), scale 1 : 500 000.
- Harrison, J., Lynds, T., Ford, A., Rainbird, R., 2016. Geology, simplified tectonic assemblage map of the Canadian Arctic Islands, Northwest Territories – Nunavut; Geological Survey of Canada, Canadian Geoscience Map 80 (preliminary), scale 1 : 2 000 000.
- Hurford, A. J., Green, P. F., 1983. The zeta age calibration of fission track dating. Chemical Geology 41/4, 285-317.
- Ketcham, R., 2005. Forward and inverse modelling of low temperature thermochronometry data. Reviews in Mineralogy and Geochemistry 58, 275-314.
- Ketcham, R., Carter, A., Donelick, R., Barbarand, J., Hurford, A., 2007a. Improved measurement of fission-track annealing in apatite using c-axis projection. American Mineralogist 9, 799-810.
- Ketcham, R., Carter, A., Donelick, R., Barbarand, J., Hurford, A., 2007b. Improved modeling of fission-track annealing in apatite. American Mineralogist 9, 789-798.
- Ketcham, R., Gautheron, C., Tassan-Got, L., 2011. Accounting of long alpha-particle stopping distances in (U-Th-Sm)/He geochronology: refinement if the baseline case. Geochimica et Cosmochimica Acta 75, 7779-7791.
- Linnemann, U., Ouzegane, K., Drareni, A., Hofmann, M., Becker, S., Gärtner, A., Sagawe, A. , 2011. Sands of West Gondwana: An archive of secular magmatism and plate interactions – A case study from the Cambro-Ordovician section of the Tassili Ouan Ahaggar (Algerian Sahara) using U-Pb LA-ICP-MS detrital zircon ages. Lithos 123, 188-203
- Ludwig, K. R., 2001. Users Manual for Isoplot/Ex rev. 2.49: Berkeley Geochronology Center Special Publication No. 1a, 1-56.
- McDowell, F., McIntosh, W., Farley, K., 2005. A precise ^{40}Ar-^{39}Ar reference age for the Durango apatite (U-Th)/He and fission track dating standard. Chemical Geology 214, 249-263.
- Peel, J., Dawes, P., Collinson, J., Christie, R., 1982. Proterozoic basal Cambrian stratigraphy across Nares Strait: correlation between Inglefield Land and Bache Peninsula. Meddelelser om Gronland, Geoscience, 8, 105-115.
- Roest, W., Srivastava, S., 1989. Sea-floor spreading in the Labrador Sea: a new reconstruction. Geology 17 (11), 1000-1003.

- Sircombe, K.N, 2004. AgeDisplay: an EXCEL workbook to evaluate and display univariate geochronological data using binned frequency histograms and probability density distributions. Computers & Geosciences 30, 21-31.
- Sláma, J., Košler, J., Condon, D.J., Crowley, J.L., Gerdes, A., Hanchar, J.M., Horstwood, M.S.A., Morris, G.A., Nasdala, L., Norberg, N., Schaltegger, U., Schoene, N., Tubrett, M.N., & Whitehouse, M.J., 2008. Plešovice zircon – a new natural reference material for U–Pb and Hf isotopic microanalysis. Chemical Geology 249, 1–35.
- Stacey, J.S., Kramers, J. D., 1975. Approximation of terrestrial lead isotope evolution by a two-stage model. Earth and Planetary Science Letters 26, 207-221.
- Thorsteinsson, R., Tozer, E.T., 1970. Geology of the Arctic Archipelago. *In*: Douglass, R.J.W. (ed.) Geology and Economic Minerals of Canada. Geological Survey of Canada, Economic Geology Report 1, 547–590.
- Thorsteinsson, R., Harrison, J., de Freitas, T., 2009. Phanerozoic bedrock geology, Vendom Fiord area, Ellesmere Island, Nunavut. Geological Survey of Canada, "A" Seris Map 2142A, Scale 1 : 125 000.
- Trettin, H., 1991. Geology of the Innuitian Orogen and Arctic platform of Canada and Greenland. Geological Survey of Canada, Geology of Canada 3, 576 p.
- West, R., Dawson, M., Hutchison, JH., Ramaekers, P., 1975. Paleontological evidence of marine sediments in the Eureka Sound Formation of Ellesmere Island, Arctic Archipelago, NWT., Canada. Canadian Journal of Earth Sciences 12, 574-579.
- Wiedenbeck, M., Alle, P., Corfu, F., Griffin, W.L., Meier, M., Oberli, F., Von Quart, A., Roddick, J.C., Spiegel, W., 1995. Three natural zircon standards for U–Th–Ph, Lu–Th, trace element and REE analyses. Geostandard Newsletters 19, 1, 1–23.
- Zeh, A. & Gerdes, A., 2012. U–Pb and Hf isotope record of detrital zircons from gold-bearing sediments of the Pietersburg Greenstone Belt (South Africa)—is there a common provenance with the Witwatersrand Basin? Precambrian Research 204–205, 46–56.

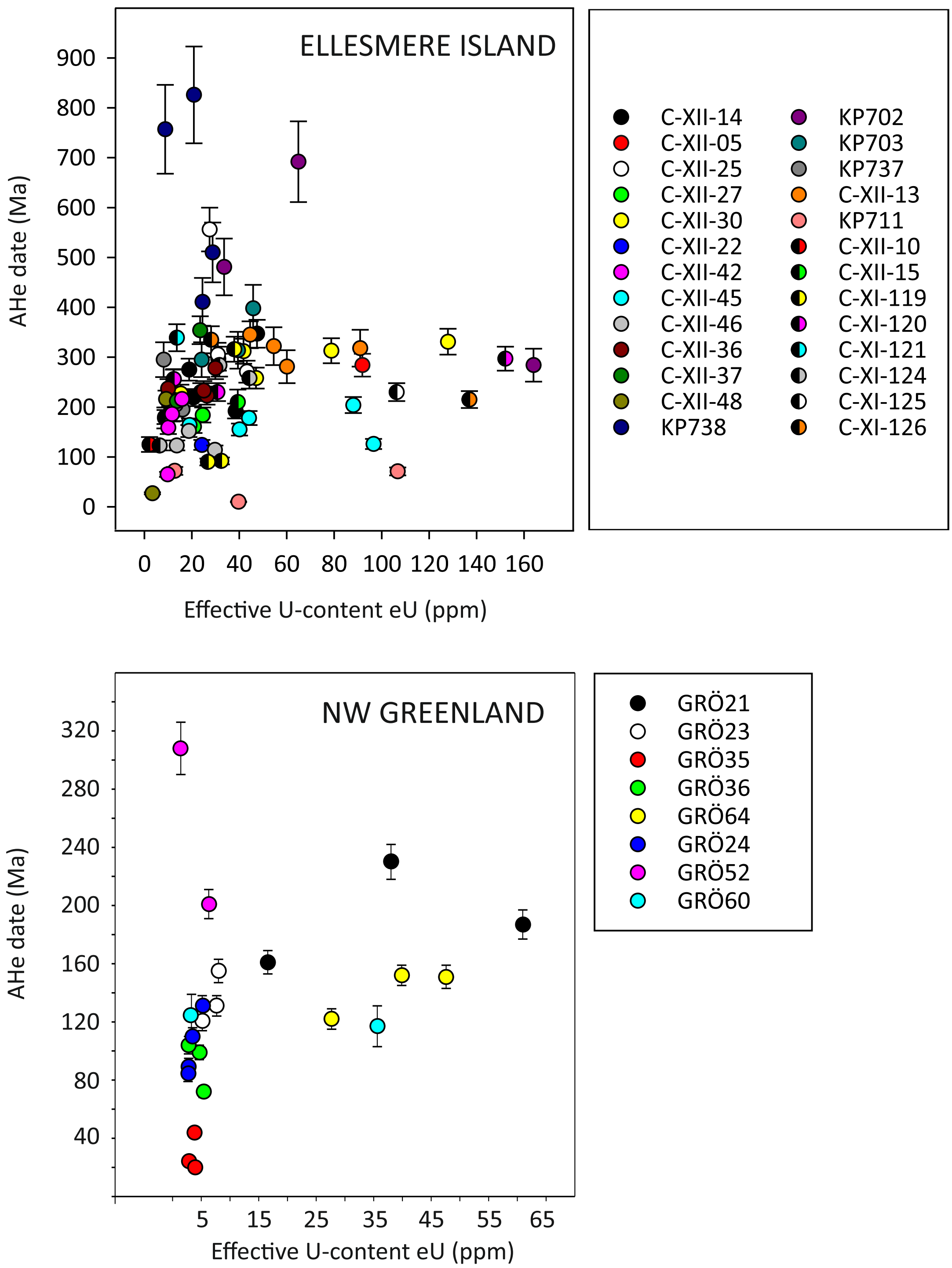

Fig. S1: relationship between AHe dates and effective Uranium contents calculated as eU = U (ppm) + 0.235 * Th (ppm) + 0.0053 *Sm (ppm). The different samples are colour-coded.

Fig. S2 (following pages):

Time-temperature paths modelled from the thermochronology data of (i) the cratonic rocks exposed in Southeast Ellesmere Island, (ii) the Devonian clastic sediments of the Franklinian Basin in Ellesmere Island (plus one Triassic sample from the Sverdrup Basin), and (iii) coastal exposures of rocks from the Thule Basin and the Rae craton of Northwest Greenland. Squares are constraint boxes introduced in the model and explained in the text and in Table S1 Blue line shows the mean path weighted according to the goodness-of-fit values. Left side: pink envelopes enclose all modelled time-temperature paths with a good statistical fit with the data observed (defined as goodness-of-fit value >0.5). Green envelopes enclose al modelled time-temperature paths with an acceptable statistical fit (defined as goodness-of-fit value >0.05). Right-side: same models as on left side, but displaying the constraint points of paths with good fit (pink) and of acceptable fit (green). Text on the left side lists the diffusion model (Farley = Farley, 2000, Flowers = Flowers et al., 2009), the number of tT-paths attempted, and the number of Tt-paths in good statistical fit with the data.

CRATON - ELLESMERE ISLAND

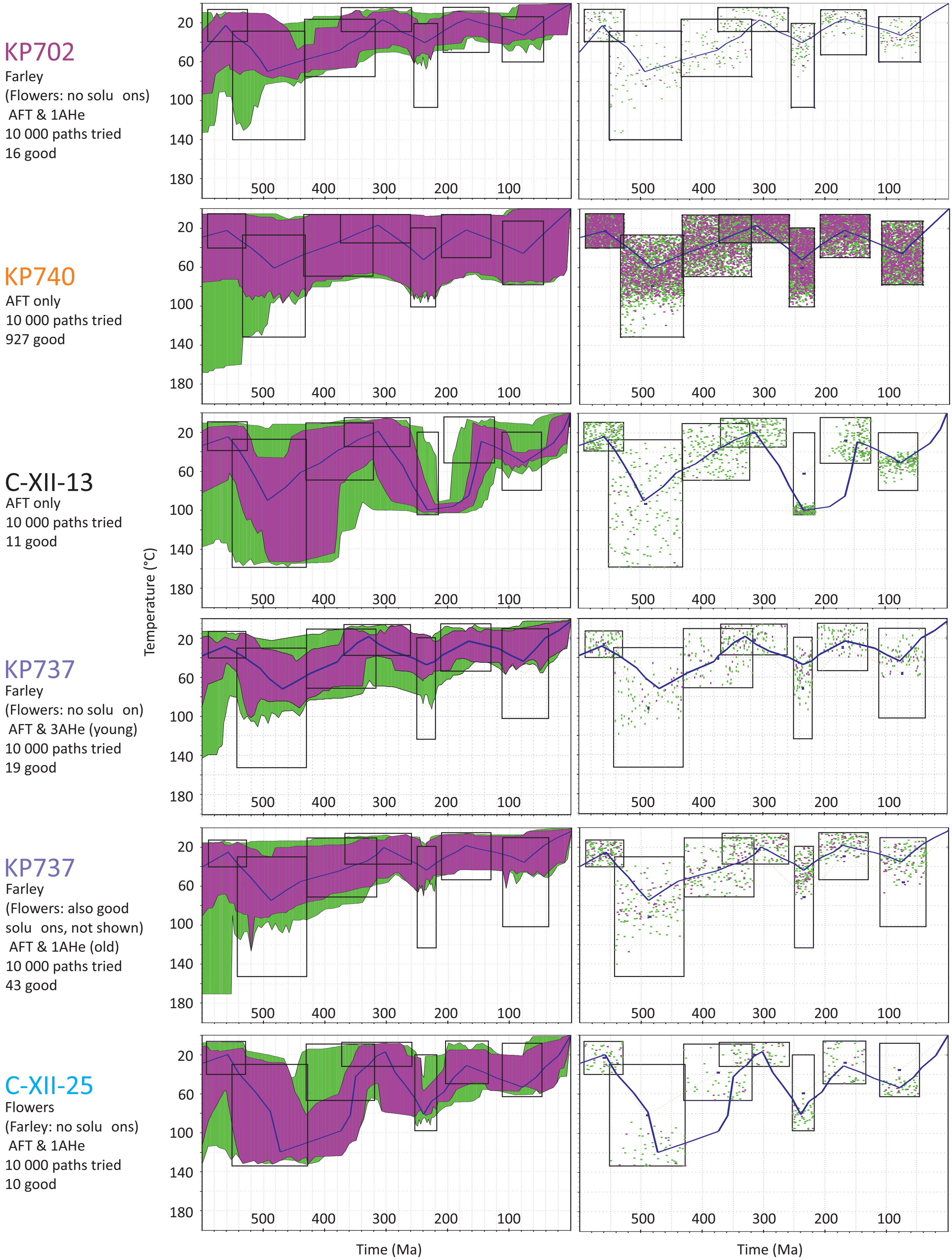

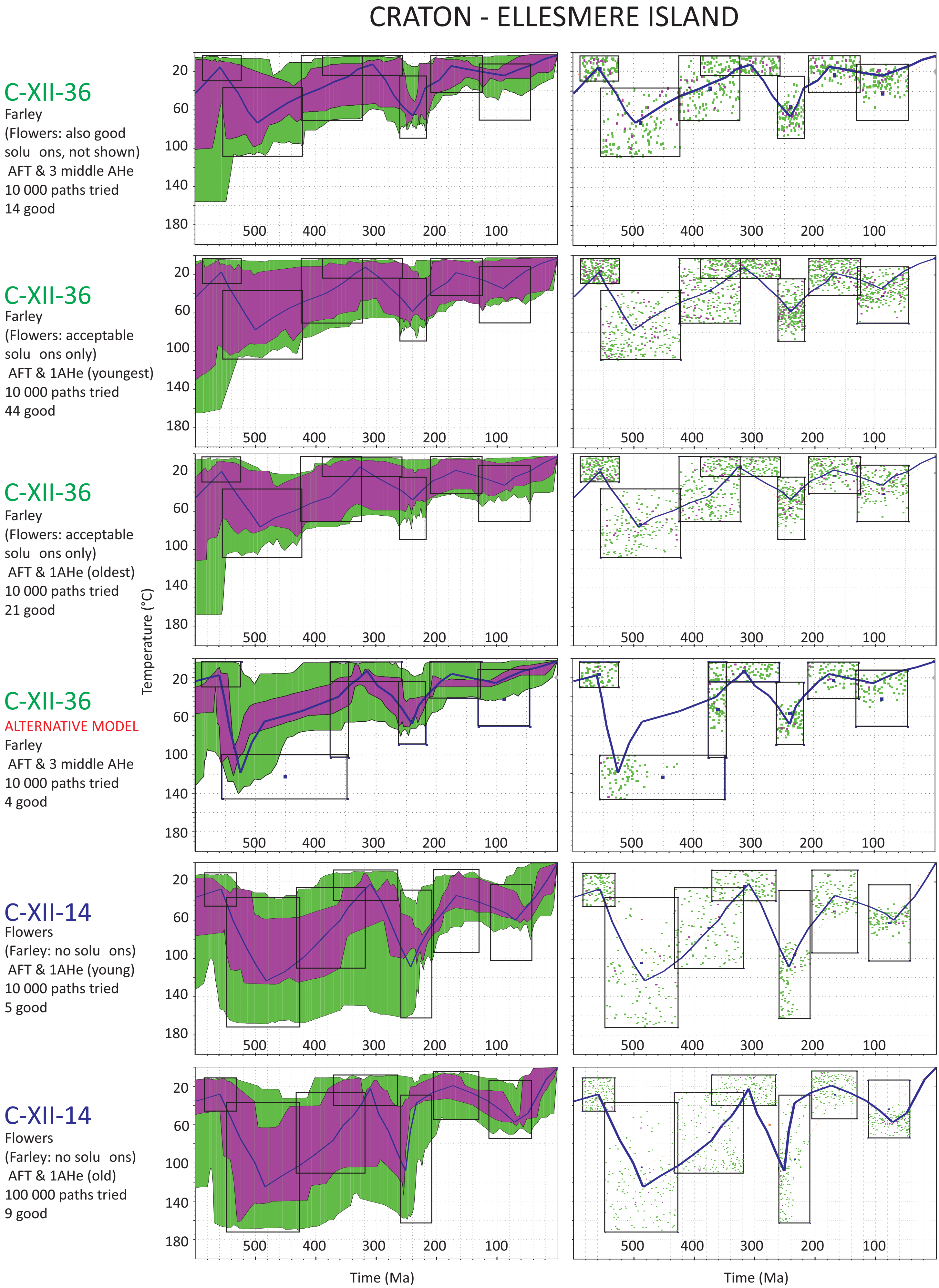
CRATON - ELLESMERE ISLAND
C-XII-36
Farley
(Flowers: also good
solu ons, not shown)
AFT & 3 middle AHe
10 000 paths tried
14 good
C-XII-36
Farley
(Flowers: acceptable
solu ons only)
AFT & 1AHe (youngest)
10 000 paths tried
44 good
C-XII-36
Farley
(Flowers: acceptable
solu ons only)
AFT & 1AHe (oldest)
10 000 paths tried
21 good
C-XII-36
ALTERNATIVE MODEL
Farley
AFT & 3 middle AHe
10 000 paths tried
4 good
C-XII-14
Flowers
(Farley: no solu ons)
AFT & 1AHe (young)
10 000 paths tried
5 good
C-XII-14
Flowers
(Farley: no solu ons)
AFT & 1AHe (old)
100 000 paths tried
9 good
Temperature (°C)
20
60
100
140
180
500
400
300
200
100
Time (Ma)
Time (Ma)

CRATON - ELLESMERE ISLAND

C-XI-121
AFT only
10 000 paths tried
66 good

C-XI-123
AFT only
50 000 paths tried
41 good

C-XII-37
Flowers
(Farley: also good
solu ons, but fewer)
AFT & 2AHe
21 000 paths tried
55 good

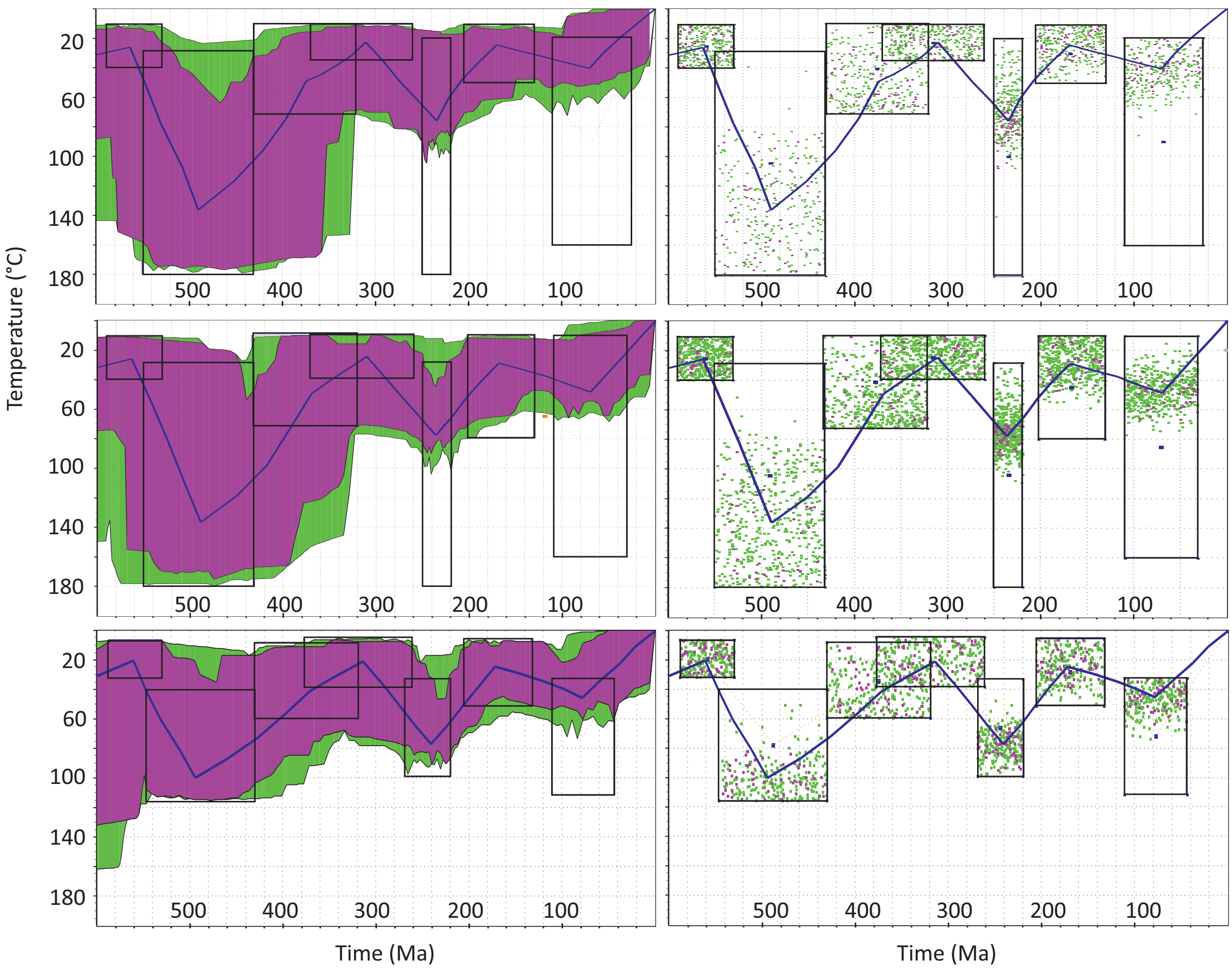

SEDIMENTARY ROCKS - ELLESMERE ISLAND

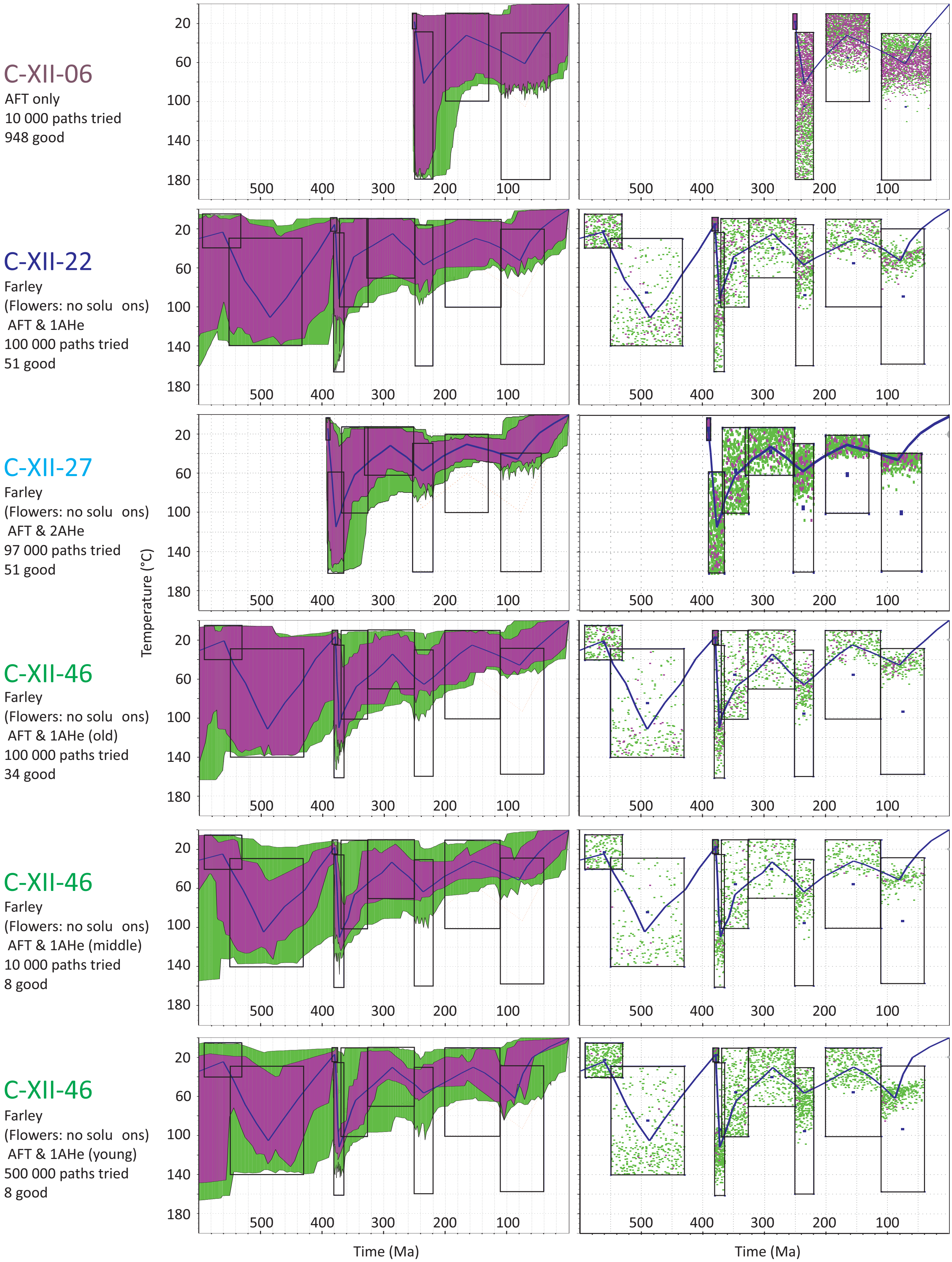

SEDIMENTARY ROCKS - ELLESMERE ISLAND

C-XI-119

Flowers
(Farley: no solu ons)
AFT & 1AHe (middle)
100 000 paths tried
17 good

C-XI-119

Flowers
(Farley: no solu ons)
AFT & 1AHe (old)
10 000 paths tried
37 good

C-XI-119

Farley
(Flowers: no solu ons)
AFT & 2AHe (young)
10 000 paths tried
14 good

C-XII-48

Farley
(Flowers: acceptable solu ons only)
AFT & 1AHe (old)
197 000 paths tried
43 good.
The youngest AHe date could not be integrated.

C-XI-120

Flowers
(Farley: acceptable solu ons only)
AFT & 1AHe (middle)
100 000 paths tried
12 good.
The 2 other AHe dates yielded either no or only acceptable solu ons.

C-XI-124

Flowers
(Farley: also good solu ons, not shown)
AFT & 1AHe (young)
100 000 paths tried
28 good.
The other AHe date yielded only acceptable solu ons.

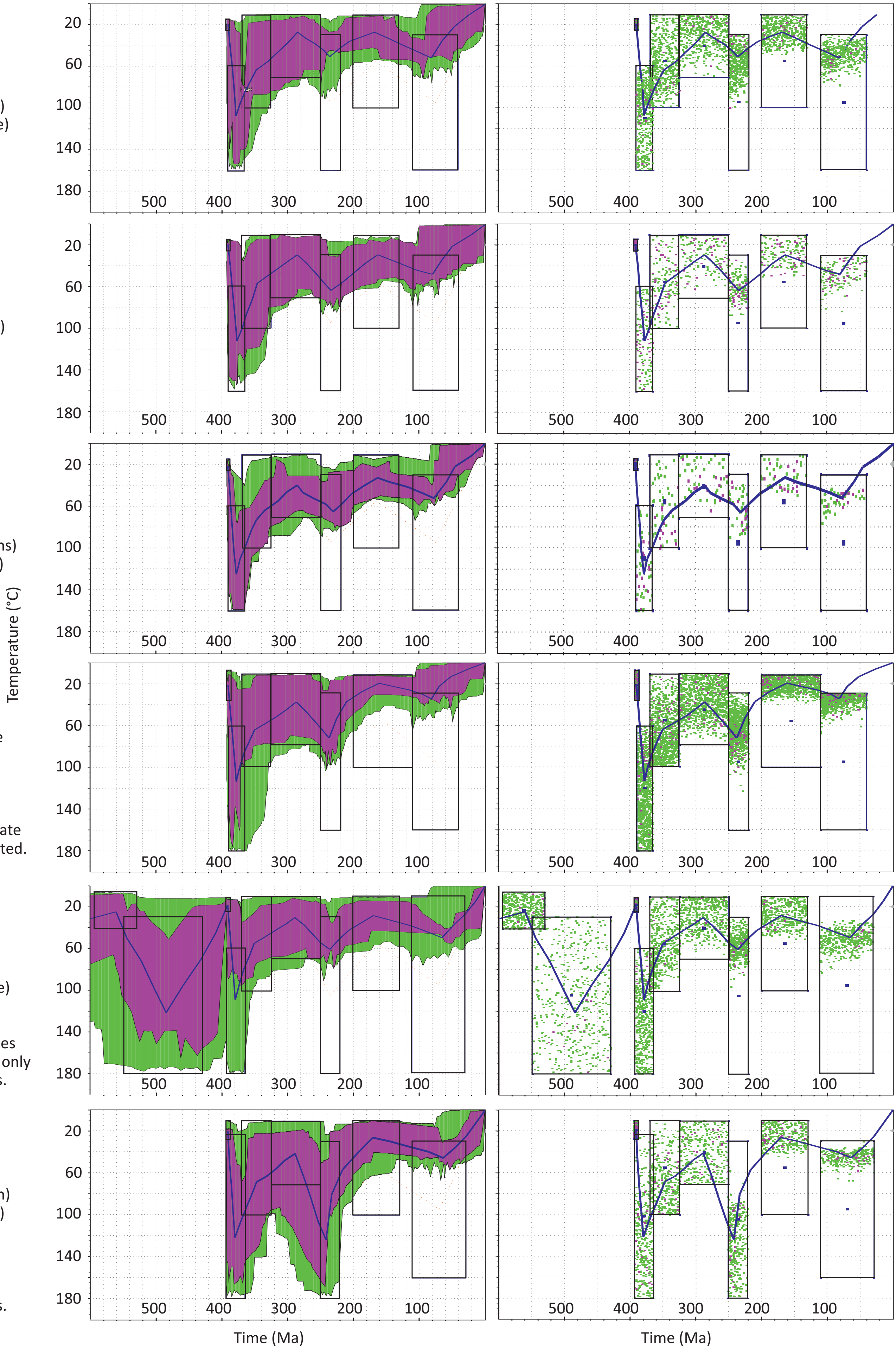

SEDIMENTARY ROCKS - ELLESMERE ISLAND

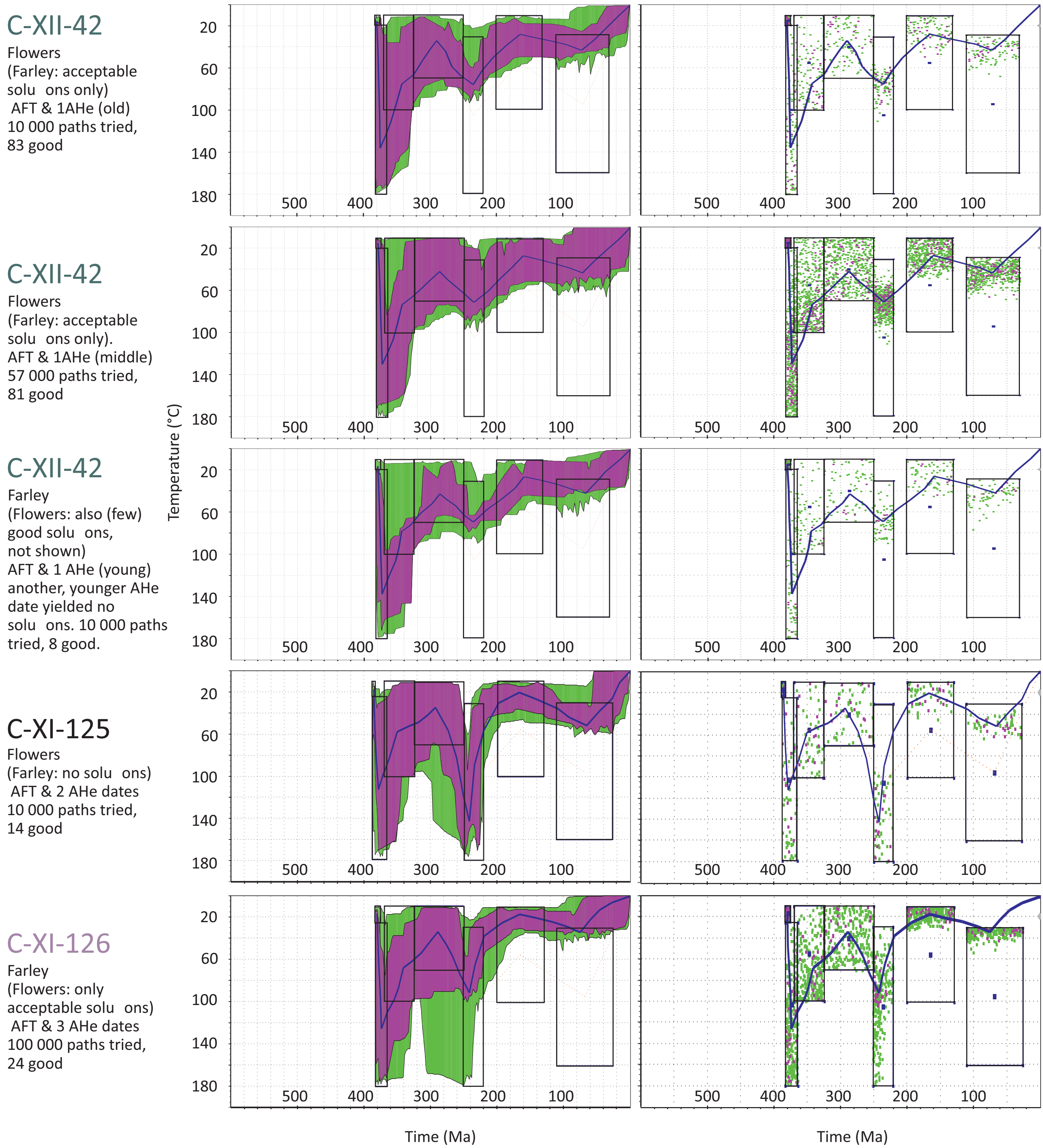

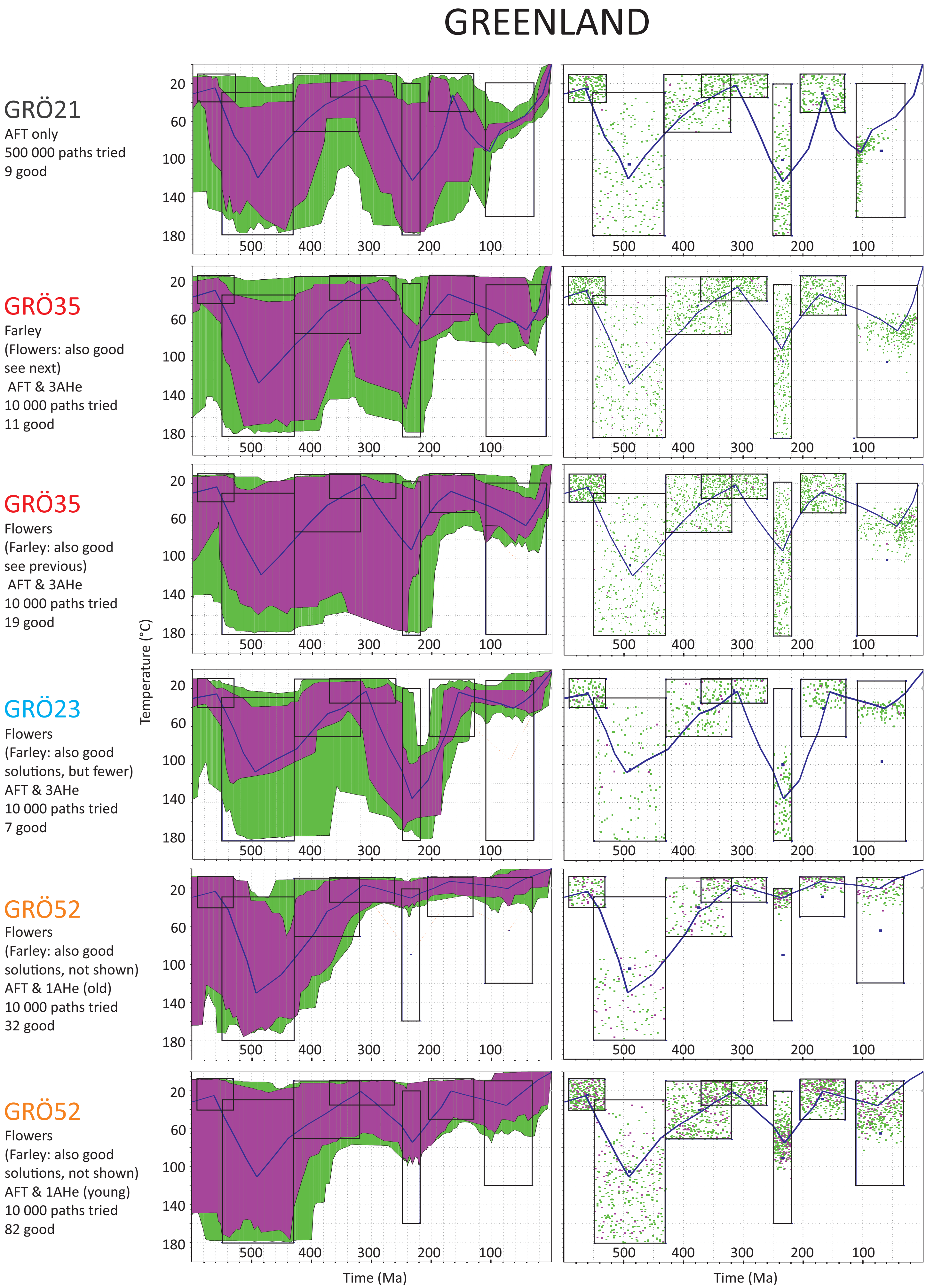
GREENLAND
GRÖ21
AFT only
500 000 paths tried
9 good
GRÖ35
Farley
(Flowers: also good
see next)
AFT & 3AHe
10 000 paths tried
11 good
GRÖ35
Flowers
(Farley: also good
see previous)
AFT & 3AHe
10 000 paths tried
19 good
GRÖ23
Flowers
(Farley: also good
solutions, but fewer)
AFT & 3AHe
10 000 paths tried
7 good
GRÖ52
Flowers
(Farley: also good
solutions, not shown)
AFT & 1AHe (old)
10 000 paths tried
32 good
GRÖ52
Flowers
(Farley: also good
solutions, not shown)
AFT & 1AHe (young)
10 000 paths tried
82 good
Temperature (°C)
20
60
100
140
180
500
400
300
200
100
Time (Ma)
Time (Ma)

GREENLAND

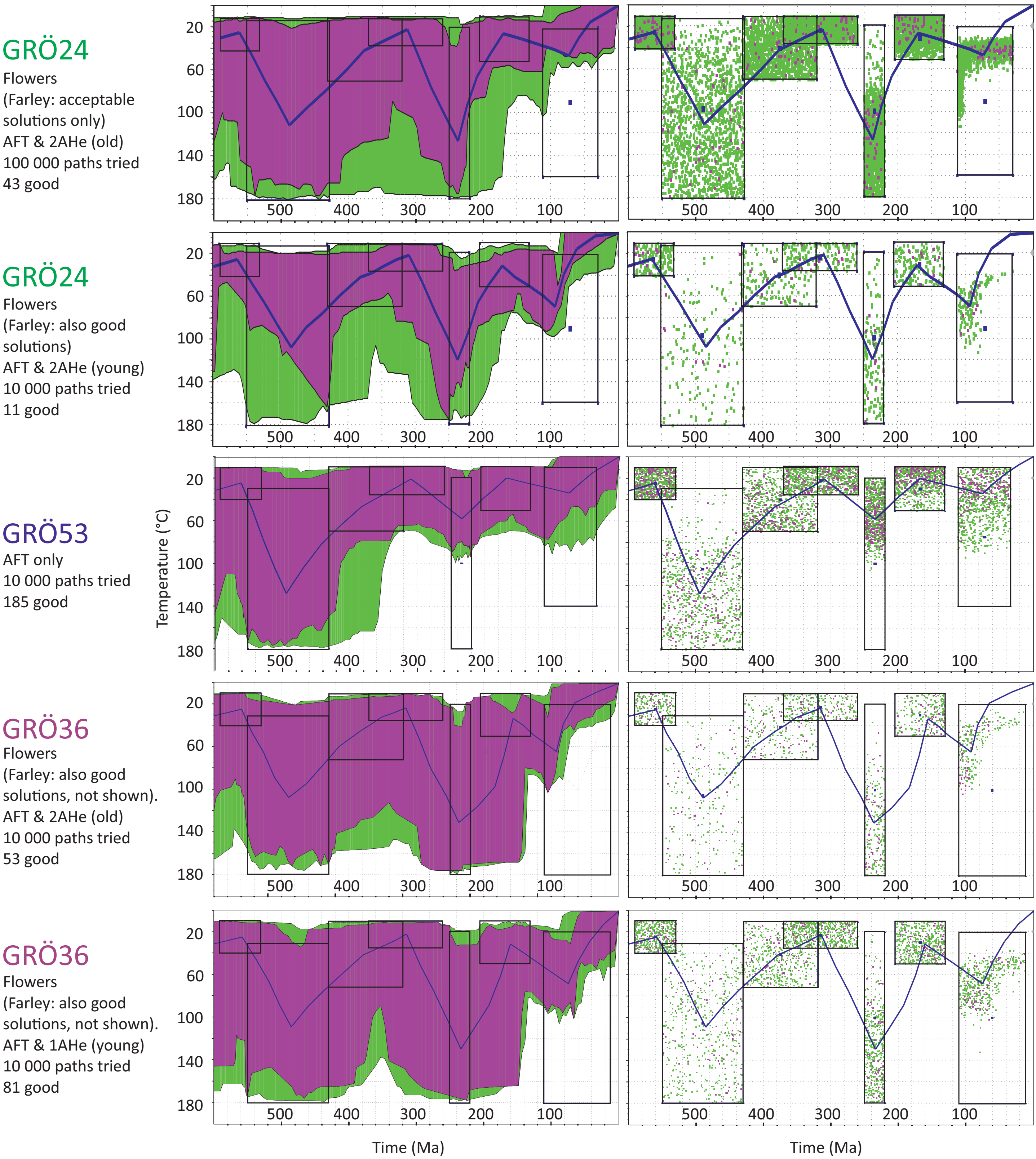
GRÖ24
Flowers
(Farley: acceptable solutions only)
AFT & 2AHe (old)
100 000 paths tried
43 good
GRÖ24
Flowers
(Farley: also good solutions)
AFT & 2AHe (young)
10 000 paths tried
11 good
GRÖ53
AFT only
10 000 paths tried
185 good
GRÖ36
Flowers
(Farley: also good solutions, not shown).
AFT & 2AHe (old)
10 000 paths tried
53 good
GRÖ36
Flowers
(Farley: also good solutions, not shown).
AFT & 1AHe (young)
10 000 paths tried
81 good
Temperature (°C)
20
60
100
140
180
500
400
300
200
100
Time (Ma)
Time (Ma)

GREENLAND

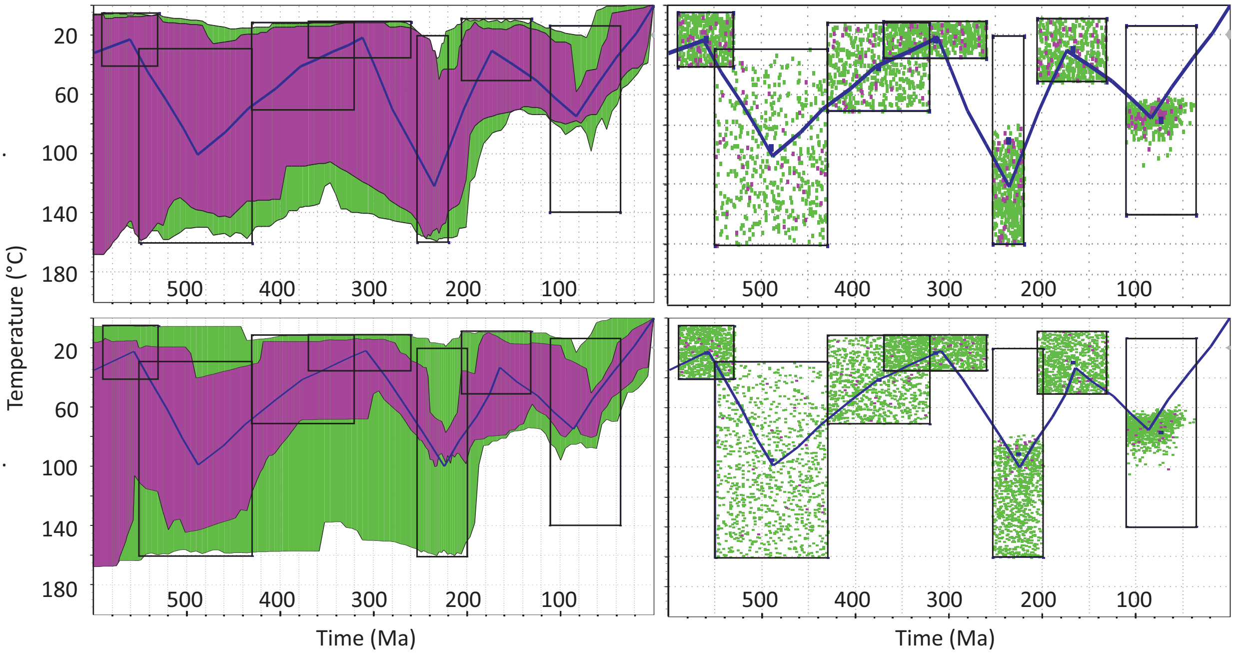

GRÖ64

Flowers
(Farley: no solutions).
AFT & 2AHe (old)
100 000 paths tried
39 good

GRÖ64

Flowers
(Farley: no solutions).
AFT & 1AHe (young)
500 000 paths tried
18 good

Table S1: Information for thermal history inversions

1: Thermochronologic data and independent geological constraints used in simulations

	AFT age	AFT length	Paths tried	AHe dates	Integration of multiple AHe dates	Constraints
CXII-06	n=10	n=9	10000	0		a
CXII-22	n=24	n=33	100000	1		b
CXII-27	n=22	n=75	97000	2	AHe dates modelled individually and simultaneously	c (from constrain 6 onwards)
CXII-46	n=16	n=79	100000 & 10000 & 500000	3	AHe dates modelled individually and separately	b
CXII-48	n=19	n=26	197000	1		c (from constrain 6 onwards)
C-XI-119	n=21	n=98	100000 & 2 x 10000	4	All AHe dates modelled individually, 2 simultaneously	c (from constrain 6 onwards)
C-XI-120	n=17	n=64	100000	1		c
C-XII-42	n=17	n=82	57000 & 2 x 10000	3	AHe dates modelled individually and separately	c (from constrain 6 onwards)
C-XI-125	n=20	n=70	10000	2	AHe dates modelled individually and simultaneously	c (from constrain 6 onwards)
C-XI-124	n=18	n=87	100000	1		c (from constrain 6 onwards)
C-XI-126	n=20	n=15	100000	3	AHe dates modelled individually and simultaneously	b (from constrain 6 onwards)
KP702	n=15	n=67	10000	1		d
KP737	n=19	n=18	2 x 10000	4	all AHe dates modelled individually, 3 simultaneously	d
KP740	n=10	n=0	10000	0		d
CXII-13	n=20	n=91	10000	0		d
CXII-14	n=18	n=58	10000 & 100000	2	AHe dates modelled individually and separately	d
CXII-25	n=26	n=99	10000	1		d
CXII-36	n=20	n=52	3 x 10000	5	All AHe dates modelled individually, 3 simultaneously	d
CXII-37	n=23	n=50	21000	2	AHe dates modelled individually and simultaneously	d
C-XI-121	n=23	n=31	10000	0		d
C-XI-123	n=13	n=40	50000	0		d
GRÖ21	n=20	n=103	500000	0		d
GRÖ23	n=19	n=28	10000	3	AHe dates modelled individually and simultaneously	d
GRÖ24	n=20	n=0	100000 & 10000	4	All AHe dates modelled individually, 2 each simultaneously	d
GRÖ35	n=18	n=1	10000	3	AHe dates modelled individually and simultaneously	d
GRÖ36	n=20	n=0	2 x 10000	3	All AHe dates modelled individually, 2 simultaneously	d
GRÖ52	n=12	n=7	2 x 10000	2	AHe dates modelled individually and separately	d
GRÖ53	n=15	n=15	10000	0		d
GRÖ64	n=20	n=97	100000 & 500000	3	All AHe dates modelled individually, 2 simultaneously	d

Constraints

a:
1: Early Triassic surface temperatures (20 ± 10°C) --> sediment deposition
2: Triassic heating between 30 and >120°C --> increased clastic discharge into the Sverdrup Basin (Embry and Beauchamp, 2008)
3: Jurassic to earliest Cretaceous T between 100 and 10°C, allowing for slow erosion or stagnation
--> no sediments of this age deposited (Thorsteinsson et al., 2009, Harrison et al., 2015), period of quiescence (Embry and Beauchamp, 2008).
4: Late Cretaceous to Paleogene T between 30 to >120°C, allowing for heating

--> late Cretaceous rifting and breakup (Roest and Srivastana, 1989), Deposition of marine-influenced Paleogene strata (West et al., 1975).
5: Present-day surface T of 0°C

b & c 1: 2000-1900 Ma: T of 800 ± 100°C --> magmatism and high-T metamorphism of cratonic rocks (Frisch and Hunt, 1988, Gilotti et al., 2018).
2: 1270 ± 50 Ma: surface T of 20 ± 10°C --> onset of deposition of Thule sediments on top of the cratonic peneplain (Dawes, 2006)
3: 1270 - 800°C: heating to T of 30 - >120°C --> deposition of Thule supergroup (Dawes, 2006)
4: 590 - 530 Ma: at or close to surface at T of 20 ± 10°C --> deposition of lower Cambrian sediments on top of the craton (Peel et al., 1982, Thorsteinsson et al., 2009)
5: 550-430 Ma: heating to T of 30 - >120°C
--> deposition of Franklinian Basin deposits, followed by local and regional uplift from 430 Ma onwards (Bothia uplift, Ellesmerian orogeny, Trettin, 1991).
6: Late Devonian (b) or lower - middle Devonian (c): surface T of 20 ± 10°C --> deposition age
7: Deposition age to 365 Ma: heating to T of 30 - >120°C
--> Duration of deposition in foreland basin of the Ellesmerian orogen (Thorsteinsson and Thozer, 1970; Embry 1988; Dewing & Hadlari, 2023).
8: 370-325 Ma: Cooling to T of 100 - 10°C --> uplift and deformation of the foreland basin (Trettin, 1991)
9: Carboniferous to Permian: T between 30 and 70°C, allowing for slow erosion or stagnation
--> Sverdrup Basin was shallow and / or did not receive significant clastic influx (Embry & Beauchamp, 2008).
10: Triassic: heating to T of 30 - >120°C: Sverdrup Basin widened and deepened, receiving increased clastic discharge (Embry and Beauchamp, 2008).
11: Jurassic to earliest Cretaceous T between 100 and 10°C, allowing for slow erosion or stagnation
--> no sediments of this age deposited (Thorsteinsson et al., 2009, Harrison et al., 2015), period of quiescence (Embry and Beauchamp, 2008).
12: Late Cretaceous to Paleogene T between 30 to >120°C, allowing for heating
--> late Cretaceous rifting and breakup (Roest and Srivastana, 1989), Deposition of marine-influenced Paleogene strata (West et al., 1975).
13: Present-day surface T of 0°C

d 1: 2000-1900 Ma: T of 800 ± 100°C --> magmatism and high-T metamorphism of cratonic rocks (Frisch and Hunt, 1988, Gilotti et al., 2018).
2: 1270 ± 50 Ma: surface T of 20 ± 10°C --> onset of deposition of Thule sediments on top of the cratonic peneplain (Dawes, 2006)
3: 1270 - 800°C: heating to T of 30 - >120°C --> deposition of Thule supergroup (Dawes, 2006)
4: 590 - 530 Ma: at or close to surface at T of 20 ± 10°C --> deposition of lower Cambrian sediments on top of the craton (Peel et al., 1982, Thorsteinsson et al., 2009)
5: 550-430 Ma: heating to T of 30 - >100°C
--> deposition of Franklinian Basin deposits, followed by local and regional uplift from 430 Ma onwards (Bothia uplift, Ellesmerian orogeny, Trettin, 1991).
6: 430 - 320 Ma: cooling to T of 10 - 70°C --> Ellesmerian orogeny (Trettin, 1991), provenance data suggest that craton underwent exhumation and erosion (this study)
7: 320 - 260 Ma: Stagnation at (near-)surface levels at T of 10-30°C
--> Sverdrup Basin was shallow and / or did not receive significant clastic influx (Embry & Beauchamp, 2008).
8: Triassic: heating to T of 30 to >100°C: Sverdrup Basin widened and deepened, receiving increased clastic discharge (Embry and Beauchamp, 2008).
9: Jurassic to earliest Cretaceous T between 100 and 10°C, allowing for slow erosion or stagnation
--> no sediments of this age deposited (Thorsteinsson et al., 2009, Harrison et al., 2015), period of quiescence (Embry and Beauchamp, 2008).
10: Late Cretaceous to Paleogene T between 30 to >60-100°C, allowing for heating
--> late Cretaceous rifting and breakup (Roest and Srivastana, 1989), Deposition of marine-influenced Paleogene strata (West et al., 1975).
11: Present-day surface T of 0°C

2: Model-specific parameters

- Modelling code: HeFTy software (Ketcham, 2005), Version 1.9.1, Monte Carlo search method, random subsegment spacing
- Statistical fitting criteria: good fit = GOF-value >0.5, acceptable fit = GOF-value >0.05

3: System-specific parameters

3.1 AFT-system

- AFT dates were calculated from single-grain data as pooled ages with 2-sigma confidence interva
- The annealing algorithm of Ketcham et al. (2007) was used
- Dpar was used as kinetic indicator for each grain on which age or length measurements were performec
- Initial track lengths were calculated from Dpar values
- c-axis projection was used
- Length reduction in age standard = 0.893

3.2 AHe-system

- All simulations were performed with both the diffusion models of Farley (2000) and Flowers et al. (2009) in different model runs
- Single grains were modelled individually, no averaged ages were use
- Single grain uncorrected AHe dates were simulatec
- Uncorrected dates were corrected for alpha-ejection in HeFTy using the stopping distances of Ketcham et al. (2011)
- Single-grain errors refer to analytical errors reported in Table 2 of this study
- No zonation data were measured
- Grain sizes for modelling refer to the equivalent sphere radius

Table S2: Summary Outcome Thermal History Inversions

	AFT age	n lengths	nAHe dates	inversion applied	integrated in model	solutions Farley (2000)	solutions Flowers et al. (2009)	Reliability
CXII-06	y	9	0	y	0	n.a.	n.a.	Very limited
CXII-13	y	91	4, 4 cross-over	y	0	n.a.	n.a.	ok
C-XII-14	y	58	5, 3 cross-over	y	2, individually modelled			good
model 1					1 AHe date: 192 Ma	none	**5 good out of 10 000 paths**	good
model 2					1 AHe date: 219 Ma	none	**9 good out of 100 000 paths**	good
C-XII-20	y	39	0	no, non-reset	n.a.	n.a.	n.a.	n.a.
C-XII-22	y	33	1	y	1 AHe date: 124 Ma	**51 out of 100 000 paths**	none	ok
CXII-25	y	99	3, 1 cross-over	y	1	none	**10 good out of 10 000 paths**	good
CXII-27	y	75	2	y	2 AHe dates: 184, 161 Ma	**51 good out of 97 000 paths**	none	very good
CXII-30	y	53	5	no, non-reset	0	n.a.	n.a.	n.a.
CXII-33	y	0	0	no, non-reset	0	n.a.	n.a.	n.a.
CXII-36	y	52	5	y	3 together, 2 individually			very good
model 1					3 AHes dates: 223, 233, 237 Ma	**14 good out of 10 000 paths**	18 good out of 10 000 paths	very good
model 2					1 AHe date: 214 Ma	**44 good out of 10 000 paths**	30 acceptable out of 10 000 paths	good
model 3					1 AHe date: 278 Ma	**21 good out of 10 000 paths**	2 acceptable out of 10 000 paths	good
CXII-37	y	50	3	y	2 AHe dates: 219, 212 Ma	3 good out of 50 000 paths	**55 good out of 22 000 paths**	very good
CXII-46	y	79	3	y	3 individually			good
model 1					1 AHe date: 152 Ma	**34 good out of 100 000 paths**	none	good
model 2					1 AHe date: 123 Ma	**8 good out of 100 000 paths**	none	good
model 3					1 AHe date: 114 Ma	**8 good out of 500 000 paths**	none	good
CXII-48	y	26	2	y	2 individually			ok
model 1					1 AHe date: 216 Ma	**43 good out of 197 000 paths**	68 acceptable out of 100 000 paths	ok
model 2					1 AHe date: 27 Ma	none	none	ok
KP702	y	67	3	y	1 AHe date: 284 Ma	**16 good out of 10 000 paths**	none	good
KP737	y	18	4	y	3 together, 1 individually			ok
model 1					AHe dates: 205, 195, 178 Ma	**19 good out of 10 000 paths**	none	ok
model 2					AHe date: 295 Ma	**43 good out of 10 000 paths**	12 out of 10 000 paths	ok
KP740	y	0	0	y	0	n.a.	n.a.	Very limited
GRÖ53	y	15	0	y	0	n.a.	n.a.	Very limited
C-XI-119	y	98	4	y	2 together, 2 individually			very good
model 1					1 AHe date: 316 Ma	none	**37 good out of 10 000 paths**	good
model 2					1 AHe date: 255 Ma	none	**17 good out of 100 000 paths**	good
model 3					2 AHe dates: 92, 90 Ma	**14 good out of 10 000 paths**	none	very good
C-XI-120	y	64	3	y	3 individually			good
model 1					1 AHe date: 230 Ma	10 acceptable out of 100 000 paths	none	good
model 2					1 AHe date: 256 Ma	39 acceptable out of 100 000 paths	**12 good out of 100 000 paths**	good
model 3					1 AHe date: 297 Ma	none	none	good

	AFT age	n lengths	nAHe dates	inversion applied	integrated in model	solutions Farley (2000)	solutions Flowers et al. (2009)	Reliability
C-XI-121	y	31	1	y	1	none	33 acceptable out of 10 000 paths	limited
C-XI-123	y	40	0	y	0	n.a.	n.a.	limited
C-XII-42	y	82	4	y	4 individually			good
model 1					1 AHe date: 216 Ma	26 acceptable out of 10 000 paths	**83 good out of 10 000 paths**	good
model 2					1 AHe date: 186 Ma	13 good out of 100 000 paths	**81 good out of 57 000 paths**	good
model 3					1 AHe date: 159 Ma	**8 good out of 10 000 paths**	2 good out of 100 000 paths	good
model 4					1 AHe date: 65 Ma	none	none	good
C-XI-124	y	87	4	y	2 individually			good
model 1					1 AHe date: 180 Ma	3 acceptable out of 100 000 paths	31 acceptable out of 10 000 paths	good
model 2					1 AHe date: 123 Ma	56 good out of 100 000 paths	**28 good out of 100 000 paths**	good
C-XI-125	y	70	2	y	2 AHe dates: 230, 230 Ma	none	**14 good out of 10 000 paths**	very good
C-XI-126	y	15	4, 1 cross-over	y	3 AHe dates: 215, 211, 210 Ma	**24 good out of 100 000 paths**	4 acceptable our of 10 000 paths	ok
GRÖ21	y	103	4, 4 cross-over	y	0	n.a.	n.a.	ok
GRÖ23	y	28	3	y	3 AHe dates: 155, 131, 121 Ma	11 good out of 100 000 paths	**7 good out of 10 000 paths**	ok
GRÖ24	y	0	4	y	2 together for each model			ok
model 1					2 AHe dates: 131, 110 Ma	511 acceptable out of 100 000 paths	**43 good out of 100 000 paths**	ok
model2					2 AHe dates: 90, 84 Ma	10 good our of 10 000 paths	**11 good out of 10 000 paths**	ok
GRÖ35	y	1	3		3 AHe dates: 44, 24, 20 Ma	**11 good out of 10 000 paths**	**19 good out of 10 000 paths**	ok
GRÖ36	y	52	3	y	2 together, 1 individually			very good
model 1					2 AHe dates: 104, 99 Ma	63 good out of 10 000 paths	**53 good out of 10 000 paths**	very good
model 2					1 AHe date: 72 Ma	94 good out of 10 000 paths	**81 good out of 10 000 paths**	good
GRÖ52	y	7	2	y	2 induvidually			ok
model 1					1 AHe date: 308 Ma	55 good out of 10 000 paths	**32 good out of 10 000 paths**	ok
model 2					1 AHe date: 201 Ma	88 good out of 10 000 paths	**82 good out of 10 000 paths**	ok
GRÖ64	y	97	3	y	2 together, 1 individually			very good
model 1					2 AHe dates: 152, 151 Ma	none	**39 good out of 100 000 paths**	very good
model 2					1 AHe date: 122 Ma	none	**18 good out of 500 000 paths**	good

Modelling solutions in bold: Used for compilation in Fig. 7 and as basis for calculating burial and erosion illustrated in Fig. 8
Quality of input data / models is colour-coded:
Green: Very reliable - 2 or more AHe dates simultaneously integrated in model, number of measured fission track lenghs >50
Blue: reliable - 1 AHe date integrated in model, number of mesured fission track lengths >50
Black: relatively reliable - 1 or more AHe dates integrated simultaneously in model, number of measured fission track lengths <50
Violett: relatively reliable - no AHe dates integrated, but number of measured fission track lengths >90
Orange: limited reliability - no AHe dates, 30 - 90 fission track lengths measured
Red: very limited reliability - no AHe dates, <30 fission track lengths measured
Grey: not used for thermal history modelling

Table S3: Interpretation: Net burial and exhumation of southeast Ellesmere Island dervied from weigthed mean paths of thermal history inversions

Sedimentary Rocks	**C-XII-06**	**C-XII-22**	**C-XII-27**	**C-XII-46**	**C-XII-48**	**C-XI-119**	**C-XI-120**	**C-XII-42**	**C-XI-125**	**C-XI-124**	**C-XI-126**
Ellesmerian Orogeny (380-370 Ma)											
Timing of peak heating (Ma)	na	372	378	373-375	379	379	380	373-375	379	378	374
T max (°C)	na	91	117	110-112	114	110-128	110	138-140	112	121	127
Assumed Geothermal Gradient	na	25°C/km	25°C/km	25°C/km	25°C/km	25°C/km	25°C/km	25°C/km	25°C/km	25°C/km	25°C/km
Overburden (km)	na	3.2	4.3	4.0 - 4.1	4.2	4.0 - 4.7	4.0	5.1 - 5.2	4.1	4.4	4.7
Onset Ellesmerian erosion (Ma)		372.0	378.0	374	379.0	379.0	380.0	374	379.0	378.0	374.0
End Ellesmerian erosion (Ma)	na	345.0	343.0	343	350.0	343	350.0	344	350.0	343.0	341.0
Ellesmerian net cooling (°C)	na	52.0	55.0	46	51.0	56-53	55.0	64	54.0	52.0	59.0
Assumed Geothermal Gradient	na	25°C/km	25°C/km	25°C/km	25°C/km	25°C/km	25°C/km	25°C/km	25°C/km	25°C/km	25°C/km
Ellesmerian Orogeny net erosion (km)	m	2.1	2.2	1.8	2.0	2.2	2.2	2.6	2.2	2.1	2.4
Triassic Burial (242-230 Ma)											
Timing of peak heating (Ma)	237	237	238	237	238	230-238	238	237	241	241	242
T max (°C)	82	58	58	57-66	72	50-65	60	68 - 77	143	124	92
Assumed Geothermal Gradient	25°C/km	25°C/km	25°C/km	25°C/km	25°C/km	25°C/km	25°C/km	25°C/km	25°C/km	25°C/km	25°C/km
Overburden	2.9	1.9	1.9	1.9 - 2.2	2.5	1.6 - 2.2	2.0	2.3 - 2.7	5.3	4.6	3.3
Late Cretaceous to Cenozoic Burial (87-62 Ma)											
Timing of peak heating (Ma)	73	79	81	80-87	80	78-80	64	65-68	63	62	75
T max (°C)	62	52	47	46-62	35	49-53	50	42	52	48	35
Assumed Geothermal Gradient	40°C/km	40°C/km	40°C/km	40°C/km	40°C/km	40°C/km	40°C/km	40°C/km	40°C/km	40°C/km	40°C/km
Overburden	1.3	1.1	0.9	0.9 - 1.3	0.6	1.0 - 1.1	1.0	0.8	1.1	1.0	0.6

Cratonic Rocks Ellesmere	**KP702**	**KP737**	**KP740**	**C-XII-13**	**C-XII-14**	**C-XII-25**	**C-XII-36**	**C-XII-37**	**C-XI-121**	**C-XI-123**
Early Paleozoic Burial (502-468 Ma)										
Timing of peak heating (Ma)	495	479-489	481	493	482-484	474	495-502	497	490	487
T max (°C)	70	73-75	62	90	123-125	120	74-79	101	138	138
Assumed Geothermal Gradient	25°C/km	25°C/km	25°C/km	25°C/km	25°C/km	25°C/km	25°C/km	25°C/km	25°C/km	25°C/km
Overburden	2.4	2.5 - 2.6	2.1	3.2	4.5 - 4.6	4.4	2.6 - 2.8	3.6	5.1	5.1
Ellesmerian Orogeny										
Net cooling "clastic wedge interval" (°C)	5.0	8	5	7.0	11	5.0	5	11.0	20.0	20.0
Assumed Geothermal Gradient	25°C/km	25°C/km	25°C/km	25°C/km	25°C/km	25°C/km	25°C/km	25°C/km	25°C/km	25°C/km
Net erosion during "clastic wedge interval" (km)*	0.2	0.3	0.2	0.3	0.4	0.2	0.2	0.4	0.8	0.8
Net cooling climax Ellesmerian Orogeny (°C)	10.0	8	8	10.0	19	56.0	10	9.0	7.0	12.0
Net erosion climax Ellesmerian Orogeny (km)*	0.4	0.3	0.3	0.4	0.8	2.2	0.4	0.4	0.3	0.5
Triassic Burial (250-238 Ma)										
Timing of peak heating (Ma)	238	237-238	239	237	242-250	240	239-240	240	238	238
T max (°C)	41	43-48	52	99	108-110	81	48-66	78	78	78
Assumed Geothermal Gradient	25°C/km	25°C/km	25°C/km	25°C/km	25°C/km	25°C/km	25°C/km	25°C/km	25°C/km	25°C/km
Overburden	1.2	1.3 - 1.5	1.7	3.6	3.9 - 4.0	2.8	1.5 - 2.2	2.7	2.7	2.7
Late Cretaceous to Cenozoic Burial (90-68 Ma)										

Timing of peak heating (Ma)	77	77	76	78	68-70	78	78-80	79	68	68
T max (°C)	33	37-44	47	51	60-58	54	24-35	47	41	49
Assumed Geothermal Gradient	40°C/km	40°C/km	40°C/km	40°C/km	40°C/km	40°C/km	40°C/km	40°C/km	40°C/km	40°C/km
Overburden	0.6	0.7 -0.9	0.9	1.0	1.2 - 1.3	1.1	0.4 - 0.6	0.9	0.8	1.0

Greenland Exposures	**GRÖ21**	**GRÖ23**	**GRÖ24**	**GRÖ35**	**GRÖ36**	**GRÖ52**	**GRÖ53**	**GRÖ64**
Early Paleozoic Burial (495-483 Ma)								
Timing of peak heating (Ma)	491	495	485-490	485-490	486	493-495	495	488
T max (°C)	120	109	112-118	119-124	107-109	110-130	128	98-102
Assumed Geothermal Gradient	25°C/km	25°C/km	25°C/km	25°C/km	25°C/km	25°C/km	25°C/km	25°C/km
Overburden	4.4	4.0	4.1 - 4.3	4.4 - 4.6	3.9 - 4.0	4.0 - 4.8	4.7	3.5 -3.7
Ellesmerian Orogeny								
Net cooling "clastic wedge interval" (°C)	9.0	12.0	9	12	8	12	8.0	9
Assumed Geothermal Gradient	25°C/km	25°C/km	25°C/km	25°C/km	25°C/km	25°C/km	25°C/km	25°C/km
Net erosion during "clastic wedge interval" (km)*	0.4	0.5	0.4	0.5	0.3	0.5	0.3	0.4
Net cooling climax Ellesmerian Orogeny (°C)	8.0	7.0	7	11	9	11	8.0	7
Net erosion climax Ellesmerian Orogeny (km)*	0.3	0.3	0.3	0.4	0.4	0.4	0.3	0.3
Triassic Burial (239-225 Ma)								
Timing of peak heating (Ma)	234	237	239	238	235-238	234-238	233	225-238
T max (°C)	122	135	122-131	88-91	129-132	31-75	59	100-122
Assumed Geothermal Gradient	25°C/km	25°C/km	25°C/km	25°C/km	25°C/km	25°C/km	25°C/km	25°C/km
Overburden	4.5	5.0	4.5 - 4.8	3.1 - 3.2	4.8 - 4.9	0.8 - 2.6	2.0	3.6 - 4.5
Late Cretaceous to Cenozoic Burial (103-40 Ma)								
Timing of peak heating (Ma)	103	63	72-93	40-42	70-93	74	73	81-85
T max (°C)	91	42	55-77	66-68	65-68	20-36	35	75-78
Assumed Geothermal Gradient	40°C/km	40°C/km	40°C/km	40°C/km	40°C/km	40°C/km	40°C/km	40°C/km
Overburden	2.0	0.8	1.1 - 1.7	1.4 - 1.5	1.4 - 1.5	0.3 - 0.7	0.6	1.6 - 1.7

*"clastic wedge interval" = time between deposition & max. burial of mid to late Devonian deposits (393-375 Ma)
*climax Ellesmerian Orogeny defined as 375 to 345 Ma
surface temperatures of the past assumed as 10°C
grey background: figures associated with high uncertainty due to later thermal resetting
orange background: numbers used for Fig. 7

Table S4: Single grain data of Apatite Fission Track analysis

C-XI-119 (Ellesmere Island, Canadian High Arctic)

Location	**Cf-irrad.**
Vendom Fiord	no
Lithology	**Zeta**
Sandstone	346
Stratigraphic	**error_Zeta**
Lower-Middle Devon.	12
Formation	**RhoD**
Strathcona Fiord Fm	1.311E+6
Lat N	**Nd**
77°35.400´	6721
Long W	**Length reduction in standard**
83°36.305´	0.893
Elevation	
292	

Ns	Ni	Age	-95%	95%	Dpar
15	12	277.1	-148	312	1.73
13	8	357.9	-210	490	2.55
30	19	348	-153	267	1.71
34	27	279.1	-112	184	1.94
14	8	384.6	-224	514	1.82
26	22	262.2	-115	201	1.74
27	15	395.3	-186	340	1.81
26	11	514.2	-260	504	2.06
11	8	304.1	-183	442	1.66
17	15	251.7	-127	251	1.92
16	12	295.1	-156	324	2.21
10	6	366.8	-234	617	2.05
34	26	289.6	-117	193	1.74
17	12	313.1	-164	337	2.1
49	31	348.4	-127	198	1.56
18	19	211.1	-101	192	2.46
18	9	437.7	-241	516	2.86
18	9	437.7	-241	516	1.6
22	18	271	-127	234	1.96
23	18	283.1	-131	240	1.91
12	8	331.1	-197	466	2.5

Length	Angle	Lo	Dpar	Lc
13.2	53	15.88	1.89	14.13
12.96	50	15.88	1.89	13.9
11.79	57	15.86	1.8	13.17
10.14	74	15.86	1.8	12.27
9.82	29	15.8	1.59	10.8
11.61	63	15.81	1.63	13.14
10.3	82	15.81	1.63	12.45

13.9	37	15.84	1.73	14.4
13.58	64	15.84	1.73	14.56
14	62	16.05	2.55	14.84
13.32	74	16.05	2.55	14.47
11.96	37	15.83	1.69	12.81
12.98	56	15.83	1.69	14.02
10.88	19	15.83	1.69	11.3
13.26	29	15.87	1.86	13.69
12.19	66	15.83	1.72	13.6
11.46	65	15.83	1.72	13.07
12.44	89	15.83	1.72	13.92
13.51	51	15.83	1.72	14.33
13.07	43	15.83	1.72	13.84
12.66	72	15.89	1.94	13.99
13.21	49	15.89	1.94	14.07
11.35	58	15.86	1.82	12.87
13.41	34	15.86	1.82	13.93
13.46	56	15.86	1.82	14.37
14.9	54	15.84	1.74	15.42
11.34	81	15.84	1.74	13.15
13.35	77	15.93	2.1	14.51
14.25	71	15.93	2.1	15.09
12.34	36	15.84	1.73	13.09
14.02	80	15.84	1.73	14.98
11.78	88	15.86	1.81	13.47
12.07	71	15.84	1.75	13.57
12.75	29	15.84	1.75	13.25
12.29	69	15.84	1.75	13.7
13.45	75	15.92	2.06	14.56
13.08	52	15.82	1.66	14.03
8.44	67	15.89	1.92	11.46
14.7	71	15.96	2.21	15.41
10.98	22	15.92	2.05	11.49
13.24	29	15.84	1.74	13.67
12.08	78	15.84	1.74	13.64
12.53	52	15.84	1.74	13.61
10.21	60	15.84	1.74	12.1
13.09	46	15.84	1.74	13.92
12.83	80	15.81	1.63	14.17
11.24	76	15.81	1.63	13.05
14.26	73	15.81	1.63	15.11
13.73	61	15.81	1.63	14.63
13.19	70	15.79	1.56	14.34
11.96	56	15.82	1.66	13.27
9.27	44	15.82	1.66	10.98
10.89	26	15.9	1.98	11.56
12.26	62	15.9	1.98	13.59
14.11	58	15.9	1.98	14.88
14.64	49	15.98	2.28	15.17
13.08	20	15.98	2.28	13.33
13.87	60	15.95	2.18	14.72
12.9	89	15.95	2.18	14.24

12.81	78	15.95	2.18	14.14
14.19	52	15.95	2.18	14.86
11.6	31	15.95	2.18	12.33
13.92	64	15.95	2.18	14.8
12.74	51	15.95	2.18	13.75
14.1	47	15.88	1.89	14.73
13.33	7	15.88	1.89	13.36
15.38	71	15.9	1.99	15.89
10.99	78	15.9	1.99	12.89
12.29	37	15.9	1.99	13.08
10.54	73	15.9	1.99	12.54
10.51	68	15.9	1.99	12.45
13.99	80	15.9	1.99	14.96
11.53	53	15.9	1.99	12.89
10.76	46	15.9	1.99	12.14
10.95	78	15.9	1.99	12.86
13.96	54	15.9	1.99	14.72
10.02	67	15.79	1.56	12.09
13.43	66	15.79	1.56	14.47
13.64	28	15.79	1.56	14
11.16	11	15.79	1.56	11.31
13.65	51	15.79	1.56	14.44
10.89	78	15.79	1.56	12.82
12.44	54	15.8	1.6	13.59
12.57	51	15.8	1.6	13.62
14.11	36	15.88	1.89	14.56
14.27	18	15.88	1.89	14.41
12.72	65	15.88	1.89	13.96
12.29	60	15.88	1.89	13.58
11.84	72	15.88	1.89	13.42
11.54	73	15.88	1.89	13.23
11.48	27	15.88	1.89	12.1
10.41	62	15.88	1.89	12.28
14.54	61	15.93	2.07	15.22
14.3	79	16.04	2.5	15.17
15.75	60	16.04	2.5	16.1
15.57	75	16.04	2.5	16.03
10.93	69	15.91	2.02	12.76
15.09	76	15.96	2.2	15.7

Table S4 (continued): Single grain data of Apatite Fission Track analysis

C-XI-120 (Ellesmere Island, Canadian High Arctic)

Location
Vendom Fiord
Lithology
Sandstone
Stratigraphic
Lower-Middle Devon.
Formation
Strathcona Fiord Fm
Lat N
77°32.931´
Long W
83°39.763´
Elevation
126

Cf-irrad.
no
Zeta
346
error_Zeta
12
RhoD
1.294E+6
Nd
6721
Length reduction in standard
0.893

Ns	Ni	Age	-95%	95%	Dpar
7	3	501.6	-372	1299	1.72
13	6	467	-289	720	1.7
26	12	467	-231	443	1.62
8	4	432.3	-302	936	1.66
20	10	432.3	-230	474	1.66
26	13	432.3	-210	397	1.84
7	4	379.8	-269	865	1.78
12	8	326.9	-194	461	1.73
16	10	348.1	-191	409	1.64
11	5	473.9	-309	834	2
15	11	297.8	-162	345	1.8
21	17	270.4	-129	241	1.74
13	7	402.3	-242	582	1.55
11	5	473.9	-309	834	1.98
28	13	464.3	-224	418	1.93
7	4	379.8	-269	865	1.76
25	17	320.6	-148	270	1.69

Length	Angle	Lo	Dpar	Lc
10.4	73	15.86	1.81	12.44
11.33	50	15.86	1.81	12.68
13.04	57	15.86	1.81	14.08
11.5	23	15.86	1.81	11.98
13.07	62	15.86	1.81	14.17
15.82	53	15.86	1.81	16.11
11.84	80	15.86	1.81	13.49
12.68	57	15.83	1.72	13.81
12.44	70	15.85	1.79	13.82
12.23	57	15.85	1.79	13.49
12.19	46	15.85	1.79	13.23
13.85	54	15.83	1.72	14.63

12.2	72	15.81	1.62	13.67
12.34	61	15.81	1.62	13.63
11.82	47	15.81	1.62	12.97
12.3	30	15.81	1.62	12.89
12.66	74	15.81	1.62	14.01
11.23	83	15.81	1.62	13.09
14.26	18	15.81	1.62	14.4
13.09	45	15.81	1.62	13.9
13.65	50	15.81	1.62	14.42
11.91	37	15.81	1.62	12.77
12.07	33	15.81	1.62	12.78
15.69	40	15.79	1.56	15.92
13.1	44	15.79	1.56	13.89
13.56	55	15.79	1.56	14.43
12.25	48	15.79	1.56	13.32
14.3	69	15.79	1.56	15.12
15.34	72	15.79	1.56	15.86
14.41	21	15.79	1.56	14.58
9.93	38	15.83	1.72	11.25
13.25	41	15.83	1.72	13.95
12.27	43	15.83	1.72	13.22
11.95	65	15.83	1.72	13.41
12.38	54	15.83	1.72	13.54
9.23	73	15.83	1.72	11.75
13.95	76	15.83	1.72	14.91
12.96	15	15.83	1.72	13.11
12.41	87	15.87	1.84	13.9
13.06	72	15.87	1.84	14.27
12.96	63	15.87	1.84	14.1
12.48	76	15.87	1.84	13.9
13.5	7	15.87	1.84	13.53
11.44	41	15.87	1.84	12.51
13.59	43	15.85	1.78	14.26
13.37	57	15.84	1.73	14.32
13.12	45	15.81	1.64	13.92
12.65	62	15.91	2	13.87
11.99	43	15.91	2	13
10.99	82	15.91	2	12.92
13.15	35	15.91	2	13.73
12.7	83	15.91	2	14.09
10.27	77	15.86	1.8	12.39
13.94	22	15.86	1.8	14.16
12.86	38	15.79	1.55	13.56
13.2	68	15.79	1.55	14.33
12.62	31	15.9	1.98	13.19
13.75	23	15.89	1.93	14
12.85	86	16	2.37	14.2
11.79	57	16	2.37	13.17
11.61	40	16	2.37	12.62
10.02	57	15.86	1.82	11.9
10.47	75	15.86	1.82	12.51
9.97	38	15.86	1.82	11.28

Table S4 (continued): Single grain data of Apatite Fission Track analysis

C-XI-121 (Ellesmere Island, Canadian High Arctic)

Location	**Cf-irrad.**
Makinson Inlet	no
Lithology	**Zeta**
Granite	346
Stratigraphic	**error_Zeta**
Paleoproterozoic	12
Formation	**RhoD**
Rae Craton	1.286E+6
Lat N	**Nd**
77°12.770´	6721
Long W	**Length reduction in standard**
80°59.900´	0.893
Elevation	
678	

Ns	Ni	Age	-95%	95%	Dpar
4	3	289.6	-226	950	1.73
16	10	346	-190	407	1.85
8	6	289.6	-190	530	1.84
12	8	324.9	-193	458	1.56
7	5	303.7	-208	631	1.67
8	5	346	-234	682	1.44
19	15	275.4	-136	265	1.68
18	10	388	-209	440	1.93
28	13	461.6	-222	416	1.66
11	8	298.4	-179	434	1.82
24	14	370	-179	339	1.84
13	8	351.3	-206	482	1.73
15	9	360	-203	450	1.65
12	14	187.7	-102	219	1.89
24	19	274.7	-125	226	1.74
27	18	324.9	-147	263	1.61
6	4	324.9	-234	788	1.75
12	8	324.9	-193	458	1.77
11	10	239.9	-139	322	1.78
11	7	340	-209	521	1.63
9	6	324.9	-210	569	1.71
7	4	377.5	-268	860	1.71
8	5	346	-234	682	1.53

Length	Angle	Lo	Dpar	Lc
10.78	60	15.91	2	12.5
11.98	58	15.82	1.68	13.32
12.28	47	15.82	1.68	13.32
13.8	79	15.82	1.68	14.83
14.33	75	15.82	1.68	15.17

11.85	16	15.82	1.68	12.09
11.45	15	15.89	1.95	11.69
10.87	43	15.89	1.95	12.14
13.68	35	15.89	1.95	14.18
13.05	81	15.88	1.9	14.32
10.76	65	15.88	1.9	12.58
13.4	40	15.86	1.81	14.05
12.4	42	15.82	1.67	13.29
14.85	32	15.82	1.67	15.13
14.01	38	15.79	1.53	14.51
10.42	33	15.82	1.65	11.44
14.91	48	15.82	1.65	15.37
13.06	18	15.81	1.61	13.27
12.1	79	15.81	1.61	13.66
13.09	47	15.83	1.69	13.94
9.69	40	15.83	1.69	11.14
11.13	75	15.83	1.69	12.96
13.89	35	15.83	1.69	14.35
12.84	47	15.83	1.69	13.75
14.61	65	15.83	1.69	15.31
9.17	38	15.83	1.69	10.68
11.67	64	15.85	1.77	13.2
12.77	81	15.85	1.77	14.13
14.71	62	15.83	1.71	15.35
15.05	45	15.83	1.71	15.45
13.19	57	15.83	1.71	14.19

Table S4 (continued): Single grain data of Apatite Fission Track analysis

C-XI-123 (Ellesmere Island, Canadian High Arctic)

Location
Makinson Inlet
Lithology
Granite
Stratigraphic
Paleoproterozoic
Formation
Rae Craton
Lat N
77°15.809´
Long W
81°03.660´
Elevation
658

Cf-irrad.
no
Zeta
346
error_Zeta
12
RhoD
1.277E+6
Nd
6721
Length reduction in standard
0.893

Ns	Ni	Age	-95%	95%	Dpar
12	8	322.7	-192	455	1.57
7	8	190.2	-122	333	1.76
15	11	294	-160	341	1.73
24	15	343.6	-164	307	1.55
25	15	357.6	-170	315	1.66
29	22	284.4	-122	210	1.62
19	14	292.6	-147	288	1.64
12	9	287.6	-167	388	1.58
20	9	472.5	-257	541	1.38
31	23	290.7	-122	208	1.6
19	14	292.6	-147	288	1.57
9	5	385.3	-257	727	1.62
42	47	194.2	-67.3	102	1.74

Length	Angle	Lo	Dpar	Lc
11.01	27	15.8	1.57	11.7
11.08	50	15.74	1.37	12.49
12.79	59	15.74	1.37	13.93
12.16	76	15.74	1.37	13.68
11.6	62	15.81	1.62	13.12
12.98	43	15.79	1.55	13.77
12.31	35	15.79	1.55	13.04
11.73	46	15.79	1.55	12.88
11.29	33	15.79	1.55	12.14
12.87	48	15.79	1.55	13.79
10.04	43	15.81	1.62	11.51
11.2	89	15.81	1.62	13.08
10	49	15.81	1.64	11.67
13.38	66	15.81	1.64	14.44
12.48	28	15.81	1.64	12.99
12.27	72	15.81	1.61	13.72

15.4	62	15.81	1.64	15.86
15.62	45	15.81	1.64	15.9
9.41	69	15.81	1.64	11.7
14.19	5	15.81	1.64	14.2
8.84	36	15.81	1.64	10.38
13.83	42	15.81	1.64	14.43
13.07	87	15.8	1.58	14.35
12.57	84	15.8	1.58	14
14.75	74	15.82	1.66	15.46
14.51	51	15.82	1.66	15.1
11.7	79	15.82	1.66	13.39
12.91	74	15.79	1.56	14.18
12.36	45	15.79	1.56	13.33
12.2	63	15.79	1.56	13.56
10.05	57	15.79	1.56	11.92
12.81	58	15.79	1.56	13.93
11.31	25	15.8	1.6	11.89
11.17	24	15.8	1.6	11.73
10.04	37	15.81	1.62	11.3
10.15	44	15.84	1.74	11.63
13.93	8	15.84	1.74	13.96
12.53	54	15.84	1.74	13.65
12.72	65	15.84	1.74	13.96
14.05	48	15.84	1.74	14.7

Table S4 (continued): Single grain data of Apatite Fission Track analysis

C-XI-124 (Ellesmere Island, Canadian High Arctic)

Location	**Cf-irrad.**
Vendom Fiord	no
Lithology	**Zeta**
Sandstone	326
Stratigraphic	**error_Zeta**
Lower-Middle Devon.	9
Formation	**RhoD**
Strathcona Fiord Fm	1.548E+6
Lat N	**Nd**
77°19.697´	7561
Long W	**Length reduction in standard**
82°28.540´	0.893
Elevation	
184	

Ns	Ni	Age	-95%	95%	Dpar
36	37	240.5	-89.5	141	2.01
13	11	291	-161	353	2.09
15	17	218.5	-110	219	2.03
3	2	367.1	-307	1635	1.91
15	18	206.5	-103	204	2.21
46	38	297.9	-105	160	2.16
28	33	210.2	-84.1	139	2.1
41	43	235.8	-83.1	127	2.35
7	9	193	-122	324	2.26
51	55	229.4	-73.8	108	2.02
28	29	238.7	-97.6	163	1.9
16	14	281.6	-145	292	2.1
1	1	247.1	-232	3026	1.65
14	12	287.3	-155	329	2.04
38	51	185	-64.4	98.1	1.99
2	3	165.8	-139	801	1.93
12	10	295.4	-169	381	2.2
4	5	198.4	-146	531	1.84

Length	Angle	Lo	Dpar	Lc
13.45	31	15.93	2.1	13.9
13.8	66	15.93	2.1	14.74
13.14	29	15.93	2.1	13.59
14.03	77	15.91	2	14.97
12.75	53	16.01	2.4	13.8
13.99	69	16.01	2.4	14.9
15.63	75	16.01	2.4	16.07
13.87	59	16.01	2.4	14.71
13.42	69	16.01	2.4	14.5
12.86	32	16.01	2.4	13.42
13.91	60	16.01	2.4	14.75
12.68	40	16.01	2.4	13.47

10.1	79	15.86	1.81	12.29
13.57	28	15.86	1.81	13.94
12.88	19	15.85	1.76	13.12
14.27	57	15.85	1.76	14.98
13.27	32	15.87	1.84	13.77
13.95	64	15.87	1.84	14.82
13.26	32	15.87	1.84	13.76
12.62	23	15.86	1.81	12.98
13.16	37	15.86	1.81	13.79
14.16	58	15.86	1.81	14.91
14.68	75	15.86	1.81	15.42
13.35	41	15.79	1.55	14.03
12.61	51	15.79	1.55	13.65
13.39	42	15.79	1.55	14.08
13.47	65	15.79	1.55	14.49
12.68	71	15.83	1.7	14
13.2	69	15.83	1.7	14.34
13.82	63	15.83	1.7	14.72
13.42	51	15.83	1.7	14.27
12.78	76	15.86	1.82	14.11
12.33	73	15.86	1.82	13.77
13.69	50	15.86	1.82	14.45
10.05	62	15.86	1.83	12.02
13.32	87	15.86	1.83	14.52
12.46	74	15.86	1.83	13.87
15.51	43	15.91	2	15.8
12.68	38	15.91	2	13.42
14.86	48	15.91	2	15.33
13.15	65	15.91	2	14.26
13.37	31	15.91	2	13.83
15.1	70	15.91	2	15.68
13.46	32	15.91	2	13.93
12.93	49	15.91	2	13.86
12.33	40	15.87	1.85	13.19
12.69	67	15.87	1.85	13.96
13.87	60	15.87	1.85	14.72
15.03	35	15.87	1.85	15.32
11.47	61	15.82	1.68	13.01
13.71	80	15.82	1.68	14.77
12.9	77	15.83	1.71	14.2
11.8	26	15.83	1.71	12.34
13.54	57	15.83	1.71	14.45
11.33	44	15.83	1.71	12.52
9.88	32	15.83	1.71	10.98
13.68	70	15.83	1.71	14.69
12.33	69	15.83	1.71	13.73
13.22	87	15.83	1.71	14.45
14.22	72	15.83	1.71	15.08
12.57	85	15.84	1.73	14.01
12.57	49	15.84	1.73	13.58
12.79	62	15.84	1.73	13.97
10.21	30	15.84	1.73	11.16

13.14	77	15.81	1.62	14.36
12.5	64	15.81	1.62	13.79
14.05	68	15.81	1.62	14.93
12.01	45	15.81	1.62	13.06
12.75	40	15.81	1.62	13.52
12.93	51	15.81	1.62	13.89
12.62	69	15.81	1.62	13.94
10.48	42	15.85	1.79	11.81
13.27	69	15.85	1.79	14.39
10.31	88	15.85	1.79	12.47
12.81	57	15.85	1.79	13.91
13.55	21	15.85	1.79	13.78
13.98	42	15.83	1.71	14.55
14.07	57	15.83	1.71	14.84
11.74	75	15.83	1.71	13.38
11.4	51	15.83	1.71	12.75
12.14	19	15.83	1.71	12.44
14.17	38	15.83	1.71	14.64
12.67	69	15.83	1.71	13.97
12.55	85	15.82	1.66	13.99
12.99	78	15.82	1.66	14.26
10.81	15	15.82	1.66	11.09
11.93	89	15.82	1.66	13.58

Table S4 (continued): Single grain data of Apatite Fission Track analysis

C-XI-125 (Ellesmere Island, Canadian High Arctic)

Location	**Cf-irrad.**
Vendom Fiord	no
Lithology	**Zeta**
Sandstone	326
Stratigraphic	**error_Zeta**
Middle Devonian	9
Formation	**RhoD**
Hecla Bay Fm	1.550E+6
Lat N	**Nd**
77°22.330´	7561
Long W	**Length reduction in standard**
82°43.569´	0.893
Elevation	
254	

Ns	Ni	Age	-95%	95%	Dpar
17	21	201	-95.9	181	2.4
19	21	224.2	-105	193	1.74
41	46	220.9	-76.9	117	1.75
3	3	247.4	-198	931	2.01
1	1	247.4	-232	3029	1.98
104	116	222.2	-53.1	69.4	1.98
12	19	157.3	-81.8	168	2.12
9	12	186.4	-109	256	2.53
28	35	198.7	-78.7	129	2.03
24	44	136.1	-54.1	89.3	1.89
3	4	186.4	-146	632	1.61
7	10	174.2	-109	283	1.86
52	59	218.5	-69.1	100	1.96
35	47	185.1	-66.6	103	1.77
97	94	255.1	-64.4	85.6	2.09
31	42	183.5	-69.1	110	2.08
13	12	267.6	-146	315	1.82
6	5	295.7	-206	649	2.11
25	26	238	-101	175	1.94
18	20	223.1	-106	199	1.87

Length	Angle	Lo	Dpar	Lc
12.33	86	15.98	2.28	13.85
12.75	70	15.98	2.28	14.04
11.52	49	15.98	2.28	12.79
14.26	81	15.98	2.28	15.15
12.48	28	15.77	1.46	12.99
12.76	53	15.77	1.46	13.8
12.77	48	15.88	1.9	13.72
13.84	10	15.85	1.77	13.89
12.93	51	15.85	1.77	13.89

11.65	49	15.85	1.77	12.89
13.81	53	15.86	1.83	14.59
15.23	73	15.86	1.83	15.79
12.77	58	15.86	1.83	13.9
11.21	41	15.86	1.83	12.34
12.13	54	15.86	1.83	13.36
13.5	70	15.86	1.83	14.56
12.43	87	15.86	1.83	13.92
12.56	65	15.86	1.83	13.85
11.36	77	15.86	1.83	13.14
12.66	18	15.8	1.6	12.89
10.61	62	15.8	1.6	12.42
14.15	72	15.8	1.6	15.03
12.79	81	15.8	1.6	14.14
13.47	58	15.87	1.86	14.41
14.58	53	15.87	1.86	15.17
14.77	56	15.87	1.86	15.35
14.39	80	15.87	1.86	15.23
13.54	18	15.87	1.86	13.72
13.96	47	15.87	1.86	14.62
13.54	18	15.89	1.95	13.72
13.96	47	15.89	1.95	14.62
11.89	45	15.89	1.95	12.97
12.4	76	15.89	1.95	13.85
14.64	43	15.89	1.95	15.1
12.18	34	15.89	1.95	12.9
12.34	28	15.89	1.95	12.87
13	24	15.89	1.95	13.35
12.01	81	15.89	1.95	13.61
13.61	41	15.88	1.91	14.24
14.01	84	15.88	1.91	14.99
13.02	76	15.88	1.91	14.27
12.3	81	15.88	1.91	13.81
11.21	27	15.88	1.91	11.87
12.45	46	15.88	1.91	13.43
12.83	33	15.88	1.91	13.42
12.03	67	15.88	1.9	13.5
12.76	29	15.88	1.9	13.26
13.17	50	15.88	1.9	14.06
12.89	90	15.88	1.9	14.23
13.82	56	15.88	1.9	14.64
13.62	50	15.88	1.9	14.4
14.03	24	15.88	1.9	14.28
11.65	73	15.88	1.9	13.3
10.26	15	15.88	1.9	10.59
12.5	69	15.88	1.9	13.85
13.94	66	15.99	2.31	14.84
13.37	70	15.99	2.31	14.47
13.34	47	15.99	2.31	14.13
12.97	66	15.89	1.95	14.15
14.6	65	15.89	1.95	15.3
13.56	51	15.89	1.95	14.37

13.1	45	15.89	1.95	13.91
13.89	47	15.89	1.95	14.56
14.2	77	15.89	1.95	15.09
12.75	50	15.89	1.95	13.74
13.41	18	15.89	1.95	13.6
13.77	87	15.89	1.95	14.83
14.69	73	15.89	1.95	15.41
12.59	55	15.89	1.95	13.71
15.63	50	15.89	1.95	15.95

Table S4 (continued): Single grain data of Apatite Fission Track analysis

C-XI-126 (Ellesmere Island, Canadian High Arctic)

Location	**Cf-irrad.**
Vendom Fiord	no
Lithology	**Zeta**
Sandstone	326
Stratigraphy	**error_Zeta**
Late Devonian	9
Formation	**RhoD**
Fram Formation	1.552E+6
Lat N	**Nd**
77°22.602´	7561
Long W	**Length reduction in standard**
83°11.272´	0.893
Elevation	
134	

Ns	Ni	Age	-95%	95%	Dpar
28	27	256.7	-106	179	2.15
46	51	223.8	-74.6	111	1.85
2	3	166.2	-139	803	1.65
1	1	247.7	-233	3032	1.65
2	1	486.2	-443	3679	1.69
15	12	308.2	-165	344	1.81
4	3	328.2	-256	1063	1.71
57	41	341.8	-114	169	1.94
7	6	288.1	-192	553	1.81
12	13	229	-125	271	1.86
2	2	247.7	-214	1392	1.87
22	20	271.9	-124	225	1.87
4	5	198.9	-146	532	1.62
17	20	211.1	-101	192	2.02
9	10	223.3	-134	324	1.99
33	29	281.1	-111	182	1.72
49	45	269.3	-90.7	135	1.54
6	9	166.2	-108	300	1.81
21	18	288.1	-135	251	1.99
30	27	274.6	-112	187	1.87

Length	Angle	Lo	Dpar	Lc
14.64	71	15.79	1.56	15.37
14.01	56	15.79	1.56	14.78
13.54	42	15.79	1.56	14.2
10.81	27	15.79	1.56	11.53
9	49	15.79	1.56	11
14.47	69	15.83	1.72	15.23
13.04	75	15.87	1.85	14.28
10.49	81	15.87	1.85	12.57

12.06	29	15.87	1.85	12.66
12.75	12	15.87	1.85	12.86
12.14	81	15.87	1.85	13.7
15.01	5	15.87	1.85	15.02
12.71	10	15.87	1.85	12.79
11.21	63	15.87	1.85	12.86
12.31	77	15.87	1.85	13.79

Table S4 (continued): Single grain data of Apatite Fission Track analysis

C-XII-06 (Ellesmere Island, Canadian High Arctic)

Location
Strathcona Fiord
Lithology
Sandstone
Stratigraphy
Early Triassic
Formation
Bjorne Fm
Lat N
78°44.185'
Long W
83°21.936'
Elevation
233

Cf-irrad.
no
Zeta
346
error_Zeta
12
RhoD
1.243E+6
Nd
3096
Length reduction in standard
0.893

Ns	Ni	Age	-95%	95%	Dpar
24	32	159.1	-66.4	113	1.96
6	8	159.1	-105	300	2.35
5	3	348.3	-266	1037	2.19
4	6	141.6	-102	360	2.21
6	3	415.8	-312	1148	2.06
6	3	415.8	-312	1148	2.11
7	4	365.2	-259	835	2.01
19	13	306.4	-156	310	1.77
27	31	184.4	-75.4	126	1.79
29	26	235.2	-97.8	165	2.03

Length	Angle	Lo	Dpar	Lc
13.13	73	15.9	1.96	14.33
10.16	70	15.9	1.96	12.24
10.8	51	15.9	1.96	12.31
12.49	46	15.9	1.96	13.46
13.23	66	15.86	1.8	14.33
12.49	32	15.86	1.8	13.11
15.22	73	15.92	2.04	15.78
10.98	5	15.92	2.04	11.01
12.95	33	15.92	2.04	13.52

Table S4 (continued): Single grain data of Apatite Fission Track analysis

C-XII-13 (Ellesmere Island, Canadian High Arctic)

Location	**Cf-irrad.**
Glacier Strathcona Fiord	no
Lithology	**Zeta**
Granite	346
Stratigraphy	**error_Zeta**
Paleoproterozoic	12
Formation	**RhoD**
Rae Craton	1.226E+6
Lat N	**Nd**
78°46.675'	6106
Long W	**Length reduction in standard**
81°02.169'	0.893
Elevation	
683	

Ns	Ni	Age	-95%	95%	Dpar
37	44	175.7	-63.3	98.3	2.19
22	31	148.6	-63.5	110	1.59
26	37	147.1	-59	97.7	2.03
26	40	136.2	-54	88.8	2.65
7	14	105	-63.3	158	1.97
33	56	123.6	-44.1	68.2	2.26
16	24	139.7	-66.3	125	2.28
36	44	171	-62	96.6	2.2
17	25	142.4	-66.4	123	2.09
17	22	161.6	-76.7	144	2.1
20	27	155	-69	123	2.24
24	35	143.6	-59.1	99.7	2.5
15	23	136.7	-66.2	127	2.32
19	32	124.5	-54.8	97	2.29
24	32	156.9	-65.5	111	1.9
83	79	218.8	-59.6	81.4	2.23
39	45	181	-64.3	98.9	1.97
32	53	126.6	-45.9	71.6	2.1
23	21	227.9	-103	185	2.24
26	25	216.6	-92.6	160	2.36

Length	Angle	Lo	Dpar	Lc
14.41	29	15.96	2.19	14.7
13.59	42	15.96	2.19	14.24
14.07	13	15.96	2.19	14.15
12.5	62	15.93	2.08	14
15.54	70	15.93	2.08	15.99
13.24	44	15.93	2.08	14
13.49	18	15.93	2.08	13.67
12.06	59	15.95	2.18	13.4

15.96	18	15.95	2.18	16.01
13.54	88	15.95	2.18	14.67
13.15	39	16.03	2.48	13.82
14.13	16	16.03	2.48	14.25
12.55	85	16.03	2.48	13.99
12.41	78	16.03	2.48	13.87
12.77	43	15.8	1.59	13.61
12.2	71	15.8	1.59	13.66
10.08	14	15.8	1.59	10.39
15.61	73	15.91	2.03	16.05
13.82	68	15.91	2.03	14.77
13.71	68	15.91	2.03	14.69
11.82	38	15.91	2.03	12.73
14.19	81	16.02	2.43	15.1
12.98	53	16.02	2.43	13.97
13.24	50	15.9	1.97	14.11
13.93	29	15.9	1.97	14.28
15.47	62	15.97	2.26	15.91
13.91	28	15.97	2.26	14.24
16.03	6	15.97	2.26	16.04
15.47	3	15.97	2.26	15.47
13.2	86	15.91	2.03	14.44
13.41	42	16.05	2.54	14.09
12.73	57	16.05	2.54	13.85
12.34	71	16.05	2.54	13.76
12.04	55	16.05	2.54	13.31
14.41	51	16.05	2.54	15.02
13.56	71	15.93	2.09	14.61
13.76	41	15.93	2.09	14.36
13.97	71	15.97	2.24	14.9
13.45	61	15.97	2.24	14.43
12.97	82	15.97	2.24	14.27
12.2	82	15.93	2.1	13.74
12.36	72	15.93	2.1	13.78
11.28	10	16.07	2.62	11.4
14.17	54	16.07	2.62	14.87
13.3	89	16.07	2.62	14.51
14.25	87	15.97	2.24	15.15
10.25	55	15.97	2.24	12.01
12.53	69	15.97	2.24	13.87
11.96	55	16.04	2.5	13.25
12.06	50	16.04	2.5	13.22
12.9	70	15.99	2.32	14.14
13.09	37	15.99	2.32	13.73
12.58	67	15.97	2.23	13.89
13.31	62	15.97	2.23	14.34
13.64	58	15.97	2.23	14.53
12.57	60	15.97	2.23	13.78
12.67	75	15.97	2.23	14.02
13.77	55	15.98	2.29	14.59
13.52	61	16.04	2.52	14.48
11.93	75	16.04	2.52	13.51

17.85	52	16.04	2.52	17.68
13.01	57	15.88	1.9	14.06
10.75	50	15.88	1.9	12.25
13.41	48	15.88	1.9	14.21
13.16	88	15.88	1.9	14.41
13.11	51	15.88	1.9	14.03
11.25	46	15.97	2.23	12.51
13.57	37	15.98	2.28	14.12
13.19	47	15.98	2.28	14.02
9.63	87	15.98	2.28	12.08
14.12	46	16.01	2.39	14.73
14.35	38	16.01	2.39	14.79
11.48	55	16.01	2.39	12.9
12.44	59	15.9	1.97	13.67
14.29	50	15.93	2.1	14.91
12.78	89	15.93	2.1	14.16
12.36	47	15.93	2.09	13.38
14.72	24	15.93	2.09	14.91
12.01	69	15.93	2.09	13.51
12.5	62	15.93	2.09	13.76
12.97	52	15.93	2.09	13.94
10.68	64	15.93	2.09	12.5
15.91	51	15.93	2.09	16.17
14.19	49	15.85	1.76	14.82
14.02	59	15.85	1.76	14.82
12.47	75	15.85	1.76	13.89
15.9	72	15.98	2.27	16.25
14.34	49	15.98	2.27	14.94
14.38	69	15.98	2.27	15.17
11.25	35	16	2.36	12.18
9.84	79	16	2.36	12.11

Table S4 (continued): Single grain data of Apatite Fission Track analysis

C-XII-14 (Ellesmere Island, Canadian High Arctic)

Location	**Cf-irrad.**
Glacier Strathcona Fiord	no
Lithology	**Zeta**
Granite	346
Stratigraphy	**error_Zeta**
Paleoproterozoic	12
Formation	**RhoD**
Rae Craton	1.227E+6
Lat N	**Nd**
78°29.645'	3096
Long W	**Length reduction in standard**
81°17.212'	0.893
Elevation	
780	

Ns	Ni	Age	-95%	95%	Dpar
26	21	257.2	-114	200	1.66
24	39	129.1	-52.4	87.6	1.81
15	12	259.7	-139	293	1.76
70	62	235	-69.7	98.3	1.85
12	10	249.5	-143	325	1.86
14	15	194.9	-102	210	1.64
9	5	370.7	-247	702	2.02
6	5	249.5	-174	554	2.02
11	9	254	-150	355	1.87
22	12	377.3	-191	377	1.92
13	7	382.1	-230	555	1.96
26	20	269.8	-120	214	1.91
22	20	229	-105	192	1.87
20	16	259.7	-126	241	1.97
25	21	247.5	-110	195	1.93
4	3	276.6	-216	911	2.03
32	33	202.3	-79.1	129	1.93
36	32	234.2	-90	144	1.96
34	30	235.9	-92.7	151	1.8
10	8	259.7	-158	393	1.74
27	22	255	-111	193	1.75
4	4	208.6	-157	611	2.02
18	20	188	-89.6	169	1.86

Length	Angle	Lo	Dpar	Lc
10.61	25	15.82	1.66	11.29
9.56	74	15.82	1.66	11.87
12.38	63	15.86	1.81	13.69
14.35	47	15.85	1.76	14.92
12.32	22	15.85	1.76	12.68

12.33	51	15.85	1.76	13.44
12.22	90	15.87	1.85	13.77
11.66	59	15.87	1.86	13.11
11.99	57	15.87	1.86	13.31
10.67	89	15.87	1.86	12.72
12.62	50	15.81	1.64	13.64
11.01	83	15.89	1.95	12.94
15.05	35	15.89	1.95	15.34
13.49	61	15.95	2.17	14.46
11.04	47	15.95	2.17	12.38
12.65	65	15.88	1.91	13.91
12.47	56	15.89	1.93	13.64
12.76	68	15.89	1.93	14.02
11.41	82	15.89	1.93	13.2
12.38	47	15.84	1.73	13.4
12.53	15	15.84	1.75	12.71
13.02	54	15.84	1.75	14.02
13.61	85	15.84	1.75	14.71
12.04	55	15.84	1.75	13.31
12.58	74	15.89	1.93	13.95
14.95	35	15.91	2.03	15.25
13.72	21	15.91	2.03	13.94
10.5	63	16.03	2.48	12.36
11.65	74	16.03	2.48	13.31
15.88	56	16.03	2.48	16.18
14.19	78	16.03	2.48	15.09
12.12	61	16.03	2.48	13.47
12.87	56	15.79	1.55	13.94
12.4	42	15.88	1.89	13.29
12.22	78	15.88	1.89	13.74
16.59	51	15.89	1.92	16.7
13.49	21	15.89	1.92	13.73
11.57	42	15.89	1.92	12.64
14.65	70	15.89	1.92	15.37
12.53	41	15.89	1.92	13.37
9.75	48	15.98	2.29	11.46
12.34	57	15.98	2.29	13.57
12.5	46	15.98	2.29	13.47
15	15	15.98	2.29	15.07
12.86	82	15.98	2.29	14.19
12.68	51	15.89	1.93	13.71
11.71	54	15.9	1.99	13.05
11.29	69	15.9	1.99	13.01
14.45	19	15.9	1.99	14.59
11.41	35	15.9	1.99	12.31
12	28	15.9	1.99	12.58
12.67	14	15.9	1.99	12.82
11.63	20	15.9	1.99	12
13.27	85	15.84	1.75	14.48
13.24	73	15.84	1.75	14.4
15	46	15.91	2.03	15.42
13.62	64	15.91	2.03	14.59

12.96	48	15.91	2.03	13.86

Table S4 (continued): Single grain data of Apatite Fission Track analysis

C-XII-20 (Ellesmere Island, Canadian High Arctic)

Location	**Cf-irrad.**
Vendom Fiord	no
Lithology	**Zeta**
Sandstone	346
Stratigraphy	**error_Zeta**
Middle Devonian	12
Formation	**RhoD**
Hecla Bay Fm	1.293E+6
Lat N	**Nd**
77°42.028'	3219
Long W	**Length reduction in standard**
83°25.127'	0.893
Elevation	
347	

Ns	Ni	Age	-95%	95%	Dpar
19	8	509.8	-286	622	1.74
10	4	535.5	-367	1073	1.86
15	6	535.5	-327	790	1.76
19	7	579.4	-335	747	2.26
15	6	535.5	-327	790	1.89
85	35	520.8	-170	248	2.06
11	4	586.7	-399	1140	2.6

Length	Angle	Lo	Dpar	Lc
14.59	77	15.84	1.74	15.36
14.65	70	15.84	1.74	15.37
13.17	29	15.84	1.74	13.61
11.81	87	15.86	1.83	13.49
13.14	27	15.86	1.83	13.54
13.63	69	15.86	1.83	14.64
13.18	2	15.86	1.83	13.18
11.17	75	15.86	1.83	12.99
14.04	77	15.86	1.83	14.98
13.55	86	15.86	1.83	14.68
14.1	2	15.86	1.83	14.1
12.91	79	15.86	1.83	14.22
13.31	74	15.87	1.86	14.46
12.03	13	15.87	1.86	12.19
13.05	60	15.83	1.7	14.13
11.72	58	15.83	1.7	13.14
12.67	77	15.83	1.7	14.04
14.48	58	15.83	1.7	15.15
12.95	89	15.83	1.7	14.27
10.41	72	15.82	1.67	12.43
13.74	60	15.82	1.67	14.63

14.9	38	15.82	1.67	15.25
12.45	44	15.83	1.69	13.38
8.7	25	15.83	1.69	9.73
11.68	76	15.83	1.69	13.35
12.35	68	15.83	1.69	13.73
14.13	37	15.85	1.76	14.59
9.48	82	15.85	1.76	11.97
11.58	61	15.85	1.76	13.09
10.81	83	15.97	2.26	12.8
10.07	82	15.97	2.26	12.29
8.46	65	15.97	2.26	11.42
12.3	40	15.97	2.26	13.16
14.7	50	15.92	2.06	15.23
14.04	67	15.92	2.06	14.92
13.45	75	15.92	2.06	14.56
12.49	44	15.92	2.06	13.41
13.45	66	15.92	2.06	14.49
9.21	81	15.92	2.06	11.89

Table S4 (continued): Single grain data of Apatite Fission Track analysis

C-XII-22 (Ellesmere Island, Canadian High Arctic)

Location	**Cf-irrad.**
Vendom Fiord	no
Lithology	**Zeta**
Sandstone	346
Stratigraphy	**error_Zeta**
Late Devonian	12
Formation	**RhoD**
Fram Formation	1.293E+6
Lat N	**Nd**
77°31.953'	3219
Long W	**Length reduction in standard**
83°11.849'	0.893
Elevation	
285	

Ns	Ni	Age	-95%	95%	Dpar
23	17	295.3	-139	256	2.03
14	7	431.9	-258	610	1.86
35	8	909.9	-480	944	2.48
9	4	483.9	-335	1006	2.19
7	2	737.9	-583	2308	2.65
18	8	483.9	-273	599	1.84
8	3	569.7	-418	1406	2.16
19	7	579.4	-335	747	1.86
6	4	326.6	-235	792	1.91
41	27	330.6	-128	207	1.68
19	5	797.4	-495	1189	2.77
44	36	267.4	-96.6	150	2.17
10	3	704.6	-508	1609	1.8
14	8	379.5	-221	508	2.11
27	11	526.2	-265	511	2.11
17	9	408.7	-227	491	2.86
11	6	397	-251	647	1.81
42	30	305.4	-115	183	1.9
23	16	313.3	-149	277	1.83
19	10	411	-220	458	1.89
13	4	687.9	-461	1267	3.46
38	20	411	-173	291	1.82
10	4	535.5	-367	1073	3.09
43	33	284.7	-105	165	1.93

Length	Angle	Lo	Dpar	Lc
13.95	85	15.91	2.03	14.95
11.68	58	16.03	2.48	13.11
13.67	44	16.03	2.48	14.34
13.83	59	16.03	2.48	14.68

12.96	21	15.87	1.84	13.24
12.8	71	15.87	1.84	14.08
13.74	57	15.95	2.16	14.59
14.1	80	15.95	2.16	15.04
14.59	68	15.95	2.16	15.31
14.1	43	16.13	2.86	14.66
14.97	56	15.86	1.81	15.49
13.28	52	15.86	1.81	14.18
13.11	37	15.88	1.9	13.75
15.67	50	15.88	1.9	15.98
12.91	56	15.88	1.9	13.97
14.01	45	15.88	1.9	14.62
13.07	63	15.88	1.9	14.18
15.01	60	15.88	1.9	15.56
15.51	47	15.86	1.83	15.83
14.23	84	15.86	1.83	15.14
12.52	69	15.88	1.89	13.87
10.79	78	15.88	1.89	12.76
13.34	12	15.86	1.82	13.43
12.06	23	15.86	1.82	12.48
14.01	45	15.86	1.82	14.62
14.2	34	15.86	1.82	14.6
13.14	63	15.86	1.82	14.23
13.49	10	15.86	1.82	13.55
13.46	72	15.83	1.69	14.55
12.13	27	15.83	1.69	12.66
11.7	36	15.83	1.69	12.57
10.68	80	15.89	1.93	12.69
13.56	25	15.89	1.93	13.87

Table S4 (continued): Single grain data of Apatite Fission Track analysis

C-XII-25 (Ellesmere Island, Canadian High Arctic)

Location	**Cf-irrad.**
Glacier Vendom Fiord	no
Lithology	**Zeta**
Migmatite	346
Stratigraphic	**error_Zeta**
Paleoproterozoic	12
Formation	**RhoD**
Rae Craton	1.218E+6
Lat N	**Nd**
78°13.142'	3096
Long W	**Length reduction in standard**
81°29.978'	0.893
Elevation	
610	

Ns	Ni	Age	-95%	95%	Dpar
16	11	299	-161	341	2.03
11	6	374.6	-237	613	1.97
23	16	295.6	-140	262	1.73
16	9	363.6	-204	447	1.76
25	21	245.7	-109	194	2.06
10	6	341.5	-218	578	2.02
5	3	341.5	-261	1018	1.74
12	7	351	-214	524	1.85
31	24	266.2	-111	188	2.07
14	11	262.4	-144	313	2.16
7	4	358.1	-254	820	1.88
7	4	358.1	-254	820	2.05
11	6	374.6	-237	613	2.08
13	11	244	-136	299	1.98
27	21	265	-116	204	1.99
12	9	274.6	-160	372	1.72
13	10	267.9	-151	339	1.64
16	11	299	-161	341	1.96
21	15	288	-141	269	1.97
18	13	284.9	-146	294	2.18
11	8	283	-170	413	1.78
66	46	295	-94.2	137	1.92
9	6	308.1	-199	541	2.01
23	19	249.8	-115	209	2.03
13	8	333.2	-196	459	1.99
14	12	240.9	-131	279	2.08

Length	Angle	Lo	Dpar	Lc
11.87	31	15.91	2.03	12.56
10.86	26	15.9	1.97	11.54
10.66	34	15.84	1.73	11.67

9	5	15.92	2.06	9.066
13.51	87	15.9	1.99	14.65
9.3	17	15.9	1.99	9.822
13.81	67	15.9	1.99	14.75
10.46	80	15.93	2.07	12.54
11.51	58	15.93	2.07	12.98
10.64	8	15.93	2.07	10.73
12.44	41	15.87	1.84	13.3
14.08	59	15.95	2.16	14.87
12.81	16	15.95	2.16	12.99
11.4	61	15.95	2.16	12.96
10.51	53	15.88	1.89	12.15
14.97	54	15.9	1.98	15.48
12.05	68	15.9	1.99	13.52
11.37	83	15.9	1.99	13.18
10.52	18	15.9	1.99	10.94
10.98	32	15.9	1.99	11.86
11.94	10	15.87	1.86	12.04
11.58	63	15.83	1.72	13.12
10.62	78	15.81	1.64	12.64
12.26	62	15.85	1.79	13.59
11.46	75	15.85	1.79	13.19
12.95	79	15.85	1.79	14.24
14.6	59	15.86	1.8	15.25
12.86	45	15.9	1.96	13.72
11.38	39	15.9	1.96	12.41
11.72	74	15.9	1.96	13.36
11.47	76	15.89	1.95	13.21
14.61	83	15.89	1.95	15.39
12.17	54	15.94	2.12	13.39
10.1	62	15.94	2.12	12.06
10.51	59	15.94	2.12	12.29
11.11	74	15.94	2.12	12.94
14.37	69	15.86	1.81	15.16
9.81	37	15.86	1.81	11.12
11.09	7	15.86	1.81	11.15
14.16	56	15.96	2.2	14.89
15.81	60	15.96	2.2	16.14
10.98	38	15.88	1.9	12.06
12.21	82	15.88	1.9	13.75
10.42	50	15.88	1.9	12.01
14.13	19	15.88	1.9	14.29
13.33	66	15.9	1.96	14.4
12.99	59	15.9	1.96	14.07
11.54	58	15.9	1.96	13.01
13.29	57	15.9	1.96	14.26
11.9	86	15.9	1.96	13.55
10.11	44	15.9	1.98	11.6
12.14	29	15.87	1.85	12.73
11.46	67	15.87	1.86	13.1
13.19	54	15.81	1.63	14.14
12.45	19	15.89	1.92	12.72

12.34	76	15.89	1.92	13.8
13.34	74	15.89	1.92	14.48
14.89	79	15.91	2.03	15.57
10.35	82	15.91	2.03	12.48
10.75	46	15.91	2.03	12.14
12.81	50	15.91	2.03	13.79
10.55	79	15.91	2.03	12.6
12.52	79	15.83	1.69	13.95
10.95	60	15.93	2.1	12.62
10.8	66	15.81	1.64	12.62
11.95	77	15.83	1.71	13.54
12.52	45	15.89	1.92	13.46
12.38	88	15.89	1.93	13.88
13.99	21	15.85	1.77	14.19
11.43	87	15.85	1.77	13.23
12.13	39	15.85	1.77	13
12.91	72	15.85	1.77	14.17
15.14	85	15.85	1.77	15.76
13.57	32	15.85	1.77	14.02
12.65	42	15.85	1.77	13.49
14.98	65	15.85	1.77	15.57
11.76	43	15.85	1.77	12.82
10.68	61	15.86	1.83	12.45
10.62	34	15.86	1.83	11.64
11.41	30	15.86	1.83	12.14
13.92	68	15.86	1.83	14.84
11.72	31	15.86	1.83	12.43
10.17	44	15.85	1.78	11.64
13.64	78	15.83	1.69	14.71
12.36	30	15.87	1.85	12.94
12.25	79	15.87	1.85	13.76
13.26	22	15.87	1.85	13.54
13.51	75	15.96	2.21	14.61
10.18	78	15.96	2.21	12.34
14.07	78	15.96	2.21	15.01
13.34	44	15.96	2.21	14.08
9.39	39	15.96	2.21	10.88
12.8	48	15.96	2.21	13.74
8.4	14	15.96	2.21	8.901
11.91	49	15.82	1.67	13.08
12.73	52	15.82	1.67	13.76
13.73	51	15.87	1.87	14.5
13.42	79	15.94	2.14	14.57
12.3	67	15.81	1.62	13.69

Table S4 (continued): Single grain data of Apatite Fission Track analysis

C-XII-27 (Ellesmere Island, Canadian High Arctic)

Location	Cf-irrad.
Vendom Fiord	no
Lithology	**Zeta**
Sandstone	346
Stratigraphy	**error_Zeta**
Lower-Middle Devon.	12
Formation	**RhoD**
Strathcona Fiord Fm	1.293E+6
Lat N	**Nd**
78°06.096'	3219
Long W	**Length reduction in standard**
82°01.213'	0.893
Elevation	
140	

Ns	Ni	Age	-95%	95%	Dpar
33	38	191.1	-72.4	116	1.72
17	7	520.8	-304	693	1.79
12	7	372	-226	553	1.76
17	8	458	-260	577	2.31
34	16	458	-205	362	1.72
31	20	337.2	-146	252	1.83
27	17	345.3	-158	285	2.21
19	9	455.1	-249	529	1.76
6	4	326.6	-235	792	1.89
13	7	402	-242	582	1.99
8	8	219.6	-138	362	2.1
9	3	637.5	-464	1509	2.17
7	4	379.5	-269	865	1.98
23	14	356.9	-174	331	2.04
11	6	397	-251	647	2.05
34	23	322	-133	224	1.95
10	3	704.6	-508	1609	1.78
54	42	281	-94.7	141	1.87
19	13	318.5	-162	322	2.12
27	23	257	-111	192	2.08
17	7	520.8	-304	693	2.07
48	36	291.1	-104	159	1.68

Length	Angle	Lo	Dpar	Lc
14.21	54	15.83	1.72	14.9
10.92	39	15.83	1.72	12.05
10.47	15	15.83	1.72	10.78
14	30	15.83	1.72	14.36
11.34	38	15.83	1.72	12.35
14.35	53	15.83	1.72	15

11.99	55	15.83	1.72	13.27
12.32	79	15.83	1.72	13.81
11.61	73	15.88	1.9	13.27
13.25	60	15.88	1.9	14.27
7.84	13	15.85	1.76	8.38
14.43	27	15.85	1.76	14.68
13.25	78	15.99	2.31	14.44
14.78	79	15.99	2.31	15.5
9.88	21	15.86	1.83	10.5
13.16	40	15.86	1.83	13.85
13.36	75	15.86	1.83	14.5
14.31	82	15.86	1.83	15.19
13.64	77	15.86	1.83	14.71
10.29	34	15.9	1.98	11.38
12.69	67	15.9	1.98	13.96
12.72	74	15.9	1.98	14.05
13.46	81	15.9	1.98	14.6
12.23	54	15.9	1.98	13.43
9.9	39	15.9	1.98	11.26
11.33	52	15.9	1.98	12.72
12.81	45	15.96	2.21	13.68
14.21	39	15.96	2.21	14.69
10.5	29	15.96	2.21	11.35
9.96	90	15.96	2.21	12.24
14.75	33	15.9	1.99	15.05
13.45	71	15.92	2.05	14.53
11.05	31	15.92	2.05	11.88
13.56	34	15.87	1.87	14.06
15.33	46	15.87	1.87	15.68
12.61	56	15.87	1.87	13.75
12.24	56	15.87	1.87	13.48
13.71	57	15.87	1.87	14.57
14.31	58	15.87	1.87	15.02
12.36	56	15.87	1.87	13.56
12.49	56	15.87	1.87	13.66
13.94	34	15.87	1.87	14.38
12.66	48	15.87	1.87	13.63
13.34	76	15.94	2.12	14.49
11.26	83	15.94	2.12	13.11
12.77	58	15.94	2.12	13.9
12.29	37	15.89	1.92	13.08
12.54	80	15.89	1.92	13.97
12.01	20	15.89	1.92	12.35
11.89	42	15.89	1.92	12.89
15.11	78	15.89	1.95	15.72
11.06	81	15.89	1.95	12.96
12.67	29	15.89	1.95	13.18
15.35	73	15.88	1.91	15.87
12.97	26	15.88	1.91	13.37
12.4	17	15.88	1.91	12.63
14.56	53	15.93	2.07	15.16
14.06	44	15.93	2.07	14.65

12.41	47	15.93	2.07	13.42
10.8	68	15.93	2.07	12.65
12.65	71	15.96	2.2	13.98
12.69	51	15.96	2.2	13.71
12.54	44	15.96	2.2	13.45
14.04	78	15.86	1.81	14.99
12.67	81	15.86	1.81	14.06
12.95	34	15.86	1.81	13.54
13.96	83	15.82	1.68	14.95
14.67	65	15.82	1.68	15.35
12.05	72	15.81	1.64	13.57
13.56	14	15.81	1.64	13.67
13.14	40	15.81	1.64	13.84
11.86	45	15.81	1.64	12.95
12.69	78	15.81	1.64	14.06
12.41	87	15.81	1.64	13.9
12.4	54	15.81	1.64	13.56

Table S4 (continued): Single grain data of Apatite Fission Track analysis

C-XII-30 (Ellesmere Island, Canadian High Arctic)

Location	**Cf-irrad.**
Strathcona Fiord	no
Lithology	**Zeta**
Sandstone	346
Stratigraphy	**error_Zeta**
Late Paleocene	12
Formation	**RhoD**
Mount Lawson Fm	1.21E+6
Lat N	**Nd**
78°48.870'	3096
Long W	**Length reduction in standard**
82°01.778'	0.893
Elevation	
272	

Ns	Ni	Age	-95%	95%	Dpar
12	4	600.3	-406	1143	2.27
5	2	504.1	-407	1821	3.17
17	6	568.4	-343	813	1.74
44	27	333	-128	205	1.7
9	4	455.4	-315	952	1.8
25	15	340.4	-162	301	2.53
15	4	742	-492	1320	1.9
10	4	504.1	-346	1017	1.8
45	31	297.5	-111	173	2.37
25	15	340.4	-162	301	1.91
3	2	307.1	-257	1401	2.16
26	17	313	-144	262	2.23
12	5	484.6	-314	834	2.76
25	15	340.4	-162	301	2.9
15	7	434.4	-258	604	2.13
19	7	545.5	-315	707	2.32
39	26	307.1	-121	198	3.11
14	6	471.7	-290	715	3.02
10	5	406.4	-268	743	3.26
27	18	307.1	-139	249	2.1
17	14	249.8	-128	256	1.53
45	25	366.9	-143	230	2.39
31	17	371.5	-167	295	1.93
23	14	335.6	-164	312	1.93
6	2	600.3	-479	2016	1.82
12	6	406.4	-254	646	1.86

Length	Angle	Lo	Dpar	Lc
12.97	85	16.04	2.53	14.28
16.38	82	15.88	1.9	16.6

13.85	71	16	2.37	14.81
11.75	37	16	2.37	12.64
12.39	65	16	2.37	13.73
14.33	64	15.94	2.11	15.1
12.98	67	15.88	1.91	14.17
10.38	51	15.88	1.91	12
10.94	37	15.97	2.23	12
13.74	52	16.14	2.9	14.52
10.44	55	15.82	1.66	12.15
9.36	44	15.82	1.66	11.04
10.95	56	15.82	1.66	12.54
10.27	33	15.82	1.66	11.32
14.26	24	16.11	2.78	14.48
14.27	30	16.11	2.78	14.59
14.04	66	16.11	2.78	14.91
16.12	44	16.11	2.78	16.3
15.14	63	16.11	2.78	15.67
13.29	12	16.11	2.78	13.38
14.08	69	16.11	2.78	14.96
15.41	50	16.11	2.78	15.78
14.64	64	16.11	2.78	15.32
12.91	86	16.11	2.78	14.24
14.17	84	16.23	3.26	15.1
13.25	20	16.23	3.26	13.49
13.28	85	15.93	2.1	14.49
14.75	82	15.93	2.1	15.49
13.07	16	16.01	2.4	13.24
12.42	69	16.01	2.4	13.8
10.92	58	16.01	2.4	12.56
12.83	46	16.01	2.4	13.72
13.35	45	16.01	2.4	14.1
15.49	73	15.88	1.88	15.97
12.45	42	15.88	1.88	13.33
11.26	52	15.88	1.88	12.67
14.59	69	15.88	1.88	15.32
13.62	63	15.85	1.79	14.58
11.13	56	15.85	1.79	12.67
11.18	45	15.93	2.1	12.43
12.04	72	15.88	1.89	13.56
12.66	59	15.88	1.89	13.83
12.85	85	15.79	1.53	14.2
11.9	29	15.79	1.53	12.52
14.51	51	16.01	2.39	15.1
11.96	67	16.01	2.39	13.45
14.23	87	15.89	1.93	15.14
16.1	71	15.89	1.93	16.39
12.54	90	15.89	1.93	13.99
11.92	61	15.89	1.93	13.33
12.97	51	15.87	1.86	13.93
11.03	48	15.94	2.14	12.4
13.87	67	15.94	2.14	14.8

Table S4 (continued): Single grain data of Apatite Fission Track analysis

C-XII-33 (Ellesmere Island, Canadian High Arctic)

Location
Strathcona Fiord
Lithology
Sandstone
Stratigraphy
Maastricht. - Paleoc.
Formation
Mount Bell Fm
Lat N
78°48.569'
Long W
83°43.909'
Elevation
194

Cf-irrad.
no
Zeta
346
error_Zeta
12
RhoD
1.243E+6
Nd
3096
Length reduction in standard
0.893

Ns	Ni	Age	-95%	95%	Dpar
8	9	188.1	-116	299	2.4
3	2	314.3	-263	1430	2
5	2	515.6	-416	1856	1.9
4	1	806.3	-715	4416	2.1
2	1	415.8	-379	3274	2.3
4	1	806.3	-715	4416	2
5	1	993.1	-874	4892	1.8
2	1	415.8	-379	3274	2.3
5	1	993.1	-874	4892	2.3

Length	Angle	Lo	Dpar	Lc

Table S4 (continued): Single grain data of Apatite Fission Track analysis

C-XII-36 (Ellesmere Island, Canadian High Arctic)

Location	**Cf-irrad.**
Glacier Strathcona Fiord	no
Lithology	**Zeta**
Orthogneiss	346
Stratigraphy	**error_Zeta**
Paleoproterozoic	12
Formation	**RhoD**
Rae Craton	1.293E+6
Lat N	**Nd**
78°24.373'	3219
Long W	**Length reduction in standard**
81°11.946'	0.893
Elevation	
797	

Ns	Ni	Age	-95%	95%	Dpar
8	3	569.7	-418	1406	2.33
14	6	501.2	-308	755	1.93
15	5	637.5	-404	1018	2
12	5	515	-333	881	2.12
13	5	556.1	-357	928	2.19
10	4	535.5	-367	1073	1.94
12	6	431.9	-270	684	1.92
5	2	535.5	-432	1915	1.97
11	4	586.7	-399	1140	1.86
20	7	608.5	-350	773	1.92
8	4	431.9	-302	936	2.03
8	4	431.9	-302	936	1.93
12	5	515	-333	881	2.01
9	3	637.5	-464	1509	1.79
19	8	509.8	-286	622	2.13
8	3	569.7	-418	1406	2.26
19	7	579.4	-335	747	1.91
10	5	431.9	-285	785	1.78
17	7	520.8	-304	693	1.57
15	6	535.5	-327	790	1.93

Length	Angle	Lo	Dpar	Lc
10.35	31	15.94	2.11	11.31
11.34	79	15.92	2.06	13.14
12.73	39	15.8	1.58	13.48
14.04	79	15.8	1.58	14.99
14.49	5	15.92	2.05	14.5
14.47	15	15.92	2.05	14.56
14.02	37	15.92	2.05	14.5
13.39	76	15.92	2.05	14.53

11.4	14	15.92	2.05	11.61
12.7	82	15.92	2.05	14.09
10.78	60	15.92	2.05	12.5
12.19	54	15.9	1.99	13.4
12.78	63	15.93	2.1	13.98
11.44	79	15.93	2.1	13.21
12.41	46	15.96	2.21	13.4
12.32	31	15.89	1.95	12.94
11.08	3	16.04	2.51	11.09
14.07	75	16.04	2.51	14.99
13.4	22	16.04	2.51	13.66
14.14	81	16.04	2.51	15.07
13.01	89	15.94	2.12	14.31
11.06	18	15.94	2.12	11.42
11.86	61	15.93	2.1	13.29
9.7	66	15.93	2.1	11.85
14.1	52	15.89	1.94	14.8
13.47	28	15.89	1.94	13.85
13.21	54	15.89	1.94	14.16
12.75	57	15.84	1.74	13.87
13.65	51	15.84	1.74	14.44
14.33	19	15.84	1.74	14.48
11.83	88	15.89	1.92	13.51
16.12	77	15.94	2.13	16.42
13.09	87	15.94	2.13	14.36
14.15	61	15.94	2.13	14.94
12.87	82	15.93	2.08	14.2
12.36	46	15.87	1.87	13.36
14.31	73	15.88	1.91	15.15
12.21	57	15.93	2.08	13.47
13.3	82	15.93	2.08	14.5
11.35	85	15.83	1.69	13.18
11.37	26	15.88	1.91	11.97
9.78	74	15.88	1.91	12.02
14.37	65	15.85	1.78	15.13
11.23	76	15.85	1.78	13.04
9.92	80	15.89	1.93	12.17
10.59	64	15.89	1.93	12.44
12.66	2	15.89	1.93	12.66
9.27	2	15.89	1.93	9.28
14.84	18	15.94	2.14	14.95
11.8	75	15.94	2.14	13.42
13.95	55	15.92	2.05	14.72
12.32	54	15.92	2.05	13.5

Table S4 (continued): Single grain data of Apatite Fission Track analysis

C-XII-37 (Ellesmere Island, Canadian High Arctic)

Location	**Cf-irrad.**
Glacier Strathcona Fiord	no
Lithology	**Zeta**
Pyroxenite	346
Stratigraphy	**error_Zeta**
Paleoproterozoic	12
Formation	**RhoD**
Rae Craton	1.293E+6
Lat N	**Nd**
78°24.425'	3219
Long W	**Length reduction in standard**
81°11.976'	0.893
Elevation	
789	

Ns	Ni	Age	-95%	95%	Dpar
23	21	240.1	-108	194	2.07
15	5	637.5	-404	1018	2.02
8	3	569.7	-418	1406	1.94
7	3	501.2	-372	1299	2.09
8	3	569.7	-418	1406	1.82
17	6	603.7	-364	858	2.37
11	4	586.7	-399	1140	1.91
22	34	142.9	-60.3	103	1.76
10	4	535.5	-367	1073	1.89
26	9	615	-325	655	1.89
5	2	535.5	-432	1915	2.32
9	4	483.9	-335	1006	1.95
32	20	347.8	-150	258	2.07
30	18	361.9	-161	284	2.17
13	5	556.1	-357	928	2.2
7	4	379.5	-269	865	1.93
5	2	535.5	-432	1915	2.41
14	6	501.2	-308	755	2.24
8	3	569.7	-418	1406	1.81
19	7	579.4	-335	747	2.12
11	5	473.6	-309	834	1.93
10	4	535.5	-367	1073	2.03
5	2	535.5	-432	1915	2.41

Length	Angle	Lo	Dpar	Lc
13.58	33	16	2.37	14.05
10.94	66	16	2.37	12.72
13.53	52	16	2.37	14.36
12.11	43	16	2.37	13.09
11.08	29	15.93	2.07	11.83

13.14	54	15.92	2.04	14.1
8.57	50	15.85	1.76	10.98
13.13	85	15.85	1.76	14.39
9.89	39	15.85	1.76	11.26
12.61	71	15.8	1.58	13.95
11.69	76	15.93	2.08	13.36
12.07	43	15.93	2.08	13.06
13.18	84	15.93	2.08	14.42
12.28	39	15.87	1.87	13.12
14.28	75	15.86	1.82	15.14
12.23	22	15.86	1.82	12.6
13.24	72	15.89	1.93	14.4
11.79	65	15.89	1.93	13.3
11.82	28	15.89	1.93	12.42
10.32	69	15.89	1.93	12.33
15	47	15.87	1.85	15.43
14.52	34	15.87	1.85	14.87
14.04	30	16.01	2.4	14.39
14.62	47	15.86	1.83	15.13
12.35	43	15.86	1.83	13.28
10.15	77	15.88	1.89	12.31
9.59	40	15.88	1.89	11.07
10.83	22	15.88	1.89	11.36
14.53	50	15.88	1.89	15.1
12.05	73	15.88	1.89	13.58
7.38	67	15.88	1.89	11.27
9.85	78	15.88	1.89	12.11
12.94	75	15.88	1.89	14.21
10.79	74	15.88	1.89	12.72
12.35	57	15.88	1.89	13.57
9.68	83	15.88	1.89	12.05
11.56	33	15.88	1.89	12.36
12.5	47	15.83	1.71	13.49
12.97	27	15.83	1.71	13.39
11.1	19	15.94	2.12	11.49
13.31	76	15.94	2.12	14.47
14.74	49	15.94	2.12	15.25
12.42	69	15.94	2.12	13.8
9.68	31	15.94	2.12	10.78
12.57	64	15.89	1.93	13.84
17.26	46	15.98	2.3	17.23
13.82	80	15.98	2.3	14.84
16.01	66	15.98	2.3	16.31
13.45	11	15.98	2.3	13.52
12.9	26	15.98	2.3	13.31

Table S4 (continued): Single grain data of Apatite Fission Track analysis

C-XII-42 (Ellesmere Island, Canadian High Arctic)

Location	Cf-irrad.
Vendom Fiord	no
Lithology	**Zeta**
Sandstone	346
Stratigraphy	**error_Zeta**
Lower-Middle Devon.	12
Formation	**RhoD**
Strathcona Fiord Fm	1.293E+6
Lat N	**Nd**
77°39.333'	3219
Long W	**Length reduction in standard**
82°45.239'	0.893
Elevation	
325	

Ns	Ni	Age	-95%	95%	Dpar
23	25	202.3	-88.6	156	1.83
12	9	291.1	-169	393	1.75
28	19	321	-143	252	1.68
13	8	353.1	-207	485	1.76
16	10	347.8	-191	409	1.75
14	11	278.2	-153	331	1.67
24	25	210.9	-91.6	160	1.42
58	57	223.4	-69.9	101	1.74
36	22	355.5	-147	247	1.75
43	32	293.4	-109	171	1.7
47	40	257.3	-89.9	137	1.93
43	33	284.7	-105	165	1.52
11	8	300	-180	437	1.42
16	10	347.8	-191	409	1.47
57	46	271	-88.8	131	1.77
46	29	344.9	-129	204	1.67
19	11	374.7	-197	403	1.66

Length	Angle	Lo	Dpar	Lc
14.26	79	15.85	1.77	15.14
14.59	39	15.85	1.77	15
13.62	79	15.85	1.77	14.7
12.58	78	15.85	1.77	13.98
11.98	41	15.82	1.68	12.94
12.95	41	15.82	1.68	13.71
9.18	66	15.82	1.68	11.58
8.15	46	15.82	1.68	10.77
9.52	65	15.82	1.68	11.71
11.56	60	15.82	1.68	13.06
9.96	65	15.82	1.68	12.02
11.41	79	15.82	1.68	13.19

15.7	36	15.82	1.68	15.9
12.26	75	15.85	1.76	13.74
12.18	53	15.84	1.75	13.37
11.32	56	15.81	1.61	12.81
10.6	86	15.81	1.61	12.67
12.2	41	15.81	1.61	13.11
12.72	72	15.81	1.61	14.03
13.13	88	15.81	1.61	14.39
13.4	87	15.81	1.61	14.58
13.74	64	15.81	1.61	14.67
14.13	60	15.81	1.61	14.91
12.45	84	15.81	1.61	13.92
13.15	77	15.81	1.61	14.37
13.53	63	15.81	1.61	14.51
13.5	77	15.81	1.61	14.61
12.47	71	15.81	1.61	13.85
11.77	64	15.81	1.61	13.27
12.56	67	15.81	1.61	13.87
12.64	47	15.81	1.61	13.59
12.88	47	15.81	1.61	13.78
13.73	23	15.81	1.61	13.99
12.53	15	15.84	1.75	12.71
13.46	73	15.84	1.75	14.56
13.19	56	15.84	1.75	14.17
13.47	9	15.84	1.75	13.52
11.04	22	15.84	1.75	11.55
13.28	56	15.84	1.75	14.24
13.45	51	15.84	1.75	14.29
10.95	63	15.84	1.75	12.68
12.33	58	15.84	1.75	13.58
14.25	82	15.84	1.75	15.14
12.4	27	15.84	1.75	12.89
10.6	58	15.84	1.75	12.33
13.63	27	15.84	1.75	13.97
14.25	29	15.83	1.7	14.56
11.13	17	15.83	1.7	11.45
10.84	18	15.83	1.7	11.22
14.1	57	15.83	1.7	14.86
14.6	79	15.83	1.7	15.38
12.36	22	15.83	1.7	12.72
11.53	49	15.83	1.7	12.8
12.79	79	15.83	1.7	14.13
12.13	47	15.83	1.7	13.2
11.57	50	15.83	1.7	12.85
14.83	8	15.83	1.7	14.85
9.62	55	15.83	1.7	11.56
13.28	49	15.83	1.7	14.12
12.64	68	15.83	1.7	13.94
14.05	43	15.83	1.7	14.62
13.7	62	15.89	1.93	14.62
12	50	15.78	1.52	13.18
11.34	66	15.78	1.52	13

13.9	29	15.78	1.52	14.25
14.65	73	15.78	1.52	15.38
11.67	84	15.76	1.42	13.39
14.21	45	15.76	1.42	14.78
13.5	81	15.76	1.42	14.63
10.21	78	15.77	1.47	12.36
11.49	66	15.77	1.47	13.11
10.05	81	15.77	1.47	12.27
9.14	53	15.77	1.47	11.17
12.54	89	15.77	1.47	13.99
14.35	49	15.77	1.47	14.95
10.3	56	15.77	1.47	12.07
14.76	26	15.77	1.47	14.97
12.08	37	15.85	1.77	12.91
12.39	78	15.85	1.77	13.85
12.04	66	15.82	1.67	13.49
11.04	87	15.82	1.67	12.97
14.27	83	15.82	1.67	15.16

Table S4 (continued): Single grain data of Apatite Fission Track analysis

C-XII-46 (Ellesmere Island, Canadian High Arctic)

Location	**Cf-irrad.**
Vendom Fiord	no
Lithology	**Zeta**
Sandstone	346
Stratigraphy	**error_Zeta**
Late Devonian	12
Formation	**RhoD**
Fram Formation	1.293E+6
Lat N	**Nd**
77°46.310'	3219
Long W	**Length reduction in standard**
83°17.415'	0.893
Elevation	
282	

Ns	Ni	Age	-95%	95%	Dpar
57	29	424.7	-154	237	2.21
15	11	297.6	-162	345	1.93
61	42	316.5	-104	154	1.83
15	8	405.8	-234	531	2.32
6	7	188.7	-126	370	2.59
15	8	405.8	-234	531	1.95
21	13	351.1	-176	344	1.76
30	12	535.5	-261	489	2.3
34	21	351.9	-149	252	2.08
90	48	405.8	-122	171	1.88
42	33	278.2	-103	162	1.79
22	14	341.8	-168	321	1.74
123	70	381	-99.1	133	4.03
22	10	473.6	-249	506	3.97
49	21	501.2	-201	326	2.51
111	54	443.5	-125	172	3.87

Length	Angle	Lo	Dpar	Lc
8.39	90	15.85	1.77	11.78
13.09	71	15.85	1.77	14.28
12.62	65	15.85	1.77	13.89
14.61	16	15.85	1.77	14.7
12.19	28	15.85	1.77	12.74
12.93	39	15.85	1.77	13.64
11.2	77	15.85	1.77	13.03
12.58	69	15.85	1.77	13.91
13.44	83	15.96	2.21	14.59
13.53	43	15.96	2.21	14.21
14.29	59	15.96	2.21	15.02
11.41	10	15.96	2.21	11.53
12.63	74	15.96	2.21	13.99

13.81	25	15.86	1.83	14.1
15.39	62	15.86	1.83	15.85
13.98	82	15.86	1.83	14.96
13.95	49	15.86	1.83	14.64
12.67	65	15.86	1.83	13.92
9.77	81	15.86	1.83	12.08
15.48	88	16.06	2.59	15.99
14.51	78	16.06	2.59	15.31
12.39	35	15.85	1.76	13.1
13.18	37	15.85	1.76	13.8
11.18	58	15.85	1.76	12.75
13.83	6	15.85	1.76	13.85
14.63	22	15.85	1.76	14.8
13.21	58	15.85	1.76	14.22
15.43	28	15.93	2.08	15.59
13.69	59	15.93	2.08	14.58
12.98	51	15.93	2.08	13.93
14.72	54	15.93	2.08	15.29
12.83	60	15.93	2.08	13.97
15.38	55	15.93	2.08	15.79
12.51	49	15.88	1.88	13.54
14.03	76	15.88	1.88	14.97
10.5	26	15.88	1.88	11.23
11.5	54	15.88	1.88	12.89
10.85	37	15.88	1.88	11.93
11.51	80	15.88	1.88	13.26
13	81	15.85	1.77	14.29
12.28	65	15.85	1.77	13.65
11	48	15.85	1.77	12.38
15.1	82	16.43	4.03	15.73
16.05	27	16.43	4.03	16.14
12.27	33	16.43	4.03	12.95
15.82	68	16.43	4.03	16.18
14.09	70	16.43	4.03	14.97
16.02	69	16.43	4.03	16.33
15.93	69	16.43	4.03	16.27
8.48	56	15.89	1.93	11.17
12.94	61	15.89	1.93	14.06
12.39	36	15.89	1.93	13.13
14.16	54	15.89	1.93	14.87
12.3	85	15.89	1.93	13.82
14.36	51	15.89	1.93	14.98
11.73	80	15.89	1.93	13.41
11.67	41	15.89	1.93	12.69
13.61	73	15.89	1.93	14.66
13.73	61	15.89	1.93	14.63
14.51	46	15.89	1.93	15.03
12.36	82	15.89	1.93	13.85
14.05	72	15.89	1.93	14.96
12.73	62	16.42	3.97	13.93
14.09	75	16.42	3.97	15.01
13.61	67	16.42	3.97	14.61

14.38	80	16.42	3.97	15.23
15.43	63	16.42	3.97	15.88
9.63	46	16.04	2.51	11.31
12.87	64	16.04	2.51	14.05
13.72	52	16.04	2.51	14.51
12.06	30	16.04	2.51	12.69
12.93	76	16.04	2.51	14.21
11.84	44	16.04	2.51	12.91
15.35	76	16.39	3.87	15.88
14.31	80	16.39	3.87	15.18
10.07	71	16.39	3.87	12.19
13.86	71	16.39	3.87	14.82
14.68	9	16.39	3.87	14.71
15.61	38	16.39	3.87	15.84

Table S4 (continued): Single grain data of Apatite Fission Track analysis

C-XII-48 (Ellesmere Island, Canadian High Arctic)

Location
Vendom Fiord
Lithology
Sandstone
Stratigraphic
Lower-Middle Devon.
Formation
Strathcona Fiord Fm
Lat N
78°07.272'
Long W
82°27.090'
Elevation
283

Cf-irrad.
no
Zeta
346
error_Zeta
12
RhoD
1.293E+6
Nd
3219
Length reduction in standard
0.893

Ns	Ni	Age	-95%	95%	Dpar
12	4	637.5	-430	1204	2.05
36	15	515	-233	411	2.62
9	3	637.5	-464	1509	1.59
13	7	402	-242	582	1.73
13	14	204.1	-109	231	1.78
38	17	480.9	-210	361	2.15
10	8	273.3	-166	412	1.72
6	3	431.9	-324	1188	1.88
18	18	219.6	-106	203	2.05
15	7	461.7	-273	638	1.93
16	12	291.1	-154	321	1.69
6	3	431.9	-324	1188	1.63
19	11	374.7	-197	403	1.87
23	13	383.5	-190	366	1.91
29	17	370.2	-168	299	1.8
14	10	305.4	-171	376	2
14	8	379.5	-221	508	2.04
16	9	385.3	-216	472	2.25
18	10	390	-211	442	2.26

Length	Angle	Lo	Dpar	Lc
15.86	48	15.88	1.91	16.12
10.25	83	15.88	1.91	12.42
9.7	84	15.92	2.05	12.07
12.42	65	16.07	2.62	13.75
14.19	85	16.07	2.62	15.11
13.83	88	16.07	2.62	14.87
14	25	16.07	2.62	14.27
13.84	59	16.07	2.62	14.69
14.54	69	15.85	1.78	15.28
14.14	56	15.85	1.78	14.88

10.57	74	15.85	1.78	12.57
12.9	88	15.85	1.78	14.24
14.62	37	15.85	1.78	15
13.25	88	15.95	2.15	14.47
11.88	32	15.95	2.15	12.6
15.53	84	15.89	1.93	16.02
14.64	19	15.83	1.69	14.77
15.01	40	15.83	1.69	15.36
13.35	79	15.86	1.8	14.52
13.93	77	15.91	2	14.91
10.51	47	15.92	2.04	11.99
13.01	57	15.97	2.26	14.06
14.1	20	15.97	2.26	14.28
14.62	23	15.97	2.26	14.8
14.17	44	15.97	2.26	14.73
11.16	55	15.97	2.26	12.67

Table S4 (continued): Single grain data of Apatite Fission Track analysis

GRÖ21 (NW Greenland)

Location
SE Kap Atholl
Lithology
Gneiss
Stratigraphy
Archean
Formation
Rae Craton
Lat N
76°21.336´
Long W
69°29.665´
Elevation
216

Cf-irrad.
no
Zeta
319
error_Zeta
9
RhoD
1.515E+6
Nd
22918
Length reduction in standard
0.893

Ns	Ni	Age	-95%	95%	Dpar
83	196	101.5	-23.7	30.9	1.44
13	55	56.86	-26.2	48.4	1.42
33	58	136	-48.1	74	1.32
63	99	152	-42.1	57.9	1.54
37	55	160.5	-55.6	84.4	1.57
4	13	73.93	-50.3	156	1.68
26	43	144.5	-56.5	92.1	1.5
5	26	46.3	-28.9	76.1	1.61
49	128	91.85	-26.4	36.9	1.63
14	28	119.7	-57.4	109	1.64
40	78	122.7	-39.7	58.3	1.42
47	105	107.3	-31.9	45.3	1.5
12	37	77.9	-37.8	73	1.41
12	20	143.4	-74.1	151	1.43
8	9	211.3	-131	334	1.53
15	61	59.15	-25.9	46	1.6
39	104	89.98	-28.3	41.2	1.55
20	102	47.21	-18.3	29.9	1.59
5	29	41.53	-25.8	67.5	1.42
22	59	89.48	-35.2	57.8	1.41

Length	Angle	Lo	Dpar	Lc
12	61	15.76	1.44	13.39
12.88	62	15.76	1.44	14.03
10.66	70.3	15.76	1.44	12.59
12.9	24.7	15.76	1.42	13.27
12.29	75.8	15.73	1.32	13.77
13.61	74.5	15.73	1.32	14.67
11.84	50	15.73	1.32	13.06
13.52	9.69	15.73	1.32	13.58

13.24	39.1	15.79	1.54	13.9
14.18	74.9	15.79	1.54	15.07
13.82	61	15.8	1.57	14.7
14.2	80.3	15.8	1.57	15.11
9.95	70.8	15.82	1.68	12.1
14.45	32.4	15.82	1.68	14.79
10.29	70.3	15.78	1.5	12.33
11.74	68	15.81	1.61	13.31
12.71	61.2	15.81	1.63	13.9
13.71	66.3	15.81	1.63	14.68
13.63	69.8	15.81	1.63	14.65
13.56	54.9	15.81	1.64	14.43
13.48	76.4	15.76	1.42	14.59
11.47	62.5	15.76	1.42	13.04
11.31	74.9	15.76	1.42	13.09
10.56	50.6	15.78	1.5	12.12
14.91	43.6	15.78	1.5	15.32
14.87	67.5	15.78	1.5	15.51
11.63	38.7	15.75	1.41	12.6
9.4	70.4	15.75	1.41	11.74
8.99	71.8	15.76	1.43	11.68
11.82	64.4	15.79	1.55	13.31
7.78	58.9	15.8	1.59	11.14
7.7	81.9	15.8	1.59	11.57
11.11	75.9	15.8	1.59	12.96
11.71	32.6	15.8	1.59	12.47
11.74	43.1	15.8	1.59	12.81
13.37	63.5	15.76	1.42	14.4
13.35	54.1	15.76	1.43	14.26
12.49	45.4	15.76	1.43	13.44
10.97	60	15.76	1.43	12.64
11.3	52.5	15.76	1.43	12.71
10.7	45.4	15.82	1.65	12.08
12.85	74	15.82	1.65	14.14
13.36	48.3	15.82	1.65	14.17
13.8	49	15.82	1.65	14.52
9.6	72.2	15.82	1.65	11.88
15.03	67.7	15.8	1.59	15.62
6.79	32.7	15.8	1.59	10
10.93	66.4	15.8	1.59	12.72
11.12	70.7	15.8	1.59	12.91
13.24	54.3	15.8	1.59	14.18
8.28	88.1	15.8	1.59	11.75
13.12	78.3	15.8	1.59	14.36
10.48	51.2	15.82	1.67	12.08
11.8	43.8	15.82	1.67	12.87
10.45	74.5	15.82	1.67	12.49
11.43	39	15.8	1.58	12.45
9.87	54.3	15.77	1.48	11.72
11.5	61.9	15.77	1.48	13.05
10.28	82.9	15.77	1.48	12.44
13.96	5.04	15.82	1.65	13.97

12.92	69.4	15.82	1.65	14.15
11.18	10.2	15.82	1.65	11.31
10.53	16	15.82	1.65	10.87
12.84	64.4	15.82	1.65	14.04
15.5	8.03	15.82	1.65	15.52
9.46	51	15.82	1.65	11.34
12.34	48.8	15.79	1.55	13.4
12.13	63.6	15.79	1.55	13.52
13.42	40.8	15.79	1.55	14.08
12.44	76.7	15.79	1.55	13.88
11.76	62.4	15.79	1.55	13.24
9.04	79.9	15.79	1.55	11.83
9.37	61.3	15.79	1.55	11.53
13.99	76.2	15.79	1.55	14.94
11.4	57.1	15.78	1.52	12.89
10.79	65	15.78	1.52	12.6
11.52	85.6	15.78	1.52	13.29
11.04	83.5	15.81	1.61	12.96
12.54	65.5	15.81	1.61	13.84
12.66	67.5	15.81	1.61	13.95
10.31	56.8	15.81	1.61	12.1
14.62	21.4	15.81	1.61	14.78
14.42	60.8	15.81	1.61	15.13
12.28	68.2	15.81	1.61	13.69
13.93	45.4	15.81	1.61	14.57
9.27	78.6	15.81	1.61	11.87
12.67	56.1	15.81	1.61	13.79
8.4	65.4	15.75	1.39	11.42
13.84	73.5	15.75	1.39	14.82
10.28	71.8	15.8	1.6	12.34
12.38	47.3	15.8	1.6	13.4
11.66	36.4	15.8	1.6	12.55
14.23	68.2	15.8	1.6	15.06
13.14	62.5	15.8	1.6	14.23
14.29	75.5	15.8	1.6	15.15
8.83	69.8	15.8	1.6	11.6
12.38	66.8	15.8	1.6	13.74
7.98	55.6	15.81	1.61	11.08
12.65	75.1	15.81	1.61	14.01

Table S4 (continued): Single grain data of Apatite Fission Track analysis

GRÖ23 (NW Greenland)

Location	**Cf-irrad.**
Kap Powell	no
Lithology	**Zeta**
Sandstone	319
Stratigraphy	**error_Zeta**
Proterozoic	9
Formation	**RhoD**
Thule Supergroup	2.021E+6
Lat N	**Nd**
77°55.106´	30579
Long W	**Length reduction in standard**
71°53.863´	0.893
Elevation	
497	

Ns	Ni	Age	-95%	95%	Dpar
5	7	226.2	-155	478	1.59
8	9	280.3	-173	437	1.64
6	15	127.7	-78.9	203	1.75
13	20	206.2	-104	208	1.77
4	8	159.2	-112	368	1.45
2	6	106.6	-85.6	422	1.45
9	15	190.6	-108	245	1.63
11	16	217.9	-118	251	1.72
11	13	267.1	-148	325	1.78
7	9	246	-155	408	1.76
5	15	106.6	-68.5	189	1.68
5	21	76.3	-48	128	1.54
4	15	85.39	-57.6	175	1.73
19	54	112.4	-46.5	78.7	1.8
8	11	230.3	-139	339	1.72
7	10	221.8	-138	357	1.62
6	9	211.4	-137	378	1.55
12	24	159.2	-80.4	160	1.64
26	53	156.2	-59.3	95	1.83

Length	Angle	Lo	Dpar	Lc
11.32	84.9	15.77	1.45	13.15
12.15	68.6	15.87	1.86	13.6
12.36	66.2	15.87	1.86	13.72
12.52	55.8	15.87	1.86	13.68
14.57	71	15.87	1.86	15.32
9.99	57.9	15.87	1.86	11.9
15.14	47.4	15.81	1.63	15.54
13.01	78	15.85	1.78	14.28
11.06	85.5	15.84	1.73	12.98
11.92	85.9	15.86	1.83	13.57

14.68	45.1	15.87	1.86	15.16
10.76	60.2	15.77	1.48	12.49
9.38	82.5	15.81	1.64	11.95
12.72	57	15.81	1.64	13.84
13.63	51.5	15.81	1.64	14.43
12.11	67.2	15.8	1.59	13.56
14.5	60.2	15.8	1.59	15.19
13.19	68.3	15.82	1.68	14.33
10.52	38	15.82	1.68	11.7
11.82	60.8	15.85	1.76	13.26
13.45	88.5	15.85	1.76	14.61
13.06	54.9	15.79	1.53	14.06
12.83	58.2	15.79	1.53	13.94
13.83	53.2	15.82	1.65	15
12.45	58.5	15.81	1.61	13.67
13.62	75.8	15.81	1.61	14.69
12.84	44.7	15.82	1.65	13.7
12.62	52.5	15.84	1.75	13.69

Table S4 (continued): Single grain data of Apatite Fission Track analysis

GRÖ24 (NW Greenland)

Location	**Cf-irrad.**
Kap Peary	no
Lithology	**Zeta**
Sandstone	319
Stratigraphy	**error_Zeta**
Proterozoic	9
Formation	**RhoD**
Thule Supergroup	2.021E+6
Lat N	**Nd**
76°49.437´	30579
Long W	**Length reduction in standard**
70°13.534´	0.893
Elevation	
7	

Ns	**Ni**	**Age**	**-95%**	**95%**	**Dpar**
4	5	252.9	-186	666	1.86
10	14	226.2	-127	281	2.33
2	3	211.4	-177	1002	1.89
4	2	614.5	-502	2276	1.47
2	8	80.09	-63.5	301	1.75
3	2	466.2	-389	2000	1.76
7	11	201.9	-125	317	1.71
3	3	314.5	-252	1156	2.18
3	1	901	-806	5035	1.82
5	5	314.5	-224	738	1.98
3	3	314.5	-252	1156	1.94
1	3	106.6	-95.9	894	1.6
1	5	64.15	-57	488	2.05
2	6	106.6	-85.6	422	1.93
4	5	252.9	-186	666	1.74
1	2	159.2	-145	1481	1.75
3	4	237.3	-185	791	1.72
4	2	614.5	-502	2276	1.96
3	8	119.8	-88.7	333	2.01
1	2	159.2	-145	1481	1.65

Length	**Angle**	**Lo**	**Dpar**	**Lc**

Table S4 (continued): Single grain data of Apatite Fission Track analysis

GRÖ32 (NW Greenland)

Location	**Cf-irrad.**
S Thule Airbase	no
Lithology	**Zeta**
Metabasite	319
Stratigraphy	**error_Zeta**
?	9
Formation	**RhoD**
Rae Craton	2.021E+6
Lat N	**Nd**
76°21.938´	30579
Long W	**Length reduction in standard**
68°48.036´	0.893
Elevation	
753	

Ns	Ni	Age	-95%	95%	Dpar
64	130	156.8	-41.5	56.2	2.33
17	37	146.4	-64.8	115	2.46
36	74	154.9	-51.7	77.2	2.49
45	72	198.4	-62.7	90.9	2.66
19	38	159.2	-68.2	118	2.55
29	52	177.3	-65.6	103	2.56
31	53	185.8	-67.4	105	2.56
17	43	126.2	-54.9	96.6	2.28

Length	Angle	Lo	Dpar	Lc
11.45	82.36	15.99	2.33	13.23
6.65	77.5	15.99	2.33	11.31
12.16	59.68	15.99	2.33	13.48
11.35	67.42	16.08	2.66	13.03
12.22	80.68	16.05	2.56	13.75
8.3	74.21	16.05	2.56	11.58

Table S4 (continued): Single grain data of Apatite Fission Track analysis

GRÖ35 (NW Greenland)

Location
NW Pitugfik Glacier
Lithology
Itabirite
Stratigraphy
Archean
Formation
Rae Craton
Lat N
76°17.187´
Long W
68°46.659´
Elevation
295

Cf-irrad.
no
Zeta
319
error_Zeta
9
RhoD
2.021E+6
Nd
30579
Length reduction in standard
0.893

Ns	Ni	Age	-95%	95%	Dpar
2	1	614.5	-559	4347	1.65
5	5	314.5	-224	738	1.65
1	2	159.2	-145	1481	1.58
1	2	159.2	-145	1481	1.57
12	25	152.9	-76.9	153	1.8
3	5	190.6	-146	594	1.63
1	1	314.5	-296	3639	1.77
3	3	314.5	-252	1156	1.54
6	5	375.7	-262	809	1.71
2	1	614.5	-559	4347	1.08
1	2	159.2	-145	1481	1.63
1	3	106.6	-95.9	894	1.85
5	5	314.5	-224	738	1.71
2	1	614.5	-559	4347	1.71
4	3	416.1	-324	1312	1.54
1	1	314.5	-296	3639	1.55
1	2	159.2	-145	1481	1.84
1	2	159.2	-145	1481	1.83

Length	Angle	Lo	Dpar	Lc

Table S4 (continued): Single grain data of Apatite Fission Track analysis

GRÖ36 (NW Greenland)

Location	**Cf-irrad.**
NW Pitugfik Glacier	no
Lithology	**Zeta**
Schist	346
Stratigraphy	**error_Zeta**
Archean	12
Formation	**RhoD**
Rae Craton	1.293E+6
Lat N	**Nd**
76°16.927´	3219
Long W	**Length reduction in standard**
68°49.888´	0.893
Elevation	
321	

Ns	Ni	Age	-95%	95%	Dpar
8	3	569.7	-418	1406	2.33
14	6	501.2	-308	755	1.93
15	5	637.5	-404	1018	2
12	5	515	-333	881	2.12
13	5	556.1	-357	928	2.19
10	4	535.5	-367	1073	1.94
12	6	431.9	-270	684	1.92
5	2	535.5	-432	1915	1.97
11	4	586.7	-399	1140	1.86
20	7	608.5	-350	773	1.92
8	4	431.9	-302	936	2.03
8	4	431.9	-302	936	1.93
12	5	515	-333	881	2.01
9	3	637.5	-464	1509	1.79
19	8	509.8	-286	622	2.13
8	3	569.7	-418	1406	2.26
19	7	579.4	-335	747	1.91
10	5	431.9	-285	785	1.78
17	7	520.8	-304	693	1.57
15	6	535.5	-327	790	1.93

Length	Angle	Lo	Dpar	Lc
10.35	31	15.94	2.11	11.31
11.34	79	15.92	2.06	13.14
12.73	39	15.8	1.58	13.48
14.04	79	15.8	1.58	14.99
14.49	5	15.92	2.05	14.5
14.47	15	15.92	2.05	14.56
14.02	37	15.92	2.05	14.5
13.39	76	15.92	2.05	14.53

11.4	14	15.92	2.05	11.61
12.7	82	15.92	2.05	14.09
10.78	60	15.92	2.05	12.5
12.19	54	15.9	1.99	13.4
12.78	63	15.93	2.1	13.98
11.44	79	15.93	2.1	13.21
12.41	46	15.96	2.21	13.4
12.32	31	15.89	1.95	12.94
11.08	3	16.04	2.51	11.09
14.07	75	16.04	2.51	14.99
13.4	22	16.04	2.51	13.66
14.14	81	16.04	2.51	15.07
13.01	89	15.94	2.12	14.31
11.06	18	15.94	2.12	11.42
11.86	61	15.93	2.1	13.29
9.7	66	15.93	2.1	11.85
14.1	52	15.89	1.94	14.8
13.47	28	15.89	1.94	13.85
13.21	54	15.89	1.94	14.16
12.75	57	15.84	1.74	13.87
13.65	51	15.84	1.74	14.44
14.33	19	15.84	1.74	14.48
11.83	88	15.89	1.92	13.51
16.12	77	15.94	2.13	16.42
13.09	87	15.94	2.13	14.36
14.15	61	15.94	2.13	14.94
12.87	82	15.93	2.08	14.2
12.36	46	15.87	1.87	13.36
14.31	73	15.88	1.91	15.15
12.21	57	15.93	2.08	13.47
13.3	82	15.93	2.08	14.5
11.35	85	15.83	1.69	13.18
11.37	26	15.88	1.91	11.97
9.78	74	15.88	1.91	12.02
14.37	65	15.85	1.78	15.13
11.23	76	15.85	1.78	13.04
9.92	80	15.89	1.93	12.17
10.59	64	15.89	1.93	12.44
12.66	2	15.89	1.93	12.66
9.27	2	15.89	1.93	9.28
14.84	18	15.94	2.14	14.95
11.8	75	15.94	2.14	13.42
13.95	55	15.92	2.05	14.72
12.32	54	15.92	2.05	13.5

Table S4 (continued): Single grain data of Apatite Fission Track analysis

GRÖ52 (NW Greenland)

Location
Kap Powell
Lithology
Sandstone
Stratigraphic
Proterozoic
Formation
Thule Supergroup
Lat N
77°55.106´
Long W
71°53.863´
Elevation
497

Cf-irrad.
no
Zeta
319
error_Zeta
9
RhoD
2.021E+6
Nd
30579
Length reduction in standard
0.893

Ns	Ni	Age	-95%	95%	Dpar
12	11	342.4	-192	422	1.94
26	12	663.1	-325	610	1.99
40	22	561	-226	368	1.95
9	14	204	-117	266	1.41
12	6	614.5	-382	938	2.16
9	19	150.9	-83.4	184	1.49
17	22	244.4	-115	215	1.35
17	16	333.7	-166	321	1.83
43	52	261.2	-87.7	131	1.54
33	9	1085	-552	1037	2.06
19	5	1121	-689	1578	2.04
20	16	390.8	-189	354	1.89

Length	Angle	Lo	Dpar	Lc
12.47	68.4	15.9	1.99	13.82
9.72	69.9	15.9	1.99	11.93
14.87	48.5	15.9	1.99	15.34
8.74	75	15.95	2.16	11.68
9.44	42.6	15.95	2.16	11.05
10.23	60.3	15.86	1.83	12.12
13.93	59.7	15.92	2.06	14.76

Table S4 (continued): Single grain data of Apatite Fission Track analysis

GRÖ53 (NW Greenland)

Location	**Cf-irrad.**
Kap Chalon	no
Lithology	**Zeta**
Sandstone	346
Stratigraphy	**error_Zeta**
Proterozoic	12
Formation	**RhoD**
Thule Supergroup	1.784E+6
Lat N	**Nd**
77°56.720´	4442
Long W	**Length reduction in standard**
72°07.920´	0.893
Elevation	
515	

Ns	Ni	Age	-95%	95%	Dpar
15	9	494.2	-278	604	1.73
9	5	532.2	-353	974	1.8
24	30	242	-102	173	1.92
7	5	417.6	-286	845	2.23
7	6	349.9	-233	663	1.72
19	13	435.4	-221	432	2.31
15	14	322	-167	340	1.83
39	26	446.5	-175	282	1.91
9	7	384.5	-242	621	1.51
10	13	232.8	-132	296	1.51
27	15	532.2	-248	450	1.87
9	5	532.2	-353	974	1.87
20	16	374.2	-181	341	1.68
16	6	773.5	-466	1080	1.91
12	5	700.2	-451	1155	1.77

Length	Angle	Lo	Dpar	Lc
12.48	36	15.86	1.8	13.2
10.92	40	15.86	1.8	12.08
13.83	27	15.8	1.59	14.15
9.88	81	15.99	2.31	12.15
13.15	57	15.99	2.31	14.16
14.41	68	15.99	2.31	15.19
12.64	84	15.99	2.31	14.05
13.78	43	15.88	1.91	14.41
11.29	42	15.88	1.91	12.43
13.05	82	15.92	2.04	14.32
10.36	43	15.92	2.04	11.75
12.63	58	15.87	1.87	13.79
10.33	62	15.87	1.87	12.22

9.14	55	15.87	1.87	11.24
14.74	66	15.85	1.77	15.41

Table S4 (continued): Single grain data of Apatite Fission Track analysis

GRÖ60 (NW Greenland)

Location	**Cf-irrad.**
Bylot Sound	no
Lithology	**Zeta**
Arkose	319
Stratigraphy	**error_Zeta**
Proterozoic	9
Formation	**RhoD**
Thule Supergroup	2.021E+6
Lat N	**Nd**
77°10.260´	30579
Long W	**Length reduction in standard**
70°36.376´	0.893
Elevation	
187	

Ns	Ni	Age	-95%	95%	Dpar
2	12	53.5	-41.9	190	1.92
34	66	164	-56.4	85.4	2.18
118	242	155.3	-31.8	39.9	2.42

Length	Angle	Lo	Dpar	Lc
11.65	70.2	15.89	1.92	13.27
6.33	48.58	15.95	2.18	10.61

Table S4 (continued): Single grain data of Apatite Fission Track analysis

GRÖ64 (NW Greenland)

Location	**Cf-irrad.**
Bylot Sound	no
Lithology	**Zeta**
Gneiss	319
Stratigraphic	**error_Zeta**
Archean	9
Formation	**RhoD**
Rae Craton	1.525E+6
Lat N	**Nd**
76°22.508´	22918
Long W	**Length reduction in standard**
69°32.543´	0.893
Elevation	
299	

Ns	Ni	Age	-95%	95%	Dpar
18	18	237.2	-115	218	1.69
30	36	198.3	-77	125	1.53
43	45	226.9	-78.4	119	1.51
30	63	114.1	-40.9	63.5	1.66
75	139	129.1	-32.5	43.3	1.6
17	34	119.7	-53.5	96.1	1.6
31	56	132.4	-47.8	74.3	1.6
28	32	208	-83.6	138	1.77
8	12	159.1	-94.9	231	1.78
55	64	204.4	-62.8	90.1	1.9
37	66	134.1	-45.2	67.9	1.74
5	7	170.3	-117	364	1.57
3	12	60.13	-43.6	156	1.39
18	25	171.7	-78.8	144	1.28
82	106	184.3	-47.2	63.2	1.64
65	73	211.6	-61.2	85.5	1.8
39	83	112.6	-36.3	53.4	1.57
20	27	176.6	-78.4	139	1.49
17	14	286.9	-146	292	1.43
59	117	120.7	-33.2	45.7	1.5

Length	Angle	Lo	Dpar	Lc
7.48	86.1	15.78	1.51	11.57
15.42	56.5	15.82	1.66	15.83
5.8	81.8	15.82	1.66	11.19
13.12	48.5	15.82	1.66	13.99
12.96	81.8	15.82	1.66	14.26
10.05	60	15.82	1.66	11.98
11.36	78.9	15.82	1.66	13.15
13.48	87.6	15.82	1.66	14.63

11.83	44.4	15.82	1.66	12.91
14.31	80.9	15.82	1.66	15.18
10.63	54.7	15.82	1.66	12.28
13.35	71.2	15.82	1.66	14.47
10.82	59.2	15.82	1.66	12.51
10.97	55.2	15.82	1.66	12.54
8.77	75.2	15.82	1.66	11.69
11.98	73.3	15.82	1.66	13.53
15.11	57.4	15.82	1.66	15.61
13.85	64.4	15.83	1.71	14.76
13.52	80.3	15.8	1.6	14.64
9.53	55.4	15.8	1.6	11.51
12.52	90	15.8	1.6	13.98
13.14	62.8	15.8	1.6	14.23
10.06	80.1	15.8	1.6	12.27
4.36	37.2	15.8	1.6	9.883
10.4	85.7	15.85	1.77	12.53
14.37	61.8	15.85	1.78	15.11
11.35	49	15.88	1.9	12.67
9.99	37.8	15.88	1.9	11.29
11.74	87.1	15.88	1.9	13.45
11.27	30.7	15.88	1.9	12.05
13.68	53	15.84	1.74	14.49
12.21	69.1	15.81	1.64	13.65
12.78	34.9	15.81	1.64	13.42
6.98	56.2	15.81	1.64	10.94
9.6	43.6	15.81	1.64	11.2
11.37	32.9	15.8	1.57	12.2
13.67	68.5	15.78	1.49	14.67
14.72	56.6	15.78	1.49	15.31
11.44	51.9	15.78	1.49	12.8
11.95	67.7	15.76	1.43	13.45
9.53	67.5	15.78	1.5	11.76
7.81	76	15.78	1.5	11.51
14.04	54.9	15.78	1.5	14.79
9.3	55.5	15.78	1.5	11.35
14.43	64.2	15.83	1.7	15.17
14.89	65.5	15.82	1.65	15.51
8.06	51.3	15.82	1.65	10.95
10.26	64.8	15.78	1.5	12.22
8.06	88.1	15.78	1.5	11.7
9.02	76.2	15.8	1.6	11.77
14.88	51	15.75	1.39	15.38
11.47	67.4	15.75	1.39	13.11
10.1	48.9	15.75	1.39	11.74
11.06	72.9	15.73	1.33	12.89
12.19	58.7	15.73	1.33	13.49
14.68	46	15.73	1.33	15.17
9.32	70.7	15.73	1.33	11.72
13.35	77	15.79	1.55	14.51
11.54	69.1	15.82	1.68	13.18
12.85	13.5	15.82	1.68	12.98

9.05	78.5	15.82	1.68	11.81
9.79	60.7	15.82	1.68	11.82
13.91	70.9	15.78	1.5	14.86
11.32	54.1	15.77	1.48	12.76
13.71	49	15.77	1.48	14.45
12.42	50.6	15.81	1.62	13.5
9.41	87.8	15.83	1.7	12.01
9.02	43.6	15.83	1.7	10.78
13.59	53.2	15.83	1.7	14.43
12.64	82.3	15.78	1.49	14.05
11.33	80.3	15.81	1.62	13.14
10.75	61.4	15.81	1.62	12.51
13.68	50.6	15.81	1.62	14.46
13.22	80.1	15.8	1.57	14.43
13.96	51.9	15.8	1.57	14.69
13.63	60.5	15.8	1.57	14.56
13.25	46.8	15.83	1.72	14.06
13.07	60.4	15.83	1.72	14.15
9.91	78.7	15.79	1.56	12.16
9.89	58.5	15.79	1.56	11.84
6.9	65.2	15.82	1.67	11.14
8.72	70.1	15.82	1.67	11.58
13.06	77.3	15.81	1.64	14.31
10.77	32.6	15.77	1.48	11.71
11.49	74.8	15.77	1.48	13.21
10.15	75.2	15.77	1.48	12.29
9.02	62.8	15.77	1.48	11.46
9.31	77.4	15.77	1.48	11.86
13.64	51.7	15.76	1.44	14.44
11.15	55.4	15.76	1.44	12.67
10.8	66.7	15.76	1.44	12.63
8.07	88.9	15.78	1.51	11.71
11.12	77.6	15.78	1.51	12.98
10.61	63.6	15.82	1.68	12.45
13.46	80.3	15.75	1.38	14.6
11.35	82.5	15.78	1.51	13.17
4.31	89.8	15.78	1.51	10.93

Table S4 (continued): Single grain data of Apatite Fission Track analysis

KP702 (Ellesmere Island, Canadian High Arctic)

Location	**Cf-irrad.**
Cape Herschel	no
Lithology	**Zeta**
Granite	346
Stratigraphic	**error_Zeta**
Paleoproterozoic	12
Formation	**RhoD**
Rae Craton	1.200E+6
Lat N	**Nd**
78°36.155'	3096
Long W	**Length reduction in standard**
74°36.284'	0.893
Elevation	
5	

Ns	Ni	Age	-95%	95%	Dpar
23	9	509.1	-273	564	2.63
15	5	593.7	-377	956	2.34
49	17	571.4	-241	405	1.98
9	3	593.7	-432	1421	2.31
42	15	555.8	-247	429	2.01
20	8	498.5	-279	603	1.93
21	7	593.7	-340	750	2.92
22	7	620.7	-354	774	2.75
11	3	718.5	-516	1609	2.66
17	5	668.9	-420	1039	2.48
12	4	593.7	-401	1132	2.18
14	5	555.8	-355	913	2.69
23	7	647.5	-367	798	2.08
19	6	625.1	-374	868	2.35
15	5	593.7	-377	956	2.7

Length	Angle	Lo	Dpar	Lc
12.64	87	16.09	2.7	14.06
14.42	41	16.09	2.7	14.89
14.66	61	16.09	2.7	15.31
12.36	77	16.09	2.7	14
9.92	57	16.09	2.7	11.82
14.89	56	16.09	2.7	15
12.23	35	16.09	2.7	12.97
14.45	51	16.09	2.7	15.05
9.99	82	15.99	2.32	12.24
13.11	61	15.99	2.32	14.19
11.19	82	15.99	2.32	13.05
9.79	43	15.99	2.32	11.32
13.96	52	15.99	2.32	14.69

12.25	77	15.99	2.32	13.75
14.5	42	15.99	2.32	14.97
16.57	87	15.99	2.34	16.73
14.76	76	16.04	2.5	15.47
12.96	73	16.07	2.63	14.21
15.54	76	16.07	2.63	16.01
10.5	57	16.07	2.63	12.24
9.67	24	16.07	2.63	10.46
12.61	71	16.04	2.53	13.95
11.93	55	15.99	2.34	13.23
10.74	86	15.99	2.34	12.76
12.8	47	15.87	1.87	13.72
12.93	46	15.87	1.87	13.8
14.69	53	15.87	1.87	15.25
12.34	44	15.87	1.87	13.29
11.32	55	15.87	1.87	12.78
11.54	63	15.87	1.87	13.09
11.67	26	15.87	1.87	12.23
13.33	55	15.87	1.87	14.26
11.8	71	15.87	1.87	13.38
13.76	13	15.87	1.87	13.85
12.76	68	15.94	2.11	14.02
11.32	58	15.94	2.11	12.85
11.7	57	15.94	2.11	13.1
12.76	43	15.94	2.11	13.6
13.31	40	16.03	2.48	13.97
10.84	27	15.91	2.01	11.56
14.06	41	15.91	2.01	14.6
12.18	44	15.91	2.01	13.17
13.92	35	15.91	2.01	14.38
12.11	86	16.04	2.51	13.7
13.62	43	16.04	2.51	14.28
14.51	19	15.89	1.93	14.65
13.45	56	15.89	1.93	14.36
11.28	56	15.89	1.93	12.78
13.25	69	15.89	1.93	14.38
14.02	87	15.89	1.93	15
13.71	79	16.08	2.66	14.76
13.31	48	16.03	2.48	14.13
14.91	48	15.95	2.18	15.37
10.59	58	15.95	2.18	12.32
12.97	63	15.95	2.18	14.11
11.92	40	16.09	2.69	12.86
14.75	68	16.09	2.69	15.43
13.78	71	15.99	2.32	14.77
13.1	54	15.99	2.32	14.07
14.02	68	15.99	2.32	14.91
12.66	21	15.99	2.32	12.97
12.36	81	15.99	2.32	13.85
14.21	51	15.99	2.32	14.87
13.67	88	15.99	2.32	14.76
11.45	53	15.99	2.32	12.84

12.6	35	15.99	2.32	13.28
12.84	24	15.99	2.32	13.2

Table S4 (continued): Single grain data of Apatite Fission Track analysis

KP737 (Ellesmere Island, Canadian High Arctic)

Location	**Cf-irrad.**
Leffert Glacier	no
Lithology	**Zeta**
Plagiogranite	346
Stratigraphy	**error_Zeta**
Paleoproterozoic	12
Formation	**RhoD**
Rae Craton	1.436E+6
Lat N	**Nd**
78°42.976´	7152
Long W	**Length reduction in standard**
76°46.732`	0.893
Elevation	
1136	

Ns	Ni	Age	-95%	95%	Dpar
7	3	554.3	-411	1417	2.29
5	2	592.1	-477	2080	2.01
3	3	243.4	-195	917	1.88
6	3	478	-359	1298	2.01
10	4	592.1	-405	1172	2.5
8	3	629.7	-461	1531	1.79
10	3	778	-560	1747	2.06
4	1	922.9	-818	4832	2.14
6	3	478	-359	1298	2.19
14	5	659.7	-420	1062	2.24
7	3	554.3	-411	1417	2.13
6	2	704.3	-561	2293	2.58
17	8	506.7	-288	633	2.32
9	3	704.3	-511	1641	2.39
11	4	648.5	-440	1243	2.4
13	4	759.7	-508	1379	2.08
17	5	792.6	-495	1203	2.49
19	6	741.3	-441	1008	2.32
6	2	704.3	-561	2293	2.25

Length	Angle	Lo	Dpar	Lc
10.97	16	15.93	2.1	11.27
14.93	52	15.99	2.33	15.43
12.28	14	15.99	2.33	12.45
13.72	51	15.89	1.94	14.49
12.97	50	15.89	1.94	13.91
15.5	80	15.91	2	16
13.35	20	16.01	2.4	13.58
13.68	66	16.01	2.4	14.65
11.45	51	16.01	2.4	12.79

12.99	31	15.95	2.16	13.51
12.39	69	15.93	2.08	13.77
13.04	72	16	2.36	14.26
13.02	58	15.92	2.05	14.08
14.22	55	15.91	2.02	14.92
15.52	33	15.91	2.02	15.72
13.89	63	15.92	2.05	14.77
8.39	48	15.97	2.25	10.88
12.54	82	16.09	2.69	13.98

Table S4 (continued): Single grain data of Apatite Fission Track analysis

KP740 (Ellesmere Island, Canadian High Arctic)

Location
North of Stygge Glacier
Lithology
Granite
Stratigraphy
Paleoproterozoic
Formation
Rae Craton
Lat N
78°37.003´
Long W
79°58.461´
Elevation
1512

Cf-irrad.
no
Zeta
346
error_Zeta
12
RhoD
1.436E+6
Nd
7152
Length reduction in standard
0.893

Ns	Ni	Age	-95%	95%	Dpar
6	3	478	-359	1298	1.84
10	3	778	-560	1747	1.87
6	2	704.3	-561	2293	1.79
4	2	478	-391	1853	1.6
5	2	592.1	-477	2080	1.6
13	4	759.7	-508	1379	1.73
4	1	922.9	-818	4832	1.36
4	1	922.9	-818	4832	1.36
5	1	1134	-997	5323	1.58
3	1	704.3	-631	4271	1.47
5	2	592.1	-477	2080	1.75
20	8	592.1	-330	704	1.62
14	5	659.7	-420	1062	1.73
7	3	554.3	-411	1417	1.72
7	3	554.3	-411	1417	1.66
4	2	478	-391	1853	1.61
5	2	592.1	-477	2080	1.52
5	2	592.1	-477	2080	1.52
7	3	554.3	-411	1417	1.55
5	2	592.1	-477	2080	1.58

Length	Angle	Lo	Dpar	Lc

Table S5: Detailed results of apatite (U-Th-Sm)/He Thermochronolo

Sample Aliquot #	Raw AHe age (Ma)	Error (Ma)	Weighted Ft	Corrected AHe age (Ma)	Error (Ma)	^{4}He (ncc)	^{147}Sm (ppm)	^{232}Th (ppm)	$^{238}U+^{235}U$ (ppm)	eU (ppm)	mass (mg)	^{147}Sm (ng)	^{232}Th (ng)	$^{238}U+^{235}U$ (ng)	equ. sphere radius (µm	Length 1 (µm)	Length 2 (µm)	Width 1 (µm)	Width 2 (µm)	Width 3 (µm)	Morphology	number pyramidal termination
Late Paleocene sandstone, Mt. Lawson Fm, 78°48.870'N, 82°1.778'W, 272 masl																						
CXII-30#1	163	10	0.72	**227**	18	0.6724	7	39	6	15	0.0022	0.014814713	0.087650000	0.012849293	54	150.0	146.0	102.0	101.0	86.0	hexagonal prism	1
CXII-30#2	204	13	0.65	**313**	25	3.7254	34	56	64	79	0.0019	0.064457256	0.107000000	0.122843243	46	164.0	162.0	81.0	64.0	81.0	hexagonal prism	2
CXII-30#3	208	13	0.63	**331**	26	5.4550	37	45	115	128	0.0017	0.412150000	0.075500000	0.195200000	45	172.4	173.4	73	65.4	68.1	hexagonal prism	2
CXII-30#4	216	13	0.69	**312**	25	2.8748	57	36	30	42	0.0028	1.057400000	0.099800000	0.083500000	56	181.9	180.3	106.7	83.2	67.2	hexagonal prism	2
CXII-30#5	177	11	0.68	**258**	21	2.2394	26	73	28	47	0.0023	0.384700000	0.164700000	0.064250000	55	132.4	130.4	97.5	91.1	84.2	hexagonal prism	2
Early Triassic sandstone, Bjorne Formation, 78°44.253'N, 83°21.230'W, 230 masl																						
CXII-05#1	208	13	0.73	**284**	23	4.8199	99	110	61	92	0.0022	1.428050000	0.237650000	0.130950000	55	137.9	134.9	102.6	99.3	98.8	hexagonal prism	1
Late Devonian sandstone, Fram Formation, 77°31.953'N, 83°11.849'W, 285 masl																						
CXII-22#1	90	6	0.72	**124**	10	1.0162	19	83	4	24	0.0040	0.076162500	0.329100000	0.014899181	59	184.0	184.0	98.0	86.0	94.0	hexagonal prism	0
Late Devonian sandstone, Fram Formation, 77°47.900'N, 82°43.047'W, 75 masl																						
CXII-45#1	113	7	0.73	**155**	12	0.6924	31	134	7	40	0.0027	0.558350000	0.357645611	0.018200000	58	154.9	155.1	111.1	102.3	96.3	hexagonal prism	1
CXII-45#2	117	7	0.66	**178**	14	0.5336	31	149	7	44	0.0025	0.503250000	0.368438174	0.018250000	51	172.1	161.6	88.1	76.7	87.9	hexagonal prism	2
CXII-45#3	115	7	0.70	**164**	13	1.3257	30	50	6	19	0.0025	0.501400000	0.125591558	0.014400000	55	114.2	118.2	99.9	96	83.1	hexagonal prism	0
CXII-45#4	152	9	0.74	**204**	16	0.4603	76	208	35	88	0.0028	1.396600000	0.572478389	0.096700000	62	150.8	157.5	112.1	102.6	100.5	hexagonal prism	1
CXII-45#5	85	5	0.67	**126**	10	1.3606	48	287	27	97	0.0016	0.530050000	0.470502837	0.043500000	47	148.3	150.3	88.2	72.9	79.5	hexagonal prism	1
Late Devonian sandstone, Fram Formation, 77°46.310'N, 83°17.415'W, 282 masl																						
CXII-46#1	114	7	0.75	**152**	12	1.3613	12	37	9	19	0.0054	0.065722500	0.199468661	0.050647214	64	237.0	237.0	114.0	108.0	92.0	hexagonal prism	2
CXII-46#3	90	6	0.80	**114**	9	2.5532	31	24	22	30	0.0082	0.256732500	0.195125402	0.183789891	77	199.0	201.0	146.0	131.0	144.0	hexagonal prism	2
CXII-46#4	90	6	0.73	**123**	10	0.5655	5	32	6	14	0.0038	0.017317500	0.124249599	0.021948793	61	145.0	145.0	119.0	119.0	100.0	hexagonal prism	2
Late Devonian sandstone, Fram Formation, 77°40.818'N, 83°18.831'W, 125 masl																						
C-XII-10#1	99	6	0.80	**125**	15	0.2248	2	6	1	2	0.0090	0.020265000	0.051350000	0.006349651	79	197.0	208.0	154.0	156.0	128.0	hexagonal prism	2
Late Devonian sandstone, Fram Formation, 77°22.602´N, 83°11.272´W, 134 masl																						
C11-126I#1	127	8	0.59	**215**	17	2.7650	46	10	132	137	0.0013	0.061238686	0.013617907	0.174842752	39	168.0	167.0	62.0	59.0	64.0	hexagonal prism	2
C11-126I#2	146	9	0.69	**211**	17	0.5360	12	40	1	11	0.0030	0.035408019	0.118941082	0.001677571	57	132.0	134.0	101.0	89.0	94.0	hexagonal prism	0
C11-126I#3	157	10	0.75	**210**	17	0.6290	4	29	4	11	0.0031	0.012605473	0.088494923	0.011884130	66	165.0	175.0	117.0	86.0	112.0	hexagonal prism	1
C11-126I#4	215	13	0.64	**335**	27	0.9070	43	36	17	28	0.0013	0.056449809	0.046509784	0.022845269	38	85.0	75.0	84.0	74.0	84.0	hexagonal prism	0
Middle Devonian sandstone, Hecla Bay Formation, 77°22.330´N, 82°43.569´W, 254 masl																						
C11-125I#1	186	12	0.81	**230**	18	3.2340	28	13	19	24	0.0063	0.178775001	0.084733862	0.120571158	84	204.0	213.0	117.0	163.0	129.0	hexagonal prism	1
C11-125I#2	193	12	0.84	**230**	18	22.6630	68	31	95	106	0.0092	0.628742452	0.289055232	0.880654744	102	283.0	290.0	169.0	173.0	188.0	ellipsoi	0
Lower-middle Devonian sandstone, Strathcona Fiord Formation, 78°06.096'N, 82°01.213'W, 140 ma																						
CXII-27#1	136	8	0.74	**184**	15	1.3015	28	60	9	25	0.0033	0.091755000	0.200850000	0.029998350	64	189.0	193.0	106.0	94.0	103.0	hexagonal prism	1
CXII-27#2	118	7	0.74	**161**	13	1.3887	8	68	5	21	0.0047	0.036757500	0.316150000	0.021548815	63	190.0	182.0	120.0	98.0	112.0	hexagonal prism	2
Lower-middle Devonian sandstone, Strathcona Fiord Formation, 77°39.333'N, 82°45.239'W, 325 ma																						
CXII-42#1	122	8	0.77	**159**	13	0.4504	4	11	7	10	0.0031	0.010785000	0.035000000	0.021898796	69	145.0	153.0	116.0	113.0	117.0	hexagonal prism	1
CXII-42#2	164	10	0.76	**216**	17	1.5821	4	22	11	16	0.0050	0.018862500	0.108900000	0.052897091	67	171.0	157.0	126.0	119.0	119.0	hexagonal prism	2
CXII-42#3	47	3	0.73	**65**	5	0.1249	5	27	3	10	0.0023	0.010785000	0.060200000	0.007349596	63	145.0	122.0	110.0	94.0	111.0	hexagonal prism	1
CXII-42#4	135	8	0.73	**186**	15	0.5034	23	12	8	12	0.0029	0.067230000	0.034550000	0.021848798	52	103.0	99.0	105.0	109.0	106.0	hexagonal prism	0
Lower-middle Devonian sandstone, Strathcona Fiord Formation, 78°07.272'N, 82°27.090'W, 283 ma																						
CXII-48#2	160	10	0.74	**216**	17	0.5916	33	8	6	9	0.0039	0.127665000	0.030530689	0.021998790	62	137.0	134.0	125.0	110.0	119.0	hexagonal prism	2
CXII-48#3	22	1	0.81	**27**	2	0.0813	8	3	2	3	0.0100	0.076845000	0.032646814	0.022348771	84	203.0	211.0	163.0	143.0	152.0	hexagonal prism	2
Lower-middle Devonian sandstone, Strathcona Fiord Formation, 77°32.839'N, 82°34.311'W, 627 ma																						
C-XII-15#1	174	11	0.83	**210**	25	6.3562	26	47	27	39	0.0078	0.203790000	0.365400000	0.209538475	86	202.0	199.0	167.0	147.0	164.0	hexagonal prism	1
C-XII-15#2	196	12	0.60	**324**	38	8.0720	634	1279	217	551	0.0006	0.407947500	0.823000000	0.139492328	37	87.0	86.0	73.0	64.0	73.0	hexagonal prism	1
Lower-middle Devonian sandstone, Strathcona Fiord Formation, 77°35.400´N, 83°36.305´W, 292 mas																						
C11-119/1#1	210	13	0.66	**316**	25	2.0160	7	47	26	38	0.0021	0.014209369	0.097831953	0.055151325	48	160.0	161.0	82.0	75.0	80.0	hexagonal prism	2
C11-119/1#2	171	11	0.67	**255**	20	0.5030	10	16	8	12	0.0020	0.021130677	0.032185845	0.016318035	48	137.0	139.0	84.0	86.0	83.0	hexagonal prism	2
C11-119/2#1	55	3	0.60	**92**	7	0.2990	29	61	16	32	0.0014	0.041643263	0.088114635	0.023681585	41	169.0	169.0	64.0	64.0	64.0	hexagonal prism	2
C11-119/2#2	54	3	0.60	**90**	7	0.1410	57	59	10	27	0.0009	0.050591510	0.052004281	0.008797589	42	122.0	121.0	67.0	62.0	67.0	hexagonal prism	1

Table S5 (continued): Detailed results of apatite (U-Th-Sm)/He Thermochronolo

Sample Aliquot #	Raw AHe age (Ma)	Error (Ma)	Weighted Ft	Corrected AHe age (Ma)	Error (Ma)	^{4}He (ncc)	^{147}Sm (ppm)	^{232}Th (ppm)	$^{238}U+^{235}U$ (ppm)	eU (ppm)	mass (mg)	^{147}Sm (ng)	^{232}Th (ng)	$^{238}U238+^{235}U$ (ng)	equ. sphere radius (µm	Length 1 (µm)	Length 2 (µm)	Width 1 (µm)	Width 2 (µm)	Width 3 (µm)	Morphology	number pyramidal termination
Lower-middle Devonian sandstone, Strathcona Fiord Formation, 77°32.931´N, 83°39.763´W, 126 mas																						
C11-120I#1	192	12	0.65	**297**	24	4.1680	74	62	134	152	0.0012	0.087567741	0.073317264	0.158766750	46	137.0	139.0	68.0	67.0	77.0	hexagonal prism	1
C11-120I#3	157	10	0.68	**230**	18	1.0400	11	25	24	31	0.0018	0.018825176	0.044873313	0.043376396	51	163.0	167.0	83.0	81.0	72.0	hexagonal prism	1
C11-120I#4	202	13	0.79	**256**	20	2.0520	5	17	8	12	0.0068	0.030841552	0.117705143	0.054707025	75	174.0	180.0	122.0	121.0	127.0	hexagonal prism	0
Lower-middle Devonian sandstone, Strathcona Fiord Formation, 77°19.697´N, 82°28.540´W, 184 mas																						
C11-124I#1	121	8	0.67	**180**	14	0.2880	8	16	5	9	0.0023	0.018234354	0.036299727	0.010731933	50	163.0	162.0	84.0	83.0	82.0	hexagonal prism	2
C11-124I#2	88	5	0.71	**123**	10	0.1980	6	16	2	6	0.0030	0.018926790	0.048469805	0.006904692	56	154.0	160.0	96.0	81.0	85.0	hexagonal prism	0
C11-124I#3	197	12	0.69	**284**	23	1.5420	19	47	20	32	0.0021	0.039577183	0.096775591	0.040807872	47	111.0	114.0	91.0	79.0	87.0	hexagonal prism	0
C11-124I#5	184	11	0.72	**258**	21	1.5470	17	42	34	44	0.0016	0.026030637	0.065765561	0.052709407	51	114.0	115.0	94.0	91.0	102.0	hexagonal prism	1
Paleoproterozoic granite, 78°29.645'N, 81°17.212'W, 780 ma:																						
CXII-14#1	150	9	0.68	**219**	17	0.6924	36	5	18	21	0.0020	0.072622500	0.009300000	0.034948078	49	135.0	128.0	83.0	71.0	79.0	hexagonal prism	0
CXII-14#2	194	12	0.65	**297**	24	0.5336	84	11	24	31	0.0008	0.459300000	0.009300000	0.019650000	42	88.3	91.1	81.2	76	79.9	hexagonal prism	1
CXII-14#3	231	14	0.66	**347**	28	1.3257	64	12	41	47	0.0010	0.449250000	0.013050000	0.043000000	43	105.7	108.9	81.3	79.8	75.2	hexagonal prism	1
CXII-14#4	187	12	0.68	**275**	22	0.4603	27	10	15	19	0.0011	0.203500000	0.011300000	0.017150000	45	108.9	103.4	84.6	84.4	81.9	hexagonal prism	1
CXII-14#5	142	9	0.74	**192**	15	1.3606	47	9	34	38	0.0021	0.100275000	0.020050000	0.072546010	66	160.0	158.0	116.0	101.0	109.0	ellipsoi	0
Paleoproterozoic migmatite, 78°13.142'N, 81°29.978'W, 610 ma:																						
CXII-25#1	177	11	0.65	**271**	22	1.8392	47	5	39	43	0.0021	0.096420000	0.011150000	0.081445520	47	185.0	184.0	71.0	77.0	72.0	hexagonal prism	2
CXII-25#2	396	25	0.71	**556**	44	3.6811	59	10	22	28	0.0030	1.183550000	0.029500000	0.065950000	56		153.1	101	95.4	94.6	hexagonal prism	2
CXII-25#3	217	13	0.71	**305**	24	1.9218	57	6	27	31	0.0025	0.952300000	0.014450000	0.067300000	54	131.5	117.8	94.1	87.2	87.9	hexagonal prism	0
Paleoproterozoic orthogneiss, 78°24.373'N, 81°11.946'W, 797 ma																						
CXII-36#1	153	9	0.71	**214**	17	0.4319	67	9	6	12	0.0027	0.179070000	0.022931990	0.016249106	56	123.0	130.0	90.0	98.0	88.0	hexagonal prism	0
CXII-36#2	203	13	0.73	**278**	22	1.5970	136	30	16	30	0.0027	0.364042500	0.080560966	0.042047687	61	166.0	175.0	107.0	95.0	88.0	hexagonal prism	1
CXII-36#3	157	10	0.67	**233**	19	0.8745	120	16	15	25	0.0023	0.278835000	0.038229336	0.034148122	50	153.0	171.0	87.0	85.0	77.0	hexagonal prism	2
CXII-36#4	170	11	0.76	**223**	18	2.9412	101	24	15	26	0.0065	0.653437500	0.154641776	0.099594522	67	268.0	273.0	112.0	100.0	110.0	hexagonal prism	2
CXII-36#5	158	10	0.67	**237**	19	0.3213	64	5	6	10	0.0023	0.147847500	0.010898537	0.012799296	49	178.0	171.0	84.0	79.0	77.0	hexagonal prism	2
Paleoproterozoic pyroxenite, 78°24.425'N, 81°11.976'W, 789 ma:																						
CXII-37#1	210	13	0.59	**354**	28	0.4025	49	30	14	24	0.0007	0.035947500	0.022255331	0.010099445	37	104.0	114.0	66.0	62.0	62.0	hexagonal prism	1
CXII-37#2	137	9	0.63	**219**	17	0.1916	15	12	7	11	0.0011	0.017160000	0.014170357	0.007949563	44	72.0	81.0	76.0	68.0	87.0	hexagonal prism	0
CXII-37#3	140	9	0.66	**212**	17	0.2573	40	10	9	14	0.0013	0.049867500	0.011975237	0.011799351	48	130.0	132.0	80.0	75.0	72.0	hexagonal prism	1
Paleoproterozic Granite, 78°46.675'N, 81°02.169'W, 683 ma:																						
CXII-13#1	239	15	0.75	**318**	37	7.8995	60	32	80	91	0.0030	0.180821808	0.096700000	0.243336616	60	160.0	182.0	109.0	103.0	98.0	hexagonal prism	1
CXII-13#2	238	15	0.74	**322**	38	7.1580	44	15	49	55	0.0046	0.205083535	0.071750000	0.225037622	62	232.0	217.0	108.0	88.0	103.0	hexagonal prism	2
CXII-13#4	206	13	0.73	**281**	33	6.5315	42	23	52	60	0.0044	0.185055212	0.103450000	0.231537265	61	223.0	226.0	103.0	95.0	94.0	hexagonal prism	2
CXII-13#5	234	15	0.68	**345**	27	3.5584	63	22	36	45	0.0030	0.100275000	0.020050000	0.072546010	50	230.0	233.0	78.0	80.0	77.0	hexagonal prism	2
Paleoproterozoic Granite, 77°12.770´N, 80°59.900´W, 678 mas																						
C11-121I#2	213	13	0.63	**339**	27	0.4920	53	17	7	14	0.0017	0.087472657	0.029002262	0.011251687	44	154.0	154.0	76.0	65.0	75.0	hexagonal prism	2
Paleoproterozoic Granite, 78°45.004´N, 75°35.258´W, 1227 mas																						
KP738#1	253	16	0.61	**411**	48	0.6377	56	4	21	25	0.0009	0.052390756	0.003650000	0.019148947	56	128.0	127.0	68.0	61.0	66.0	hexagonal prism	1
KP738#2	482	30	0.58	**826**	97	1.1118	37	8	17	21	0.0010	0.035378517	0.007550000	0.016249106	37	98.0	100.0	69.0	67.0	68.0	hexagonal prism	2
KP738#3	456	28	0.60	**757**	89	0.4734	24	2	7	9	0.0011	0.025482070	0.002100000	0.007549585	24	98.0	98.0	74.0	67.0	76.0	hexagonal prism	2
KP738#4	344	21	0.67	**510**	60	1.4762	40	1	26	29	0.0013	0.051584089	0.001800000	0.033598152	40	124.0	124.0	82.0	81.0	75.0	hexagonal prism	1
Paleoproterozoic Granite, 78° 36.155'N, 74° 36.284'W, 5 ma																						
KP702#2	503	31	0.73	**692**	81	7.9038	61	20	57	65	0.0020	0.121342500	0.038850000	0.114293714	53	138.0	134.0	108.0	94.0	86.0	hexagonal prism	1
KP702#3	200	12	0.71	**284**	33	6.0564	118	37	149	164	0.0015	0.182842500	0.057550000	0.231037292	54	133.0	112.0	99.0	90.0	80.0	hexagonal prism	1
KP702#4	332	21	0.69	**481**	57	2.6429	37	7	30	34	0.0020	0.072870000	0.014450000	0.059896706	46	110.0	107.0	89.0	82.0	84.0	hexagonal prism	0
Paleoproterozoic Granite, 78° 32.338'N, 74° 57.598'W, 25 ma																						
KP703#2	312	19	0.78	**398**	47	12.9018	76	6	40	46	0.0078	0.594229070	0.046600000	0.316532590	75	249.0	244.0	130.0	127.0	114.0	hexagonal prism	2
KP703#3	240	15	0.76	**314**	37	5.1805	64	47	25	39	0.0048	0.308723605	0.223700000	0.120293384	65	246.0	238.0	112.0	100.0	105.0	hexagonal prism	1
KP703#4	218	14	0.74	**295**	35	2.5792	55	24	16	24	0.0044	0.246540514	0.107100000	0.069096200	62	208.0	193.0	110.0	97.0	103.0	hexagonal prism	2

Table S5 (continued): Detailed results of apatite (U-Th-Sm)/He Thermochronolo

Sample Aliquot #	Raw AHe age (Ma)	Error (Ma)	Weighted Ft	Corrected AHe age (Ma)	Error (Ma)	^{4}He (ncc)	^{147}Sm (ppm)	^{232}Th (ppm)	$^{238}U+^{235}U$ (ppm)	eU (ppm)	mass (mg)	^{147}Sm (ng)	^{232}Th (ng)	$^{238}U238+^{235}U$ (ng)	equ. sphere radius (µm	Length 1 (µm)	Length 2 (µm)	Width 1 (µm)	Width 2 (µm)	Width 3 (µm)	Morphology	number pyramidal termination
Paleoproterozoic Granite, 78° 42.976'N, 76° 46.732'W, 1136 ma																						
KP737#1	140	9	0.72	**195**	23	0.4693	33	20	10	16	0.0019	0.062512500	0.037250000	0.018099005	58	134.0	130.0	99.0	93.0	93.0	hexagonal prism	1
KP737#3	147	9	0.72	**205**	24	0.4643	31	11	9	13	0.0022	0.067072500	0.024650000	0.019398933	57	154.0	162.0	101.0	93.0	78.0	hexagonal prism	1
KP737#4	231	14	0.78	**295**	35	1.6535	24	7	5	8	0.0082	0.197872500	0.058200000	0.042847643	74	266.0	260.0	135.0	114.0	119.0	hexagonal prism	2
KP737#5	121	8	0.68	**178**	21	0.2460	29	9	5	9	0.0023	0.067290000	0.020350000	0.011349376	51	149.0	148.0	95.0	94.0	69.0	hexagonal prism	2
Early Cambrian Quartzite, Dallas Bugt Formation, 79° 32.283'N, 75° 1.220'W, 486 m																						
KP711#1	46	3	0.66	**71**	8	0.5070	72	73	86	107	0.0009	0.063090000	0.063500000	0.074645894	47	98.0	88.0	86.0	78.0	74.0	hexagonal prism	1
KP711#4	54	3	0.75	**72**	8	0.3060	59	5	9	13	0.0046	0.274657500	0.021700000	0.039347836	64	149.0	153.0	128.0	113.0	123.0	hexagonal prism	2
KP711#6	7	0.4	0.70	**10**	1	0.0482	63	14	33	40	0.0015	0.095430000	0.021250000	0.049947253	52	125.0	128.0	89.0	89.0	81.0	hexagonal prism	1
Archean Gneiss, 76°21.336 N, 69°29.665 W, 216 mas																						
GRO21#1	124	1	0.77	**161**	8	1.6415	24	5	15	17	0.0065	0.153600000	0.031000000	0.099994500	70	235.3	234.5	127.3	93.7	125.8	hexagonal prism	2
GRO21#2	146	1	0.78	**187**	10	3.8914	49	16	57	61	0.0036	0.173925000	0.056500000	0.203488808	72	160.9	158.7	118.7	127.7	112.8	hexagonal prism	1
GRO21#3	162	2	0.7	**230**	12	1.9840	40	8	36	38	0.0026	0.105000000	0.020500000	0.094494803	53	136.0	139.2	96.0	88.6	102.9	hexagonal prism	2
Archean Gneiss, 76°24.710 N, 69°32.388 W, 388 mas																						
GRO23#1	107	1	0.69	**155**	8	0.2897	25	3	7	8	0.0028	0.069776000	0.009000000	0.019500000	57	209.5	210.7	84.6	84.6	86.9	hexagonal prism	1
GRO23#2	94	1	0.72	**131**	7	0.2654	17	3	7	8	0.0030	0.049875000	0.010000000	0.020498873	56	138.5	143.3	115.4	103.3	85.4	hexagonal prism	1
GRO23#3	89	2	0.74	**121**	7	0.2088	22	2	5	5	0.0037	0.082050000	0.007000000	0.016999065	60	152.9	141.6	106.9	117.0	105.2	hexagonal prism	2
Banded Iron Formation, 76°17.187 N, 68°46.659 W, 295 mas																						
GRO35#1	12	0.4	0.63	**20**	1	0.0078	5	7	2	4	0.0013	0.006994000	0.009000000	0.003000000	44	160.3	174.3	56.5	72.9	68.1	hexagonal prism	1
GRO35#2	15	1	0.62	**24**	1	0.0082	5	5	2	3	0.0016	0.008625000	0.008500000	0.002499863	43	154.7	154.8	60.5	78.3	70.9	hexagonal prism	2
GRO35#3	30	1	0.69	**44**	3	0.0254	3	4	3	4	0.0018	0.005250000	0.008000000	0.004999725	51	157.3	162.9	88.4	69.8	84.1	hexagonal prism	1
Archean Schist, 76°16.927 N, 68°49.888 W, 321 mas																						
GRO36#1	68	1	0.68	**99**	5	0.0912	27	3	4	5	0.0023	0.062307000	0.006500000	0.009000000	50	151.1	152.9	86.2	87.7	83.8	hexagonal prism	2
GRO36#2	54	1	0.75	**72**	4	0.0943	19	5	4	5	0.0027	0.050325000	0.014500000	0.010499423	65	152.7	139.7	101.8	107.5	114.4	hexagonal prism	1
GRO36#3	71	2	0.68	**104**	6	0.0537	22	3	2	3	0.0022	0.048375000	0.005500000	0.004499753	51	117.3	113.2	90.9	101.7	93.6	hexagonal prism	2
Archean Gneiss, 76°22.508 N, 69°32.543 W, 299 mas																						
GRO64#1	116	1	0.77	**152**	7	1.5526	18	13	37	40	0.0027	0.048141000	0.036500000	0.100500000	68	128.6	145.4	119.8	112.5	115.1	hexagonal prism	1
GRO64#2	105	1	0.69	**151**	8	1.0988	26	19	43	48	0.0018	0.047175000	0.033500000	0.077995710	52	157.9	154.2	91.3	63.1	92.4	hexagonal prism	1
GRO64#3	87	2	0.71	**122**	7	0.4744	18	14	24	28	0.0016	0.028500000	0.022500000	0.039497828	55	127.3	122.0	93.6	92.6	86.8	hexagonal prism	1
Proterozoic sandstone, Thule Group, 76°49.437 N, 70°13.534 W, 7 ma																						
GRO24#1	81	1	0.74	**110**	6	0.1707	45	5	2	3	0.0028	0.125300000	0.026000000	0.009500000	62	221.9	215.2	90.9	99.3	90.0	hexagonal prism	0
GRO24#2	86	1	0.66	**131**	7	0.1144	46	10	3	5	0.0021	0.095325000	0.019500000	0.005499698	46	174.9	172.7	75.0	63.9	66.8	hexagonal prism	0
GRO24#3	61	1	0.68	**90**	5	0.0612	42	6	1	3	0.0022	0.117225000	0.016000000	0.003499808	48	212.6	204.8	73.5	78.4	66.8	hexagonal prism	0
GRO24#4	61	1	0.72	**84**	5	0.0758	36	6	1	3	0.0037	0.130125000	0.022000000	0.003999780	59	158.0	166.1	89.2	108.8	86.2	hexagonal prism	0
Proterozoic sandstone, Thule Group, 77°55.106 N, 71°53.863 W, 497 ma																						
GRO52#1	138	2	0.69	**201**	10	0.1389	53	9	4	6	0.0013	0.068757000	0.011500000	0.005000000	51	114.6	117.1	80.2	89.9	81.3	hexagonal prism	1
GRO52#2	212	6	0.69	**308**	18	0.0792	1	3	1	1	0.0021	0.001200000	0.006500000	0.001499918	54	75.2		100.6	112.2	105.2	hexagonal prism	0
Proterozoic sandstone, Thule Group, 77°10.260 N, 70°36.376 W, 187 ma																						
GRO60#1	81	5	0.69	**117**	14	0.9037	33	29	29	36	0.0026	0.085500000	0.073500000	0.073995930	51	167.9	169.2	83.7	87.8	85.7	hexagonal prism	2
GRO60#2	96	6	0.77	**124**	15	0.1279	4	3	3	3	0.0036	0.012900000	0.010000000	0.008499533	71	125.6	125	125.6	125		ellipsoi	0

Cross-over ages are marked in re

Table S6: Zircon U-Pb-Th LA-ICP-MS data of Devonian sandstones from Ellesmere Island (Canada)

LA-ICP-MS analysis was carried out at Institute for Geosciences, Goethe-University Frankfurt, Germany (samples CXI-124, -120, -119 -125) and at Museum für Mineralogie und Geologie, GeoPlasma Lab, Senckenberg naturhistorische Sammlungen Dresden, Germany (sample CXI-126).

CXI-124 (Frankfurt)

Concordant (100 ±10 %) measurments: 99 (of 117)

spot number	^{207}Pb [a] (cps)	U [b] (ppm)	Pb [b] (ppm)	Th [b] / U	^{206}Pbc [c] (%)	$^{206}Pb/^{238}U$ [d]	±2σ (%)	$^{207}Pb/^{235}U$ [d]	±2σ (%)	$^{207}Pb/^{206}Pb$ [d]	±2σ (%)	rho [e]	$^{206}Pb/^{238}U$	±2σ (Ma)	$^{207}Pb/^{235}U$	±2σ (Ma)	$^{207}Pb/^{206}Pb$	±2σ (Ma)	conc. (%)
A04	1881	2	0.4	0.73	0.2	0.1950	3.1	2.054	4.8	0.0764	3.6	0.64	1148	32	1134	33	1106	73	104
A05	50213	35	8.3	0.40	0.6	0.2194	3.2	2.586	3.6	0.08551	1.7	0.89	1278	37	1297	26	1327	32	96
A06	198953	28	18.0	0.72	0.2	0.4956	2.9	12.52	3.1	0.1833	0.9	0.96	2595	63	2645	29	2683	15	97
A07	68976	56	10.2	0.01	2.2	0.1853	2.9	1.928	3.6	0.07547	2.2	0.80	1096	29	1091	25	1081	44	101
A08	16091	9	2.7	0.67	0.1	0.2410	3.1	2.921	3.4	0.0879	1.5	0.90	1392	39	1387	26	1380	28	101
A09	23675	32	9.8	0.68	0.0	0.2567	2.8	3.303	3.2	0.09331	1.4	0.90	1473	38	1482	25	1494	26	99
A10	28817	33	10.1	0.27	0.1	0.2909	2.9	4.044	3.2	0.1008	1.4	0.90	1646	42	1643	27	1640	26	100
A11	81409	26	11.8	0.70	29.0	0.1962	4.1	3.241	7.8	0.1198	6.7	0.52	1155	44	1467	63	1953	119	59
A12	120980	39	16.0	0.25	35.0	0.1883	4.7	1.990	10.0	0.07664	8.8	0.47	1112	48	1112	70	1112	175	100
A13	21982	11	2.8	0.30	1.5	0.2117	3.0	3.077	4.8	0.1054	3.7	0.63	1238	34	1427	37	1721	68	72
A14	54684	18	7.4	0.49	0.0	0.3508	3.1	5.774	3.3	0.1194	0.9	0.96	1938	53	1943	29	1947	16	100
A15	43531	12	5.8	0.88	0.0	0.3816	2.9	6.771	3.0	0.1287	0.9	0.96	2084	52	2082	27	2080	16	100
A16	19165	7	1.8	0.36	10.6	0.1836	3.2	1.930	5.8	0.07625	4.9	0.55	1086	32	1091	40	1102	98	99
A17	66786	20	16.8	1.13	2.5	0.5053	2.8	15.25	4.4	0.2189	3.4	0.64	2636	62	2831	43	2973	55	89
A18	37320	0	0.0	0.45	1.0	0.2189	2.9	2.481	3.5	0.08219	1.8	0.85	1276	34	1266	25	1250	36	102
A19	49781	30	13.2	0.60	1.7	0.3338	2.8	6.425	3.2	0.1396	1.5	0.89	1857	46	2036	28	2222	25	84
A20	65984	14	7.2	0.95	6.8	0.3282	3.0	5.353	4.3	0.1183	3.1	0.70	1830	48	1877	37	1930	55	95
A21	126293	7	4.8	0.56	0.3	0.5463	3.3	15.25	3.4	0.2024	0.9	0.96	2810	75	2831	33	2846	15	99
A22	48650	8	3.1	0.51	4.3	0.3361	3.1	5.502	4.3	0.1187	3.0	0.72	1868	50	1901	37	1937	53	96
A23	94375	3	2.6	0.39	24.8	0.3226	4.1	8.078	6.4	0.1816	4.9	0.64	1802	64	2240	59	2668	82	68
A24	86100	92	32.5	0.43	1.5	0.3150	2.8	5.123	3.2	0.1180	1.5	0.88	1765	43	1840	27	1925	26	92
A25	101656	16	7.5	0.59	4.8	0.2716	3.0	3.583	3.5	0.09568	1.8	0.86	1549	42	1546	28	1542	34	100
A26	67841	4	4.2	0.58	28.8	0.4655	4.1	10.75	7.2	0.1676	5.9	0.57	2464	85	2502	69	2533	98	97
A27	38133	14	3.8	0.55	0.0	0.1979	3.4	3.224	4.1	0.1182	2.3	0.83	1164	36	1463	32	1929	41	60
A28	99639	21	13.0	0.15	b.d.	0.4870	3.5	13.18	4.0	0.1962	1.9	0.88	2558	75	2692	38	2795	31	92
A32	13894	21	5.6	0.35	0.1	0.2463	3.6	3.178	3.9	0.09361	1.6	0.91	1419	46	1452	31	1500	31	95
A33	90450	17	15.9	1.11	4.8	0.5948	2.9	21.00	3.4	0.2561	1.7	0.86	3009	70	3139	33	3223	27	93
A34	29373	24	3.3	0.44	6.7	0.1009	3.2	1.024	5.5	0.07364	4.5	0.57	619	19	716	29	1032	91	60
A35	196768	29	17.7	0.50	2.6	0.5194	3.2	13.41	3.8	0.1872	1.9	0.86	2697	72	2709	36	2718	31	99

A36	94274	24	21.5	1.13	2.3	0.5950	3.1	18.91	3.4	0.2306	1.4	0.91	3010	74	3037	33	3056	23	98
A37	71654	7	5.5	1.15	18.2	0.3956	3.6	8.830	6.3	0.1619	5.2	0.56	2149	65	2321	59	2475	88	87
A38	70880	37	9.6	0.59	5.2	0.2013	2.9	2.297	5.3	0.08276	4.4	0.55	1182	32	1211	38	1264	86	94
A39	68359	12	6.4	0.17	2.0	0.4686	3.2	10.62	3.7	0.1644	1.9	0.86	2477	67	2491	35	2502	32	99
A40	220341	43	19.9	0.13	0.2	0.4477	2.9	11.09	3.0	0.1796	0.9	0.96	2385	58	2530	29	2649	14	90
A41	2271	2	0.5	0.29	0.2	0.2059	3.1	2.237	5.6	0.0788	4.7	0.55	1207	34	1193	40	1167	93	103
A42	74688	39	11.1	0.33	1.9	0.2540	3.0	3.271	3.9	0.09339	2.5	0.76	1459	39	1474	31	1496	48	98
A43	49216	25	8.7	0.65	0.0	0.2923	2.9	4.102	3.2	0.1018	1.2	0.92	1653	43	1655	26	1656	22	100
A44	25351	13	5.1	0.76	0.0	0.3292	3.0	6.089	3.4	0.1342	1.6	0.88	1834	48	1989	30	2153	29	85
A45	18422	22	3.5	0.30	0.0	0.1520	2.9	1.457	3.2	0.06953	1.2	0.92	912	25	913	19	914	25	100
A46	24440	16	4.1	0.39	0.0	0.2385	3.0	2.871	3.2	0.08732	1.1	0.94	1379	38	1374	25	1368	21	101
A47	66556	10	5.9	1.32	16.9	0.3173	3.3	5.929	5.9	0.1355	4.9	0.56	1777	51	1966	53	2171	86	82
A48	30333	9	3.4	0.30	0.0	0.3668	2.9	6.346	3.0	0.1255	0.9	0.95	2014	50	2025	27	2036	16	99
A49	64150	91	24.9	0.26	b.d.	0.2632	2.8	3.392	2.9	0.09349	0.7	0.97	1506	38	1503	23	1498	14	101
A50	23603	22	8.0	0.72	0.4	0.2923	3.0	4.117	3.6	0.1022	2.0	0.84	1653	44	1658	30	1664	36	99
A51	131316	69	15.3	0.05	0.2	0.2251	3.0	3.441	3.3	0.1108	1.3	0.92	1309	36	1514	26	1813	24	72
A52	95421	11	8.0	0.70	0.0	0.5873	2.9	17.94	3.2	0.2215	1.5	0.89	2979	69	2986	32	2992	24	100
A53	67726	53	11.8	0.45	0.6	0.1984	2.8	2.250	3.2	0.08226	1.5	0.89	1167	30	1197	23	1252	29	93
A54	68833	69	13.7	0.25	0.0	0.1935	3.0	2.062	3.1	0.0773	0.9	0.96	1140	31	1136	21	1129	17	101
A55	44280	15	5.3	0.33	0.4	0.3233	3.1	5.216	3.3	0.117	1.1	0.95	1806	49	1855	28	1911	19	95
A59	117183	37	15.4	0.77	1.6	0.3338	2.9	5.444	3.2	0.1183	1.5	0.89	1857	47	1892	28	1931	26	96
A60	23030	24	2.9	0.22	9.2	0.1025	3.0	0.871	6.8	0.06163	6.0	0.45	629	18	636	32	661	130	95
A61	86344	15	6.4	0.57	21.3	0.2600	3.6	3.363	7.5	0.09384	6.6	0.48	1490	48	1496	61	1505	125	99
A62	13214	9	2.2	0.73	1.8	0.2022	3.0	2.465	3.8	0.0884	2.3	0.80	1187	33	1262	28	1391	43	85
A63	77907	22	8.3	0.26	3.8	0.3231	2.9	5.209	3.6	0.1169	2.2	0.79	1805	45	1854	32	1910	40	95
A64	67712	31	12.0	1.21	0.0	0.2738	2.8	3.812	3.0	0.101	1.1	0.94	1560	39	1595	25	1642	20	95
A65	88303	90	16.0	0.03	2.2	0.1833	2.9	1.933	3.7	0.07645	2.3	0.79	1085	29	1092	25	1107	45	98
A66	75809	27	8.9	0.69	3.4	0.2572	3.1	3.439	4.2	0.09696	2.9	0.73	1476	41	1513	34	1567	55	94
A67	40630	30	7.6	0.49	0.0	0.2270	2.9	2.672	3.1	0.08537	0.9	0.95	1319	35	1321	23	1324	18	100
A68	45390	4	2.6	0.50	31.6	0.3134	4.3	4.604	8.1	0.1065	6.9	0.53	1757	67	1750	70	1741	126	101
A70	7637	6	1.4	0.38	0.0	0.2108	2.1	2.395	2.7	0.08241	1.8	0.76	1233	23	1241	20	1255	34	98
A71	1094	1	0.2	0.91	0.0	0.1819	2.7	1.898	4.2	0.07567	3.3	0.64	1077	27	1080	29	1086	65	99
A72	30154	11	3.7	0.48	0.0	0.2977	2.1	4.164	2.3	0.1014	1.0	0.91	1680	31	1667	19	1651	18	102
A73	41170	38	6.7	0.11	0.4	0.1788	2.1	1.877	2.5	0.07617	1.3	0.86	1060	21	1073	16	1100	25	96
A74	74200	6	4.9	0.86	8.9	0.4856	2.3	12.76	3.6	0.1906	2.8	0.64	2552	49	2662	34	2747	45	93
A75	39080	4	3.0	0.51	0.0	0.5601	2.3	16.29	2.5	0.211	1.0	0.92	2867	53	2894	24	2913	16	98
A76	40423	21	7.5	1.16	0.0	0.2730	2.1	3.683	2.7	0.09784	1.7	0.77	1556	29	1568	22	1583	32	98
A77	27563	4	2.1	0.60	7.9	0.2968	2.2	4.229	3.4	0.1033	2.7	0.63	1675	32	1680	29	1685	50	99
A78	81035	37	10.8	0.27	0.0	0.2788	2.0	3.865	2.1	0.1006	0.8	0.93	1585	28	1606	17	1634	14	97
A79	14693	8	2.5	1.09	0.0	0.2197	3.1	2.949	3.4	0.09735	1.5	0.90	1280	36	1395	26	1574	28	81
A80	82188	42	12.2	0.28	0.1	0.2725	2.0	3.642	2.3	0.09693	1.0	0.90	1553	28	1559	18	1566	19	99

A81	17560	18	3.3	0.24	0.1	0.1836	2.1	1.938	2.4	0.07655	1.3	0.85	1087	21	1094	16	1110	26	98
A82	129043	71	20.2	0.54	1.5	0.2583	2.3	3.405	2.8	0.09562	1.5	0.83	1481	31	1506	22	1540	29	96
A83	21805	12	3.2	0.29	0.0	0.2600	2.0	3.374	2.4	0.09413	1.3	0.85	1490	27	1498	19	1511	24	99
A84	178057	80	18.8	0.25	9.0	0.1973	2.6	2.180	5.8	0.08017	5.2	0.44	1161	27	1175	41	1201	102	97
A88	50915	4	2.4	0.59	47.6	0.1641	5.7	1.803	23.6	0.0797	22.9	0.24	980	52	1047	167	1190	453	82
A89	28079	13	4.3	0.52	0.1	0.2904	2.1	4.062	2.4	0.1014	1.2	0.86	1644	31	1647	20	1651	23	100
A90	31481	21	5.2	0.46	0.0	0.2198	2.3	2.594	2.9	0.08559	1.8	0.80	1281	27	1299	22	1329	34	96
A91	7808	5	1.3	0.45	2.8	0.2309	2.0	2.759	3.4	0.08667	2.7	0.60	1339	25	1345	26	1353	53	99
A92	9485	10	1.9	0.28	b.d.	0.1831	2.1	1.895	2.6	0.07505	1.5	0.82	1084	21	1079	17	1070	30	101
A93	44213	14	4.8	0.29	1.1	0.3161	2.0	5.186	2.3	0.119	1.1	0.87	1771	31	1850	20	1941	20	91
A94	37086	30	6.9	0.30	2.8	0.2169	2.1	2.494	5.5	0.08339	5.1	0.37	1265	24	1270	41	1278	100	99
A95	29072	28	4.6	0.22	1.3	0.1566	2.0	1.556	2.5	0.07203	1.6	0.78	938	17	953	16	987	32	95
A96	52500	12	4.2	0.29	0.2	0.3288	2.8	5.379	3.1	0.1187	1.1	0.93	1832	45	1882	27	1936	21	95
A97	192023	27	14.0	0.40	14.3	0.3375	2.7	5.463	5.5	0.1174	4.8	0.49	1875	44	1895	48	1917	85	98
A98	44211	7	5.8	2.06	0.0	0.5175	2.2	13.22	2.4	0.1853	0.8	0.94	2688	49	2695	22	2701	13	100
A99	176308	20	13.5	0.62	1.5	0.5335	2.2	14.25	2.5	0.1938	1.4	0.85	2756	48	2767	24	2774	22	99
A100	211079	38	17.0	0.40	6.1	0.3497	2.2	5.826	3.8	0.1208	3.1	0.58	1933	37	1950	34	1969	56	98
A102	95472	70	18.9	0.23	0.3	0.2643	2.2	3.460	3.0	0.09494	2.1	0.72	1512	29	1518	24	1527	39	99
A103	14043	6	2.3	1.34	3.7	0.2412	2.1	3.376	4.0	0.1015	3.4	0.53	1393	26	1499	31	1652	62	84
A104	5876	2	0.6	0.61	11.5	0.2306	2.5	2.782	7.1	0.08751	6.6	0.36	1337	30	1351	54	1372	127	97
A105	35804	8	3.5	0.46	2.8	0.3469	1.9	5.768	2.6	0.1206	1.8	0.73	1920	32	1942	23	1965	32	98
A106	99726	11	6.0	0.50	27.6	0.2647	3.4	3.535	7.5	0.09686	6.7	0.45	1514	46	1535	61	1564	126	97
A107	20079	11	3.3	0.50	0.0	0.2613	2.1	3.341	2.3	0.09274	1.0	0.90	1496	28	1491	18	1483	19	101
A108	77814	6	3.1	0.29	66.3	0.0787	18.2	1.360	35.5	0.1253	30.4	0.51	488	86	872	232	2033	539	24
A109	90329	11	6.2	0.46	16.0	0.3319	2.7	5.300	6.0	0.1158	5.3	0.46	1847	44	1869	52	1893	95	98
A110	53087	9	5.4	0.72	0.1	0.4782	2.6	11.34	2.7	0.172	0.8	0.95	2519	54	2552	25	2577	13	98
A111	37815	18	7.0	1.29	0.0	0.2836	2.0	3.932	2.1	0.1006	0.8	0.93	1609	28	1620	17	1634	14	98
A112	43906	20	6.4	0.93	0.1	0.2361	2.1	3.351	2.3	0.1029	1.0	0.91	1366	26	1493	19	1678	18	81
A113	11136	6	1.9	0.77	0.0	0.2736	2.0	3.710	2.5	0.09833	1.4	0.81	1559	28	1573	20	1593	27	98
A118	29392	16	4.5	0.31	0.1	0.2650	2.1	3.453	2.3	0.09452	1.0	0.90	1515	28	1517	18	1519	19	100
A119	137177	41	16.8	0.40	2.7	0.3434	2.1	5.637	3.1	0.1191	2.3	0.68	1903	35	1922	27	1942	41	98
A120	9457	8	1.6	0.38	0.2	0.1798	2.1	1.901	2.8	0.07668	1.8	0.77	1066	21	1081	19	1113	36	96
A121	26954	9	3.5	0.43	0.4	0.3524	2.6	5.778	3.1	0.1189	1.7	0.84	1946	44	1943	27	1940	30	100
A122	75370	34	10.3	0.47	1.6	0.2695	3.1	3.738	3.9	0.1006	2.4	0.80	1538	43	1580	32	1635	44	94
A123	171198	65	22.1	0.25	0.1	0.3223	2.4	4.933	2.6	0.111	1.0	0.92	1801	38	1808	22	1816	19	99
A124	6910	4	1.1	0.55	0.0	0.2404	2.1	3.159	2.6	0.0953	1.5	0.81	1389	26	1447	20	1534	29	91
A125	98613	15	5.6	0.53	28.4	0.1630	3.8	1.694	10.0	0.07534	9.3	0.38	974	34	1006	66	1078	187	90
A126	59114	7	4.0	0.71	31.9	0.2882	4.2	4.039	8.8	0.1017	7.8	0.48	1632	61	1642	74	1655	144	99
A127	54046	22	6.0	0.47	5.4	0.2082	2.8	2.754	4.1	0.09593	3.0	0.68	1219	31	1343	31	1546	57	79
A128	68009	9	4.2	0.38	27.4	0.2441	3.5	3.124	8.7	0.09281	8.0	0.40	1408	44	1439	69	1484	152	95
A129	132925	44	13.1	0.22	5.5	0.2640	2.3	3.537	4.0	0.09718	3.2	0.57	1510	31	1536	32	1571	61	96

A130	41099	23	6.4	0.30	0.0	0.2575	2.2	3.304	2.5	0.09307	1.2	0.88	1477	29	1482	19	1489	23	99
A131	4594	4	0.8	0.34	0.0	0.1861	2.3	1.956	3.1	0.0762	2.1	0.75	1100	23	1100	21	1100	41	100
A132	62333	21	7.8	0.38	0.0	0.3383	2.1	5.351	2.2	0.1147	0.9	0.92	1879	34	1877	19	1875	16	100
A133	75269	4	3.4	0.48	47.5	0.2298	6.2	2.782	9.2	0.08779	6.9	0.67	1334	75	1351	71	1378	132	97
A134	76768	21	11.9	0.69	17.1	0.4609	5.0	10.30	10.4	0.1621	9.1	0.49	2443	103	2462	101	2478	153	99
A135	41171	33	7.8	0.45	0.0	0.2167	2.3	2.505	2.6	0.08385	1.3	0.86	1264	26	1273	19	1289	26	98
Pleso [g]	28030	660	34	0.10	0.17	0.0540	1.0	0.3946	1.0	0.05303	0.6	0.87	339	3	338	3	330	15	103
91500 [g]	3496	63	11	0.33	0.19	0.1793	2.0	1.850	3.3	0.07484	2.1	0.60	1063	20	1063	22	1064	42	100

Spot size = 26 µm; depth of crater ~15µm. $^{206}Pb/^{238}U$ error is the quadratic additions of the within run precision (2 SE) and the external reproducibility (2 SD) of the reference zircon. $^{207}Pb/^{206}Pb$ error propagation (^{207}Pb signal dependent) following Gerdes & Zeh (2009). $^{207}Pb/^{235}U$ error is the quadratic addition of the $^{207}Pb/^{206}Pb$ and $^{206}Pb/^{238}U$ uncertainty.

[a] Within run background-corrected mean ^{207}Pb signal in cps (counts per second).

[b] U and Pb content and Th/U ratio were calculated relative to GJ-1 reference zircon.

[c] percentage of the common Pb on the ^{206}Pb. b.d. = below dectection limit.

[d] corrected for background, within-run Pb/U fractionation (in case of $^{206}Pb/^{238}U$) and common Pb using Stacy and Kramers (1975) model Pb composition and subsequently normalised to GJ-1 (ID-TIMS value/measured value); $^{207}Pb/^{235}U$ calculated using $^{207}Pb/^{206}Pb/(^{238}U/^{206}Pb*1/137.88)$

[e] rho is the $^{206}Pb/^{238}U/^{207}Pb/^{235}U$ error correlation coefficient.

[f] degree of concordance = $^{206}Pb/^{238}U$ age / $^{207}Pb/^{206}Pb$ age x 100

[g] Accuracy and reproducibilty was checked by repeated analyses (n = 6) of reference zircon Plesovice and 91500; data given as mean with 2 standard deviation uncertainties

Sample CXI-120 (Frankfurt)

Concordant (100 ±10 %) measurments: 91 (of 102)

spot number	$^{207}Pb^{a}$ (cps)	U^{b} (ppm)	Pb^{b} (ppm)	$\frac{Th^{b}}{U}$	$^{206}Pbc^{c}$ (%)	$\frac{^{206}Pb^{d}}{^{238}U}$	±2σ (%)	$\frac{^{207}Pb^{d}}{^{235}U}$	±2σ (%)	$\frac{^{207}Pb^{d}}{^{206}Pb}$	±2σ (%)	rho^{e}	$\frac{^{206}Pb}{^{238}U}$	±2σ (Ma)	$\frac{^{207}Pb}{^{235}U}$	±2σ (Ma)	$\frac{^{207}Pb}{^{206}Pb}$	±2σ (Ma)	conc. (%)
A04	35080	7	2.4	0.63	16.4	0.2118	2.9	2.343	6.7	0.08023	6.0	0.44	1239	33	1226	49	1203	118	103
A05	8771	15	1.9	0.65	1.1	0.1095	2.4	0.946	3.5	0.06269	2.6	0.67	670	15	676	18	698	56	96
A07	139941	37	14.5	0.38	0.3	0.3487	2.7	5.808	2.9	0.1208	1.1	0.93	1929	45	1948	25	1968	19	98
A08	158284	49	18.5	0.46	0.1	0.3412	2.5	5.530	2.6	0.1175	0.7	0.96	1893	41	1905	23	1919	13	99
A09	143919	95	35.6	0.68	4.7	0.2880	2.5	4.070	3.7	0.1025	2.8	0.67	1632	36	1648	31	1670	51	98
A10	214367	226	76.1	0.64	1.3	0.2937	2.6	4.088	3.0	0.1009	1.4	0.88	1660	39	1652	25	1642	26	101
A11	85360	23	16.2	1.10	2.2	0.4949	2.3	12.16	3.2	0.1783	2.2	0.71	2592	48	2617	30	2637	37	98
A12	373001	131	72.4	0.48	0.0	0.4782	2.3	10.92	2.4	0.1656	0.6	0.97	2519	49	2516	22	2513	10	100
A13	83919	39	10.7	0.34	0.5	0.2548	2.3	3.298	2.6	0.09387	1.1	0.90	1463	31	1481	20	1505	21	97
A14	338419	76	19.7	0.17	17.5	0.1683	2.9	2.275	6.1	0.09803	5.3	0.48	1003	27	1204	44	1587	99	63
A15	214205	60	21.5	0.39	0.0	0.3238	2.3	5.283	2.3	0.1183	0.6	0.97	1808	36	1866	20	1931	11	94
A16	17231	8	2.3	0.45	0.0	0.2545	2.3	3.307	2.7	0.09427	1.4	0.86	1461	30	1483	21	1513	26	97
A17	63245	31	14.8	0.28	b.d.	0.4213	2.3	9.928	2.4	0.1709	0.9	0.93	2267	43	2428	22	2566	14	88
A18	122615	0	0.0	0.41	17.6	0.2637	3.0	3.395	6.1	0.09338	5.3	0.49	1509	40	1503	49	1496	101	101
A19	11601	13	1.9	0.53	12.9	0.0889	2.6	0.856	8.1	0.06983	7.7	0.32	549	14	628	39	923	158	59
A20	290281	87	32.8	0.42	0.0	0.3425	2.4	5.648	2.5	0.1196	0.6	0.97	1899	39	1923	22	1950	11	97
A21	236993	24	10.0	0.43	1.1	0.3603	2.5	6.047	2.7	0.1217	1.1	0.91	1984	42	1983	24	1981	20	100
A22	39121	10	2.4	0.29	0.0	0.2405	2.3	2.931	2.5	0.08841	1.0	0.92	1389	29	1390	19	1391	19	100
A23	61567	19	4.4	0.58	0.0	0.2083	2.4	2.330	2.6	0.08114	0.9	0.94	1220	27	1222	18	1225	17	100
A24	5375	11	2.2	0.70	0.0	0.1699	2.5	1.790	3.2	0.0764	2.0	0.77	1012	23	1042	21	1105	41	92
A25	114740	29	10.6	0.35	4.6	0.3070	2.5	4.761	3.5	0.1125	2.5	0.70	1726	37	1778	30	1840	45	94
A26	114252	22	9.6	0.88	11.2	0.2854	2.7	3.943	5.7	0.1002	5.0	0.47	1619	38	1623	47	1628	93	99
A27	95396	31	11.3	0.55	1.1	0.3081	2.3	4.480	2.7	0.1055	1.4	0.86	1731	36	1727	23	1722	26	101
A28	58486	4	3.1	1.53	40.4	0.3129	4.7	4.999	9.1	0.1159	7.8	0.52	1755	73	1819	80	1893	140	93
A32	49009	46	16.3	0.77	0.0	0.2922	2.3	4.125	2.5	0.1024	1.0	0.92	1653	33	1659	20	1668	18	99
A33	38416	38	12.8	0.80	0.1	0.2777	2.3	3.790	2.6	0.09898	1.3	0.88	1580	32	1591	21	1605	24	98
A34	306267	46	21.6	0.48	9.1	0.3415	2.5	5.540	4.3	0.1176	3.5	0.58	1894	41	1907	37	1921	63	99
A35	87995	30	10.2	0.42	0.2	0.3178	2.2	4.734	2.8	0.108	1.7	0.80	1779	35	1773	24	1767	30	101
A36	21614	32	7.0	0.27	0.0	0.2105	2.5	2.483	2.7	0.08556	1.2	0.89	1231	28	1267	20	1328	24	93
A37	74084	35	9.7	0.41	0.0	0.2568	2.2	3.300	2.4	0.09319	0.9	0.93	1473	29	1481	19	1492	17	99
A38	76566	9	4.6	0.05	2.7	0.5030	2.3	12.47	3.1	0.1798	2.1	0.73	2627	50	2640	30	2651	36	99
A39	9323	8	1.7	0.86	0.0	0.1852	2.5	1.978	3.0	0.07745	1.6	0.84	1095	25	1108	20	1133	32	97
A40	360951	198	34.2	0.82	4.7	0.1350	3.0	2.029	4.1	0.1090	2.7	0.75	817	23	1125	28	1782	50	46
A41	280145	31	16.0	0.61	10.6	0.3374	3.9	5.547	5.8	0.1192	4.3	0.67	1874	63	1908	51	1945	77	96
A42	106043	37	13.0	0.59	0.0	0.3032	2.4	4.408	2.5	0.1054	0.7	0.96	1707	36	1714	21	1722	13	99
A43	35372	4	3.0	1.16	0.1	0.5261	2.4	13.72	2.6	0.1891	0.9	0.94	2725	54	2730	25	2734	15	100

A44	35371	20	4.7	0.30	0.0	0.2234	2.3	2.690	2.5	0.0873	1.0	0.92	1300	27	1326	19	1367	19	95
A45	146121	65	18.2	0.36	0.9	0.2550	2.3	3.298	2.6	0.09381	1.4	0.86	1464	30	1481	21	1504	26	97
A46	378256	101	35.8	0.50	1.1	0.3056	2.5	4.733	2.8	0.1123	1.2	0.90	1719	37	1773	23	1837	22	94
A47	714004	121	63.2	0.08	2.8	0.4863	2.5	11.09	3.0	0.1654	1.7	0.83	2555	52	2531	28	2512	28	102
A48	146151	52	16.9	0.74	1.9	0.2574	2.6	4.113	3.1	0.1159	1.7	0.83	1476	34	1657	25	1894	31	78
A49	396665	156	69.9	0.43	7.3	0.3425	2.4	5.539	3.8	0.1173	3.0	0.63	1899	40	1907	33	1915	53	99
A50	215731	124	46.9	0.28	1.1	0.3475	2.5	5.714	2.8	0.1192	1.2	0.90	1923	42	1933	24	1945	21	99
A51	110124	25	11.7	1.54	7.8	0.2812	2.5	3.901	4.4	0.1006	3.7	0.56	1597	35	1614	36	1636	68	98
A52	31753	29	5.1	0.29	0.1	0.1683	2.4	1.687	2.7	0.07271	1.2	0.88	1003	22	1004	17	1006	25	100
A53	36292	30	5.4	0.37	0.2	0.1699	2.3	1.718	2.5	0.07330	1.0	0.92	1012	22	1015	16	1022	21	99
A54	53931	18	6.3	0.52	0.2	0.3095	2.4	4.518	2.6	0.1059	1.0	0.93	1738	37	1734	22	1729	18	101
A55	706674	92	55.6	0.75	0.1	0.4754	2.2	11.84	2.6	0.1806	1.4	0.84	2507	47	2592	25	2659	24	94
A59	39201	19	5.2	0.34	0.1	0.2530	2.4	3.191	2.7	0.09147	1.2	0.89	1454	31	1455	21	1456	23	100
A60	164671	46	16.7	0.40	0.8	0.3265	2.3	5.307	2.6	0.1179	1.2	0.88	1821	36	1870	22	1924	22	95
A61	82378	31	9.5	0.35	0.3	0.2862	2.6	4.004	3.2	0.1015	2.0	0.79	1622	37	1635	27	1652	37	98
A62	275327	54	20.8	0.80	12.8	0.2376	2.6	3.054	5.3	0.0932	4.6	0.49	1374	32	1421	41	1492	87	92
A63	12697	7	1.8	0.39	0.0	0.2198	2.4	2.602	2.7	0.08585	1.4	0.87	1281	28	1301	20	1335	26	96
A64	224840	96	26.3	0.20	0.9	0.2682	2.3	3.779	2.6	0.1022	1.1	0.90	1532	32	1588	21	1664	21	92
A65	229416	28	18.5	0.96	0.0	0.5104	2.3	12.940	2.4	0.1839	0.7	0.95	2658	49	2675	23	2688	12	99
A66	159767	89	16.6	0.30	4.5	0.1610	2.5	1.578	4.1	0.0711	3.2	0.61	962	22	962	26	960	66	100
A67	59274	24	7.6	0.50	0.0	0.2842	2.4	4.022	2.6	0.1027	0.9	0.93	1612	34	1639	21	1673	17	96
A68	40760	13	5.0	0.85	0.0	0.3171	2.3	4.869	2.5	0.1114	0.9	0.93	1775	37	1797	21	1822	17	97
A69	91362	53	12.5	0.29	0.0	0.2265	2.2	2.681	2.4	0.08583	0.8	0.95	1316	27	1323	18	1334	15	99
A70	144203	183	12.8	1.13	20.8	0.0473	3.6	0.340	11.1	0.0521	10.5	0.32	298	10	297	29	290	240	103
A71	130810	100	20.2	0.40	0.0	0.1875	1.7	1.998	1.9	0.07728	0.8	0.90	1108	18	1115	13	1128	16	98
A72	31068	21	4.7	0.47	0.0	0.2022	1.8	2.266	2.0	0.08130	1.0	0.88	1187	19	1202	14	1229	19	97
A73	46720	17	3.9	0.51	8.4	0.1601	1.8	1.717	4.9	0.07781	4.5	0.37	957	16	1015	32	1142	90	84
A74	133243	15	9.1	0.37	0.0	0.5409	1.6	14.91	1.8	0.1999	0.6	0.93	2787	37	2809	17	2825	11	99
A75	228289	35	14.7	2.14	31.3	0.1508	3.5	1.526	9.2	0.07339	8.5	0.39	905	30	941	58	1025	172	88
A76	217733	57	22.5	0.44	0.1	0.3500	1.8	5.806	2.0	0.1203	0.8	0.92	1934	30	1947	17	1961	14	99
A77	174801	43	16.2	0.50	0.0	0.3293	1.7	5.528	1.9	0.1218	0.7	0.93	1835	28	1905	16	1982	12	93
A78	126625	58	16.7	0.68	0.0	0.2531	1.6	3.266	1.7	0.09359	0.8	0.90	1455	20	1473	14	1500	15	97
A79	161026	33	9.3	0.33	11.1	0.1465	1.9	4.160	3.9	0.2060	3.4	0.50	881	16	1666	33	2874	55	31
A80	148243	47	16.5	0.45	0.1	0.3177	1.6	4.720	1.9	0.1078	0.9	0.87	1778	26	1771	16	1762	17	101
A81	117850	38	12.7	0.32	0.4	0.3090	1.6	4.563	1.9	0.1071	1.0	0.84	1736	24	1743	16	1750	18	99
A82	36592	14	4.5	0.49	0.0	0.2779	1.8	3.848	2.0	0.1004	0.9	0.89	1581	25	1603	16	1632	17	97
A83	51808	73	9.0	1.23	1.7	0.0892	1.7	1.008	4.0	0.08196	3.7	0.42	551	9	708	21	1245	72	44
A84	91899	24	8.5	0.42	4.7	0.2949	1.9	4.155	3.6	0.1022	3.0	0.53	1666	28	1665	30	1664	56	100
A88	111027	25	9.6	0.33	1.4	0.3348	1.7	5.506	2.1	0.1193	1.2	0.82	1862	27	1901	18	1945	21	96
A89	126243	40	11.3	0.24	3.2	0.2512	1.7	3.301	3.1	0.09531	2.6	0.56	1445	22	1481	24	1534	49	94
A90	283751	86	28.3	0.15	0.7	0.3199	1.7	5.126	1.9	0.1162	0.9	0.89	1789	27	1840	17	1899	16	94
A91	359330	44	23.3	0.11	0.0	0.5040	1.9	12.29	2.0	0.1768	0.6	0.95	2631	42	2626	19	2623	10	100
A92	66278	9	3.5	0.61	23.3	0.2002	2.8	2.533	6.6	0.09176	6.0	0.43	1176	30	1281	49	1462	114	80

A93	458879	121	50.2	0.74	0.0	0.3471	1.9	5.844	2.0	0.1221	0.6	0.95	1921	32	1953	18	1987	11	97
A94	60229	20	5.3	0.44	9.2	0.2116	1.9	2.407	6.5	0.08251	6.2	0.29	1237	21	1245	48	1258	122	98
A95	26209	8	3.4	1.23	0.0	0.3229	1.7	5.137	2.0	0.1154	1.0	0.85	1804	27	1842	17	1886	19	96
A96	318379	89	33.0	0.48	0.0	0.3315	1.7	5.214	1.8	0.1141	0.7	0.93	1846	27	1855	16	1865	12	99
A97	94237	6	4.7	0.81	60.3	0.3235	6.4	4.779	12.5	0.1071	10.7	0.51	1807	102	1781	111	1751	196	103
A98	80493	45	9.9	0.27	0.0	0.2107	1.6	2.519	1.8	0.08669	0.7	0.91	1233	18	1277	13	1354	14	91
A99	61072	24	8.0	1.09	0.0	0.2680	1.5	3.874	1.7	0.1048	0.8	0.88	1531	21	1608	14	1711	15	89
A100	32350	10	3.8	0.74	0.0	0.3195	1.6	4.949	1.9	0.1124	0.9	0.87	1787	25	1811	16	1838	17	97
A101	60419	48	9.0	0.32	0.0	0.1789	1.7	1.860	1.9	0.07538	0.8	0.90	1061	17	1067	13	1079	16	98
A102	78651	65	10.7	0.25	1.0	0.1594	1.9	1.593	2.9	0.07247	2.2	0.64	954	16	967	18	999	45	95
A103	12916	12	2.1	0.70	0.0	0.1523	2.1	1.510	2.6	0.07188	1.5	0.82	914	18	934	16	983	30	93
A104	53913	26	3.3	0.71	19.2	0.0708	2.5	0.698	7.1	0.07147	6.6	0.36	441	11	537	30	971	135	45
A105	74315	41	10.9	0.17	0.3	0.2622	1.6	3.489	1.8	0.09649	1.0	0.85	1501	21	1525	15	1557	18	96
A106	14765	16	2.8	0.66	1.2	0.1584	1.7	1.587	2.8	0.07267	2.2	0.61	948	15	965	17	1005	44	94
A107	24768	19	3.5	0.35	0.3	0.1821	1.7	1.865	3.8	0.07426	3.4	0.45	1079	17	1069	26	1049	69	103
A108	210089	46	19.2	0.64	1.8	0.3412	1.7	5.623	2.1	0.1195	1.3	0.79	1893	28	1920	18	1949	23	97
A109	149980	42	12.2	0.45	9.4	0.2200	2.1	2.624	5.2	0.08648	4.8	0.41	1282	25	1307	39	1349	92	95
A110	14335	10	2.1	0.60	0.0	0.1868	1.9	2.064	2.4	0.08014	1.4	0.81	1104	19	1137	16	1200	27	92
A111	11213	8	2.0	1.24	0.0	0.1833	1.7	1.956	2.3	0.07739	1.6	0.72	1085	17	1100	16	1131	32	96
A112	13032	9	1.8	0.31	2.2	0.1809	1.7	1.934	3.0	0.07755	2.4	0.57	1072	17	1093	20	1135	48	94
A113	10058	5	1.2	0.46	1.6	0.2115	1.7	2.557	2.8	0.08767	2.2	0.62	1237	19	1288	20	1375	42	90
A114	118345	20	9.0	0.49	4.7	0.3577	1.9	6.210	2.9	0.1259	2.2	0.66	1971	33	2006	26	2042	39	97
A115	81649	60	12.7	0.61	0.0	0.1850	1.7	1.961	1.9	0.07689	0.7	0.93	1094.0	17.4	1102.2	12.6	1118	14	98
Pleso [g]	35365	713	36	0.09	0.07	0.05345	2.0	0.3923	1.9	0.05324	0.7	0.87	336	6	336	5	339	15	100
91500 [g]	5896	13	2	0.31	0.18	0.18040	1.2	1.8646	3.0	0.07496	2.1	0.63	1069	12	1069	20	1067	41	100

Spot size = 26 µm; depth of crater ~15µm. $^{206}Pb/^{238}U$ error is the quadratic additions of the within run precision (2 SE) and the external reproducibility (2 SD) of the reference zircon. $^{207}Pb/^{206}Pb$ error propagation (^{207}Pb signal dependent) following Gerdes & Zeh (2009). $^{207}Pb/^{235}U$ error is the quadratic addition of the $^{207}Pb/^{206}Pb$ and $^{206}Pb/^{238}U$ uncertainty.

[a]Within run background-corrected mean ^{207}Pb signal in cps (counts per second).

[b] U and Pb content and Th/U ratio were calculated relative to GJ-1 reference zircon.

[c] percentage of the common Pb on the ^{206}Pb. b.d. = below dectection limit.

[d] corrected for background, within-run Pb/U fractionation (in case of $^{206}Pb/^{238}U$) and common Pb using Stacy and Kramers (1975) model Pb composition and subsequently normalised to GJ-1 (ID-TIMS value/measured value); $^{207}Pb/^{235}U$ calculated using $^{207}Pb/^{206}Pb/(^{238}U/^{206}Pb*1/137.88)$

[e] rho is the $^{206}Pb/^{238}U/^{207}Pb/^{235}U$ error correlation coefficient.

[f] degree of concordance = $^{206}Pb/^{238}U$ age / $^{207}Pb/^{206}Pb$ age x 100

[g] Accuracy and reproducibilty was checked by repeated analyses (n = 5) of reference zircon Plesovice and 91500; data given as mean with 2 standard deviation uncertainties

Sample CXI-119 (Frankfurt)

Concordant (100 ±10 %) measurments: 82 (of 99)

spot number	$^{207}Pb^{a}$ (cps)	U^{b} (ppm)	Pb^{b} (ppm)	Th^{b}/U	$^{206}Pbc^{c}$ (%)	$^{206}Pb^{d}/^{238}U$	±2σ (%)	$^{207}Pb^{d}/^{235}U$	±2σ (%)	$^{207}Pb^{d}/^{206}Pb$	±2σ (%)	rho^{e}	$^{206}Pb/^{238}U$	±2σ (Ma)	$^{207}Pb/^{235}U$	±2σ (Ma)	$^{207}Pb/^{206}Pb$	±2σ (Ma)	conc. (%)
A04	253866	17	14.5	0.77	0.0	0.6282	2.8	24.69	3.0	0.285	1.0	0.94	3142	70	3296	29	3391	16	93
A05	168915	20	12.5	0.66	0.0	0.5088	2.8	12.65	2.9	0.1803	0.7	0.97	2652	62	2654	28	2656	12	100
A06	70280	47	6.1	0.12	7.5	0.1129	3.5	1.35	5.5	0.08647	4.3	0.64	690	23	866	33	1349	82	51
A07	95972	32	11.2	0.49	0.7	0.312	3.0	4.65	3.3	0.1081	1.2	0.93	1751	47	1758	28	1767	23	99
A08	66271	59	5.3	0.41	6.8	0.06351	3.5	0.53	7.2	0.0608	6.4	0.48	397	13	433	26	632	137	63
A09	76044	26	17.0	0.82	0.8	0.5338	2.8	14.15	3.1	0.1922	1.4	0.89	2757	62	2760	30	2761	23	100
A10	36711	28	9.5	0.58	0.3	0.2875	2.8	4.40	3.0	0.1111	1.1	0.93	1629	41	1713	25	1817	20	90
A11	27325	44	8.2	0.20	0.0	0.1873	2.9	2.05	3.1	0.07936	1.0	0.94	1107	29	1132	21	1181	20	94
A12	78208	168	30.8	0.57	0.0	0.1636	2.8	1.68	3.1	0.0744	1.3	0.91	977	26	1000	20	1052	26	93
A13	24947	20	3.8	0.38	0.0	0.1817	3.0	1.96	3.5	0.07829	1.9	0.85	1076	30	1102	24	1154	37	93
A14	44533	25	5.6	0.30	0.0	0.2123	2.9	2.46	3.0	0.08394	0.8	0.96	1241	32	1259	22	1291	17	96
A15	43959	10	1.8	0.37	24.9	0.06547	4.3	0.53	12.8	0.05912	12.1	0.34	409	17	434	46	572	263	72
A16	37217	13	4.4	0.77	0.0	0.2828	2.8	4.12	3.1	0.1057	1.1	0.93	1605	40	1659	25	1727	21	93
A17	30046	22	9.1	1.17	0.1	0.3130	3.2	4.61	3.6	0.1068	1.7	0.89	1755	50	1751	31	1746	30	101
A18	16220	0	0.0	1.13	0.0	0.2910	2.9	4.03	3.1	0.1003	1.2	0.92	1646	42	1639	26	1630	22	101
A19	148298	101	38.5	0.21	6.0	0.3411	3.1	5.61	4.5	0.1193	3.3	0.68	1892	50	1918	39	1946	58	97
A20	58298	37	7.1	0.36	2.5	0.1707	2.8	1.75	4.3	0.0744	3.3	0.65	1016	26	1028	28	1052	66	97
A21	21808	1	0.6	1.21	11.5	0.1927	3.2	2.13	4.9	0.0803	3.7	0.65	1136	34	1160	35	1204	73	94
A22	14394	2	0.5	0.93	14.4	0.1520	4.0	2.14	7.6	0.1023	6.5	0.52	912	34	1163	54	1667	120	55
A23	45123	5	2.0	0.56	0.0	0.3395	2.9	5.72	3.1	0.1221	1.0	0.94	1884	47	1934	27	1988	19	95
A24	3088	6	1.5	0.97	0.0	0.2195	3.3	2.55	5.2	0.08436	4.1	0.63	1279	38	1287	39	1301	79	98
A25	34964	54	4.4	0.80	6.2	0.06202	2.9	0.47	6.2	0.05519	5.5	0.46	388	11	393	21	420	124	92
A26	47826	13	4.9	0.64	3.7	0.2932	2.8	4.15	3.6	0.1027	2.4	0.76	1658	41	1665	30	1674	44	99
A28	62278	53	9.4	0.51	1.8	0.1584	3.2	1.55	3.9	0.07096	2.2	0.83	948	29	950	24	956	44	99
A32	233832	43	23.6	0.61	1.5	0.4457	2.8	10.06	3.0	0.1637	1.3	0.90	2376	55	2440	29	2494	22	95
A33	6668	9	2.3	0.54	0.0	0.224	2.8	2.60	3.4	0.08431	1.9	0.83	1303	33	1302	25	1300	37	100
A34	25074	17	6.2	0.50	0.0	0.3217	2.8	5.05	3.0	0.1137	1.0	0.95	1798	45	1827	26	1860	18	97
A35	29866	11	3.7	0.61	0.0	0.2939	2.8	4.42	3.0	0.109	1.0	0.94	1661	42	1715	25	1783	19	93
A36	64181	54	9.9	0.27	b.d.	0.1782	2.9	1.83	3.0	0.07432	0.8	0.96	1057	28	1055	20	1050	17	101
A37	10724	26	5.4	1.32	0.0	0.1567	2.8	1.57	3.4	0.07267	1.9	0.84	938	25	958	21	1005	38	93
A38	112202	30	13.7	1.03	0.0	0.3554	3.0	5.90	3.1	0.1204	0.7	0.97	1960	50	1961	27	1962	13	100
A39	32336	38	4.8	0.81	0.0	0.09347	2.8	1.60	5.5	0.1241	4.8	0.51	576	16	970	35	2016	84	29
A40	267217	59	20.3	0.03	1.3	0.3286	2.9	7.83	3.0	0.1728	0.8	0.96	1831	46	2212	27	2585	14	71
A41	25524	22	7.4	0.51	0.0	0.3298	2.9	5.32	4.0	0.1171	2.7	0.74	1837	47	1873	35	1912	48	96
A42	81253	35	10.4	0.32	2.6	0.2737	3.1	3.62	3.7	0.09589	2.0	0.85	1559	43	1554	30	1546	37	101
A43	152719	13	9.3	0.44	6.1	0.5398	3.0	14.92	3.6	0.2005	2.1	0.82	2783	68	2810	35	2830	34	98

A44	112513	28	10.0	0.48	14.8	0.2639	3.8	3.67	7.8	0.101	6.9	0.48	1510	51	1566	65	1642	128	92
A45	40605	12	4.7	0.79	0.0	0.3178	2.8	4.88	2.9	0.1113	0.9	0.95	1779	43	1798	25	1820	16	98
A46	139594	22	11.9	0.63	0.0	0.4559	2.9	9.93	3.0	0.1581	0.6	0.98	2421	59	2429	28	2435	10	99
A47	87873	25	8.4	0.14	0.0	0.3314	2.9	5.34	3.0	0.117	0.9	0.96	1845	46	1876	26	1910	16	97
A48	277328	27	17.0	0.30	1.7	0.5400	3.0	14.54	3.1	0.1953	0.9	0.96	2783	67	2786	30	2788	14	100
A49	3177	2	0.5	0.62	0.0	0.1823	2.9	2.00	4.1	0.07945	2.9	0.71	1079	29	1114	28	1183	57	91
A50	31248	9	5.4	0.70	8.2	0.4109	3.1	8.97	4.9	0.1582	3.9	0.62	2219	58	2335	46	2437	65	91
A51	9004	31	3.9	0.66	0.1	0.1075	2.8	1.01	3.9	0.06835	2.7	0.73	658	18	710	20	879	55	75
A52	108502	28	10.2	0.38	0.0	0.3268	2.8	5.48	2.9	0.1215	0.7	0.97	1823	44	1897	25	1979	12	92
A53	39323	18	5.2	0.53	0.0	0.2595	2.8	3.37	3.0	0.09421	0.9	0.95	1488	38	1498	24	1512	18	98
A54	78441	19	8.0	1.05	2.3	0.2959	2.8	4.88	3.5	0.1195	2.1	0.80	1671	42	1798	30	1949	38	86
A55	38561	23	4.7	0.19	0.0	0.2033	2.8	2.33	3.0	0.08326	1.0	0.95	1193	31	1223	22	1275	19	94
A59	121643	22	8.3	0.75	18.8	0.2329	3.9	2.81	8.3	0.0875	7.3	0.47	1350	48	1358	64	1372	141	98
A60	186849	44	14.7	0.16	0.0	0.3235	2.9	6.50	3.0	0.1456	0.9	0.95	1807	46	2045	27	2295	15	79
A61	150794	20	9.7	0.50	23.3	0.3174	3.7	4.84	6.9	0.1107	5.8	0.54	1777	58	1793	60	1810	105	98
A62	138222	19	6.6	0.53	31.9	0.1595	4.4	1.63	8.3	0.07392	7.0	0.53	954	39	980	54	1039	142	92
A63	46465	11	4.5	0.41	0.0	0.3574	2.9	5.97	3.1	0.121	1.0	0.95	1970	50	1971	27	1972	17	100
A64	32010	12	4.7	1.47	0.0	0.2743	2.7	3.79	2.9	0.1003	1.0	0.94	1563	38	1591	23	1629	18	96
A65	182656	38	15.2	0.36	7.7	0.3229	3.2	5.00	4.9	0.1122	3.7	0.66	1804	51	1819	42	1836	66	98
A66	32481	15	5.0	0.66	b.d.	0.2848	4.1	4.05	4.4	0.1031	1.8	0.92	1615	58	1644	37	1681	33	96
A67	66792	94	11.1	0.23	0.1	0.1172	2.9	1.46	3.0	0.09022	0.8	0.96	715	20	913	18	1430	16	50
A68	32354	15	3.8	0.53	6.1	0.2154	3.1	2.50	5.6	0.08432	4.6	0.56	1258	36	1273	41	1300	89	97
A69	87159	22	10.2	1.25	3.1	0.3191	3.9	5.02	4.7	0.114	2.7	0.82	1785	61	1822	41	1865	48	96
A70	20851	40	3.9	0.63	0.0	0.08543	2.8	0.82	3.6	0.06957	2.2	0.78	528	14	608	16	916	46	58
A71	78701	31	11.1	0.81	1.3	0.3132	2.2	5.11	3.0	0.1182	1.9	0.75	1757	34	1837	25	1929	35	91
A72	38096	14	3.9	0.58	0.1	0.2514	2.0	3.34	2.7	0.09625	1.9	0.73	1446	26	1489	21	1553	35	93
A73	19984	14	2.7	0.12	0.4	0.1972	2.5	2.20	3.1	0.0809	1.9	0.81	1160	27	1181	22	1219	37	95
A74	48068	18	5.5	0.37	0.2	0.2876	2.5	4.06	2.7	0.1023	1.0	0.92	1629	36	1645	22	1665	19	98
A75	178097	13	8.1	0.55	17.2	0.3656	3.1	6.69	6.8	0.1326	6.1	0.46	2009	54	2071	62	2133	106	94
A76	103519	49	14.3	0.58	0.0	0.2605	1.9	3.37	2.1	0.09373	0.9	0.91	1493	26	1497	17	1503	16	99
A77	28306	12	3.8	0.80	0.6	0.2647	2.1	3.62	2.5	0.09904	1.3	0.84	1514	28	1553	20	1606	25	94
A78	140418	37	12.7	0.11	4.0	0.3134	2.2	4.69	3.1	0.1086	2.2	0.70	1758	34	1766	27	1775	41	99
A79	171000	15	11.0	0.72	2.6	0.5391	2.5	14.66	2.8	0.1972	1.2	0.90	2780	56	2793	27	2803	20	99
A80	108460	54	13.5	0.27	0.0	0.2411	2.2	2.99	2.3	0.08995	0.7	0.95	1392	27	1405	17	1424	14	98
A81	87938	83	12.8	0.03	1.9	0.1586	2.4	1.55	3.0	0.07069	1.9	0.78	949	21	949	19	948	39	100
A82	69994	22	8.6	0.93	1.5	0.3015	2.1	4.81	2.5	0.1156	1.4	0.83	1699	31	1786	21	1890	24	90
A83	30485	29	3.0	0.64	8.9	0.07528	2.2	0.80	5.7	0.07694	5.2	0.38	468	10	596	26	1120	104	42
A84	34546	23	5.5	0.88	3.1	0.1948	2.3	2.11	4.0	0.07848	3.3	0.57	1147	24	1151	28	1159	66	99
A88	17547	12	2.4	0.34	0.8	0.1821	1.9	1.98	3.7	0.0788	3.2	0.52	1078	19	1108	25	1167	63	92
A89	63900	16	6.3	0.61	0.3	0.3098	1.9	4.77	4.9	0.1118	4.5	0.38	1740	29	1780	42	1828	82	95
A90	217248	24	12.3	3.42	26.4	0.2976	5.2	6.88	8.6	0.1677	6.9	0.61	1680	78	2096	80	2535	115	66
A91	50677	15	5.8	0.69	0.0	0.3181	2.0	5.20	2.3	0.1186	1.1	0.87	1780	31	1853	20	1935	20	92
A92	3409	2	0.7	2.24	0.8	0.1842	2.2	2.05	4.2	0.08081	3.5	0.53	1090	22	1133	29	1217	70	90

A93	94102	14	7.4	0.51	2.9	0.3984	2.1	7.39	2.6	0.1346	1.6	0.80	2162	38	2160	24	2158	28	100
A94	48612	10	4.3	0.59	7.3	0.337	2.1	5.64	4.4	0.1214	3.9	0.48	1872	35	1922	39	1976	69	95
A95	65936	15	5.5	0.38	2.5	0.3262	2.7	5.98	4.3	0.133	3.3	0.63	1820	43	1973	38	2138	58	85
A96	99610	72	13.2	0.04	0.5	0.1927	1.9	2.07	2.1	0.07782	0.8	0.92	1136	20	1138	14	1142	16	99
A97	117074	25	10.8	0.77	4.1	0.3381	2.0	5.61	3.1	0.1204	2.4	0.65	1877	33	1918	27	1962	43	96
A98	47568	20	5.8	0.41	0.1	0.2671	2.0	3.50	2.4	0.09517	1.4	0.82	1526	27	1528	19	1531	25	100
A99	33252	24	4.7	0.23	0.2	0.1938	2.3	2.10	2.5	0.07856	0.9	0.93	1142	24	1148	17	1161	19	98
A100	132918	45	15.3	0.39	0.6	0.3085	1.9	4.71	2.0	0.1106	0.7	0.93	1733	28	1768	17	1810	13	96
A101	2694	7	0.6	0.89	0.0	0.06958	2.1	0.55	4.2	0.0574	3.6	0.51	434	9	445	15	507	79	86
A102	10827	3	1.3	1.56	0.6	0.3247	2.1	5.23	2.9	0.1168	1.9	0.75	1813	34	1857	25	1908	34	95
A103	192037	41	15.4	0.83	4.9	0.3126	2.1	5.11	3.4	0.1185	2.6	0.62	1754	32	1838	29	1934	47	91
A104	12431	20	3.4	0.47	0.0	0.1749	2.0	1.76	2.5	0.07309	1.6	0.77	1039	19	1032	16	1016	32	102
A105	110461	56	12.3	0.37	4.9	0.1872	2.2	2.04	4.1	0.07916	3.5	0.53	1106	22	1130	28	1176	69	94
A106	63534	24	5.5	0.39	6.7	0.176	2.0	1.89	4.3	0.07772	3.7	0.47	1045	19	1076	29	1140	75	92
A107	109242	28	10.4	0.46	1.8	0.3201	2.2	5.31	2.8	0.1203	1.8	0.78	1790	34	1871	24	1961	31	91
A108	77681	22	8.3	0.35	0.0	0.3556	2.1	5.84	2.3	0.1191	0.8	0.93	1961	36	1952	20	1942	15	101
A109	15092	50	3.4	0.43	0.0	0.06314	1.9	0.49	2.3	0.0565	1.4	0.81	395	7	406	8	472	31	84
A110	8134	16	1.4	0.13	0.1	0.08994	2.1	0.74	2.6	0.05943	1.6	0.80	555	11	561	11	583	34	95
A111	1811	5	0.3	0.17	0.1	0.06996	2.2	0.58	3.5	0.05969	2.7	0.63	436	9	462	13	592	58	74
A112	108216	23	6.1	0.28	36.6	0.1526	4.8	1.40	16.9	0.06653	16.2	0.28	915	41	889	105	823	337	111
Pleso [g]	90715	1830	93	0.11	0.01	0.053598	2.1	0.3919	2.2	0.05303	0.6	0.93	336.6	6.8	335.8	6.2	330	14	101
91500 [g]	7068	16	3	0.32	0.22	0.17858	2.6	1.8310	1.3	0.07437	1.4	0.64	1059	26	1057	9	1051	29	101

Spot size = 26 µm; depth of crater ~15µm. ^{206}Pb/^{238}U error is the quadratic additions of the within run precision (2 SE) and the external reproducibility (2 SD) of the reference zircon. ^{207}Pb/^{206}Pb error propagation (^{207}Pb signal dependent) following Gerdes & Zeh (2009). ^{207}Pb/^{235}U error is the quadratic addition of the ^{207}Pb/^{206}Pb and ^{206}Pb/^{238}U uncertainty.

[a] Within run background-corrected mean ^{207}Pb signal in cps (counts per second).

[b] U and Pb content and Th/U ratio were calculated relative to GJ-1 reference zircon.

[c] percentage of the common Pb on the ^{206}Pb. b.d. = below dectection limit.

[d] corrected for background, within-run Pb/U fractionation (in case of ^{206}Pb/^{238}U) and common Pb using Stacy and Kramers (1975) model Pb composition and subsequently normalised to GJ-1 (ID-TIMS value/measured value); ^{207}Pb/^{235}U calculated using ^{207}Pb/^{206}Pb/(^{238}U/^{206}Pb*1/137.88)

[e] rho is the ^{206}Pb/^{238}U/^{207}Pb/^{235}U error correlation coefficient.

[f] degree of concordance = ^{206}Pb/^{238}U age / ^{207}Pb/^{206}Pb age x 100

[g] Accuracy and reproducibilty was checked by repeated analyses (n = 5) of reference zircon Plesovice and 91500; data given as mean with 2 standard deviation uncertainties

Sample CXI-125 (Frankfurt)

Concordant (100 ±10 %) measurments: 87 (of 100)

spot number	^{207}Pb[a] (cps)	U[b] (ppm)	Pb[b] (ppm)	Th[b]/U	^{206}Pbc[c] (%)	^{206}Pb[d]/^{238}U	±2σ (%)	^{207}Pb[d]/^{235}U	±2σ (%)	^{207}Pb[d]/^{206}Pb	±2σ (%)	rho[e]	^{206}Pb/^{238}U	±2σ (Ma)	^{207}Pb/^{235}U	±2σ (Ma)	^{207}Pb/^{206}Pb	±2σ (Ma)	conc.[f] (%)
j04	21487	334	33	1.20	b.d.	0.0855	1.1	0.6992	1.5	0.05931	1.0	0.74	529	6	538	6	578	22	91
j05	23418	44	5.6	0.06	17.27	0.06048	2.5	0.446	5.7	0.05348	5.2	0.44	379	9	374	18	349	117	108
j06	176393	357	140	1.43	0.43	0.3481	1.1	6.266	1.5	0.1306	1.0	0.73	1925	19	2014	13	2106	18	91
j07	214734	78	64	0.44	2.51	0.6199	1.1	20.82	1.5	0.2436	1.1	0.69	3110	26	3130	15	3144	18	99
j08	430779	102	110	0.59	2.23	0.7775	1.2	37.50	1.6	0.3499	1.1	0.75	3708	35	3707	16	3706	16	100
j09	21072	344	25	0.48	0.10	0.07096	1.1	0.5567	1.6	0.0569	1.2	0.68	442	5	449	6	488	26	91
j10	197631	322	120	0.66	b.d.	0.3356	1.0	5.576	1.2	0.1205	0.6	0.86	1865	17	1912	10	1964	11	95
j11	337638	56	390	1.18	1.81	0.3044	1.3	4.523	1.9	0.1078	1.3	0.72	1713	20	1735	16	1762	24	97
j12	31988	46	15	1.55	6.73	0.1942	1.2	2.123	4.7	0.07931	4.5	0.26	1144	13	1156	33	1180	90	97
j13	103890	467	83	0.33	0.14	0.1718	1.2	2.322	1.4	0.09803	0.8	0.82	1022	11	1219	10	1587	16	64
j14	342746	503	200	0.60	b.d.	0.3569	1.2	6.069	1.5	0.1233	0.9	0.80	1967	21	1986	13	2005	16	98
j15	173216	428	120	0.53	0.00	0.2705	1.4	4.437	1.7	0.1190	0.9	0.84	1543	19	1719	14	1941	16	80
j16	75376	203	61	1.01	0.26	0.2533	1.3	3.349	1.5	0.09587	0.8	0.86	1456	17	1492	12	1545	14	94
j17	47320	414	38	0.87	2.97	0.07456	1.3	0.607	2.7	0.05905	2.4	0.47	464	6	482	10	569	52	81
j18	6165	26	6	0.50	0.02	0.2095	1.3	2.331	2.2	0.0807	1.8	0.59	1226	15	1222	16	1214	36	101
j19	15258	31	13	1.85	0.00	0.3037	1.1	4.612	1.7	0.1101	1.3	0.65	1710	17	1751	15	1801	24	95
j20	191343	254	78	0.59	8.62	0.2098	1.8	2.374	4.2	0.08205	3.8	0.43	1228	20	1235	30	1247	74	99
j21	103544	350	80	0.38	2.59	0.2113	1.5	2.541	2.1	0.08719	1.5	0.69	1236	16	1284	16	1365	30	91
j22	23166	77	16	0.39	7.27	0.1742	1.3	2.114	4.1	0.08798	3.9	0.31	1035	12	1153	29	1382	75	75
j23	67800	256	65	1.11	0.00	0.2122	1.1	2.424	1.4	0.08285	0.9	0.78	1240	12	1250	10	1266	17	98
j26	34855	140	28	0.21	0.05	0.1983	1.6	2.229	1.9	0.08151	1.1	0.83	1166	17	1190	13	1234	21	95
j27	29470	176	17	0.90	8.66	0.07161	1.2	0.5925	4.2	0.06001	4.0	0.30	446	5	472	16	604	86	74
j28	50113	536	44	0.62	3.50	0.07296	1.2	0.5776	2.6	0.05742	2.3	0.46	454	5	463	10	508	52	89
j29	91325	183	63	0.73	0.00	0.3046	1.1	4.551	1.3	0.1084	0.7	0.87	1714	17	1740	11	1772	12	97
j30	205720	176	81	0.86	11.76	0.3266	1.5	5.297	4.0	0.1176	3.7	0.38	1822	24	1868	35	1920	67	95
j31	622849	154	150	0.63	17.91	0.3571	2.2	5.954	5.4	0.1209	4.9	0.40	1968	37	1969	48	1970	88	100
j32	153087	175	93	0.69	0.53	0.3593	1.2	6.63	1.9	0.1338	1.6	0.60	1979	20	2063	17	2149	27	92
j33	9229	6	4.4	0.64	4.35	0.5104	1.7	13.36	5.1	0.1898	4.7	0.35	2658	38	2705	49	2740	78	97
j34	166108	280	100	0.51	0.05	0.3301	1.3	5.502	1.5	0.1209	0.7	0.89	1839	21	1901	13	1969	12	93

j35	19645	237	21	0.83	1.09	0.07484	1.2	0.5868	4.0	0.05686	3.8	0.30	465	5	469	15	486	83	96
j36	68071	101	40	0.57	1.98	0.3463	1.8	5.731	2.5	0.1200	1.7	0.73	1917	30	1936	22	1956	30	98
j37	127622	95	56	0.95	8.18	0.3880	1.4	7.14	3.3	0.1335	3.0	0.44	2113	26	2129	30	2144	52	99
j38	10231	31	9.5	1.09	0.04	0.2615	1.5	3.442	2.0	0.09547	1.4	0.71	1498	19	1514	16	1537	27	97
j39	289818	741	320	1.12	0.00	0.4005	1.3	7.265	1.6	0.1316	0.9	0.82	2171	24	2144	14	2119	16	102
j40	255135	389	140	0.24	0.15	0.3531	1.1	6.151	1.2	0.1263	0.6	0.87	1949	18	1998	11	2048	11	95
j41	12273	25	11	2.08	0.00	0.311	1.2	4.629	1.7	0.1080	1.2	0.72	1745	19	1755	14	1766	22	99
j42	90097	257	64	0.80	0.00	0.2183	1.1	3.097	1.3	0.1029	0.7	0.84	1273	13	1432	10	1677	13	76
j43	19117	40	17	2.03	0.86	0.3026	1.3	4.559	2.2	0.1093	1.8	0.58	1704	19	1742	18	1788	32	95
j44	16122	34	12	0.98	0.17	0.3119	1.2	4.709	1.8	0.1095	1.4	0.67	1750	19	1769	16	1791	25	98
j45	80835	123	50	0.80	0.32	0.3449	1.0	5.968	1.4	0.1255	0.9	0.76	1910	17	1971	12	2035	16	94
j48	242874	311	150	1.33	1.07	0.3765	1.1	6.984	1.8	0.1345	1.4	0.61	2060	20	2109	16	2158	25	95
j49	175026	473	150	0.46	0.00	0.307	1.7	4.484	1.9	0.1059	0.7	0.92	1726	26	1728	16	1730	13	100
j50	89887	494	86	0.19	3.44	0.1695	1.4	1.747	2.9	0.07477	2.5	0.48	1009	13	1026	19	1062	51	95
j51	22039	48	18	0.95	0.85	0.2952	1.2	4.156	2.3	0.1021	1.9	0.53	1667	18	1665	19	1663	36	100
j52	465422	243	100	0.43	28.91	0.07633	3.1	0.605	6.9	0.05749	6.1	0.45	474	14	480	27	510	135	93
j53	41343	195	36	0.34	0.17	0.1791	1.1	1.901	1.6	0.07698	1.1	0.70	1062	11	1082	11	1121	23	95
j54	26278	88	24	0.84	0.07	0.2345	1.1	2.921	1.5	0.09033	1.1	0.71	1358	13	1387	11	1432	20	95
j55	111561	195	73	0.55	0.20	0.3425	1.1	5.716	1.4	0.1210	0.8	0.81	1899	19	1934	12	1972	15	96
j56	67468	119	47	1.01	1.65	0.3172	1.0	4.675	1.7	0.1069	1.4	0.59	1776	16	1763	15	1747	26	102
j57	139659	232	96	0.78	0.13	0.3607	1.1	6.182	1.3	0.1243	0.7	0.84	1986	18	2002	11	2019	12	98
j58	986314	524	370	0.60	0.86	0.5744	1.2	18.53	1.5	0.2340	0.9	0.78	2926	27	3018	14	3080	15	95
j59	861771	410	290	1.16	11.94	0.3567	1.5	5.91	3.1	0.1202	2.7	0.49	1966	26	1963	27	1959	48	100
j60	306862	286	140	0.41	10.21	0.2618	1.5	3.494	3.3	0.09681	2.9	0.46	1499	20	1526	26	1563	55	96
j61	79514	126	54	0.68	0.63	0.3703	1.2	6.478	2.1	0.1269	1.8	0.57	2031	21	2043	19	2055	31	99
j62	48786	144	40	0.55	0.22	0.2573	1.1	3.337	1.4	0.09407	0.8	0.80	1476	14	1490	11	1510	16	98
j63	165770	400	120	0.42	3.29	0.2676	1.1	3.486	2.2	0.09449	1.9	0.49	1528	15	1524	17	1518	36	101
j64	18442	184	16	0.74	4.06	0.07180	1.4	0.5646	3.6	0.05703	3.3	0.38	447	6	455	13	493	73	91
j65	16326	143	13	0.79	6.04	0.07083	1.2	0.5546	5.0	0.05678	4.9	0.24	441	5	448	18	483	108	91
j66	154797	194	93	0.89	3.92	0.3803	1.3	6.984	2.1	0.1332	1.6	0.62	2078	23	2109	18	2140	28	97
j67	219687	348	150	0.82	0.66	0.3738	1.3	6.416	1.8	0.1245	1.2	0.71	2047	22	2034	16	2021	22	101
j70	52789	734	55	0.26	0.68	0.07387	1.3	0.5792	1.8	0.05687	1.2	0.74	459	6	464	7	486	27	94
j71	52905	49	28	0.74	0.46	0.4782	1.6	11.17	1.7	0.1695	0.7	0.91	2519	33	2538	16	2552	12	99
j72	31232	27	16	0.69	0.83	0.4740	1.4	11.12	1.7	0.1701	1.0	0.82	2501	29	2533	16	2558	16	98
j73	257922	85	86	0.98	4.57	0.682	1.1	25.76	1.5	0.2740	1.1	0.73	3352	30	3338	15	3329	17	101

j74	669016	830	510	1.49	0.00	0.5162	1.7	15.21	2.0	0.2137	1.1	0.84	2683	37	2829	19	2934	17	91
j75	94550	332	91	0.54	0.01	0.2584	1.3	3.355	1.5	0.09416	0.7	0.89	1482	17	1494	12	1511	13	98
j76	243781	428	190	0.99	0.42	0.3665	1.4	6.481	1.7	0.1283	1.0	0.79	2013	23	2043	15	2074	18	97
j77	65382	109	47	1.01	0.22	0.3547	1.1	6.012	1.4	0.1229	0.8	0.80	1957	19	1978	12	1999	15	98
j78	59964	100	40	0.79	0.62	0.346	1.4	5.998	1.7	0.1257	0.9	0.84	1915	23	1976	15	2039	16	94
j79	368142	430	190	0.52	9.39	0.3057	1.4	5.379	3.5	0.1276	3.2	0.39	1720	21	1882	30	2065	56	83
j80	8257	27	6	0.44	3.35	0.1828	1.9	1.914	3.8	0.07595	3.2	0.50	1082	19	1086	25	1094	65	99
j81	137578	162	75	1.20	10.67	0.3116	1.8	4.65	3.5	0.1082	3.0	0.51	1748	28	1758	30	1770	56	99
j82	172187	382	140	0.38	0.37	0.3342	1.1	5.656	1.4	0.1227	0.9	0.76	1859	18	1925	13	1997	17	93
j83	108494	67	110	0.66	12.61	0.2023	1.8	2.165	7.4	0.07763	7.2	0.24	1188	19	1170	53	1137	144	104
j84	14089	63	13	0.65	1.39	0.1846	1.2	1.928	3.2	0.0758	2.9	0.39	1092	12	1091	22	1089	59	100
j85	463909	234	180	0.61	18.65	0.3606	1.7	5.694	3.9	0.1145	3.5	0.43	1985	29	1930	34	1872	64	106
j86	447656	718	290	1.80	0.01	0.3129	1.9	5.716	2.3	0.1325	1.3	0.82	1755	29	1934	20	2132	23	82
j87	10279	173	14	0.46	0.39	0.07735	1.3	0.6195	2.5	0.05809	2.1	0.54	480	6	490	10	533	46	90
j88	12380	143	12	0.49	5.92	0.07387	1.5	0.5741	4.1	0.0564	3.8	0.37	459	7	461	15	467	84	98
j89	75942	141	55	0.59	0.00	0.3516	1.1	5.861	1.3	0.1209	0.7	0.83	1942	18	1955	11	1970	13	99
j92	20489	97	24	0.69	0.27	0.2207	1.1	2.617	1.9	0.08600	1.6	0.56	1286	13	1306	14	1338	31	96
j93	13796	63	14	0.61	0.15	0.2050	1.2	2.404	1.9	0.08506	1.5	0.61	1202	13	1244	14	1317	30	91
j94	105677	412	49	0.82	8.55	0.07242	2.7	0.9194	10.2	0.09208	9.8	0.27	451	12	662	51	1469	186	31
j95	8543	70	7	1.24	5.49	0.07042	1.7	0.7041	8.8	0.07252	8.6	0.19	439	7	541	37	1001	175	44
j96	320854	381	170	0.62	6.35	0.3189	1.6	5.317	3.3	0.1209	2.8	0.51	1784	26	1872	28	1970	50	91
j97	2088	8	2.5	1.51	1.27	0.2389	1.9	3.496	12.7	0.1061	12.6	0.15	1381	24	1526	106	1733	230	80
j98	70042	233	81	0.81	1.11	0.3128	3.4	4.693	3.6	0.1088	1.3	0.94	1754	53	1766	31	1780	23	99
j99	41076	84	32	0.64	0.00	0.3417	1.1	5.804	1.4	0.1232	0.9	0.76	1895	18	1947	12	2003	16	95
j100	11008	48	10	0.25	0.79	0.2094	1.3	2.417	2.4	0.08368	2.0	0.54	1226	15	1248	17	1285	39	95
j101	606862	198	210	1.08	b.d.	0.7821	1.2	37.99	1.4	0.3523	0.6	0.91	3725	35	3720	14	3717	9	100
j102	10206	25	11	2.00	0.27	0.3117	2.0	4.673	2.6	0.1087	1.6	0.78	1749	31	1762	22	1778	29	98
j103	313368	106	100	0.62	0.00	0.7257	1.2	34.15	1.4	0.3413	0.7	0.86	3517	32	3615	14	3669	11	96
j104	21699	86	23	0.69	0.01	0.2414	1.1	3.043	1.6	0.09141	1.2	0.66	1394	14	1418	13	1455	23	96
j105	60746	117	50	1.16	2.73	0.3211	1.3	5.353	2.3	0.1209	1.9	0.56	1795	20	1877	20	1970	34	91
j106	20861	60	26	2.34	0.00	0.2924	1.2	4.291	1.6	0.1064	1.1	0.75	1654	17	1692	13	1739	20	95
j107	368349	316	180	0.57	0.00	0.4868	1.1	13.00	1.3	0.1937	0.7	0.84	2557	24	2680	13	2774	12	92
j108	13435	69	15	0.51	0.00	0.2091	1.2	2.393	1.8	0.08299	1.3	0.65	1224	13	1241	13	1269	26	96
j109	11377	193	16	0.87	1.51	0.07092	1.2	0.6564	5.7	0.06713	5.6	0.21	442	5	512	23	842	117	52
j110	13669	195	16	0.71	0.18	0.07114	1.6	0.589	3.1	0.0601	2.7	0.50	443	7	471	12	607	58	73

j111	7328	117	7.8	0.51	2.55	0.0596	2.1	0.4931	3.9	0.06001	3.3	0.54	373	8	407	13	604	71	62

Spot size = 23 µm; depth of crater ~15µm. $^{206}Pb/^{238}U$ error is the quadratic additions of the within run precision (2 SE) and the external reproducibility (2 SD) of the reference zircon. $^{207}Pb/^{206}Pb$ error propagation (^{207}Pb signal dependent) following Gerdes & Zeh (2009). $^{207}Pb/^{235}U$ error is the quadratic addition of the $^{207}Pb/^{206}Pb$ and $^{206}Pb/^{238}U$ uncertainty.

[a]Within run background-corrected mean ^{207}Pb signal in cps (counts per second).

[b] U and Pb content and Th/U ratio were calculated relative to GJ-1 reference zircon.

[c] percentage of the common Pb on the ^{206}Pb. b.d. = below dectection limit.

[d] corrected for background, within-run Pb/U fractionation (in case of $^{206}Pb/^{238}U$) and common Pb using Stacy and Kramers (1975) model Pb composition and subsequently normalised to GJ-1 (ID-TIMS value/measured value); $^{207}Pb/^{235}U$ calculated using $^{207}Pb/^{206}Pb/(^{238}U/^{206}Pb*1/137.88)$

[e] rho is the $^{206}Pb/^{238}U/^{207}Pb/^{235}U$ error correlation coefficient.

[f] degree of concordance = $^{206}Pb/^{238}U$ age / $^{207}Pb/^{206}Pb$ age x 100

[g] Accuracy and reproducibilty was checked by repeated analyses (n = 5) of reference zircon 91500; data given as mean with 2 standard deviation uncertainties

Sample CXI-126 (Dresden)

Concordant (100 ±10 %) measurments: 50 (of 120)

spot number	^{207}Pb[a] (cps)	U[b] (ppm)	Pb[b] (ppm)	Th[b]/U	^{206}Pb[c]/^{204}Pb	^{206}Pb[c]/^{238}U	2 σ %	^{207}Pb[c]/^{235}U	2 σ %	^{207}Pb[c]/^{206}Pb	2 σ %	rho[d]	^{206}Pb/^{238}U	2 σ (Ma)	^{207}Pb/^{235}U	2 σ (Ma)	^{207}Pb/^{206}Pb	2 σ (Ma)	conc %
a01	7147	33	13	0.44	292	0.3031	3.5	4.37	9.8	0.1046	9.2	0.35	1707	52	1707	85	1708	169	100
a09	3413	56	12	0.42	4171	0.2027	3.4	2.29	4.4	0.082	2.8	0.77	1190	37	1209	32	1245	55	96
a10	5008	46	15	0.43	382	0.2971	3.2	4.35	7.1	0.1061	6.3	0.45	1677	48	1702	60	1733	116	97
a11	4326	171	17	0.24	2007	0.0967	3.7	0.8	11.4	0.06	10.8	0.32	595	21	597	53	605	234	98
a12	22592	212	67	0.48	14808	0.2776	3.2	3.77	3.9	0.0985	2.2	0.82	1579	45	1586	31	1596	41	99
a13	7790	97	25	0.38	8540	0.2424	3.5	3.05	5	0.0911	3.6	0.7	1399	44	1419	39	1449	68	97
a19	8122	88	27	0.37	797	0.2946	3.6	4.26	4.1	0.1048	2.1	0.87	1664	53	1685	35	1711	38	97
a21	15647	84	46	0.6	197	0.4339	4.5	9.81	8.9	0.164	7.7	0.5	2323	88	2417	86	2497	130	93
a22	56947	100	76	0.42	8422	0.621	3.4	21.01	3.6	0.2454	1.1	0.95	3114	85	3139	35	3156	18	99
a23	29946	69	49	0.58	4739	0.5645	3.4	15.8	3.6	0.203	1.3	0.93	2885	79	2865	35	2850	21	101
a24	16092	256	45	0.11	512	0.1665	3.4	1.63	8.2	0.0711	7.5	0.41	993	31	983	53	960	153	103
a25	1680	70	8	0.47	2737	0.105	3.4	0.89	5.8	0.0612	4.7	0.59	643	21	644	28	646	101	100
a29	3684	22	12	1.15	1408	0.3805	3.4	6.93	5.1	0.1321	3.8	0.66	2079	60	2103	46	2126	67	98
a30	6565	51	19	0.17	973	0.3388	3.4	5.2	6.3	0.1113	5.3	0.54	1881	56	1853	55	1821	96	103
a33	17710	245	70	0.34	827	0.2636	3.7	3.34	4.8	0.0919	3.1	0.77	1508	50	1490	38	1465	58	103
a35	15374	45	27	0.35	817	0.496	3.8	12.48	4.5	0.1825	2.4	0.84	2597	82	2641	43	2676	40	97
a37	12471	172	49	0.36	6998	0.2584	4.1	3.49	6.2	0.098	4.6	0.66	1482	54	1526	50	1587	87	93
a39	11479	151	32	0.31	554	0.1872	3.6	1.95	5	0.0754	3.6	0.71	1106	36	1097	34	1080	71	102
a42	8692	88	25	0.22	2313	0.275	3.8	3.62	4.7	0.0955	2.7	0.81	1566	53	1555	38	1539	51	102
a44	21070	111	46	0.41	431	0.3784	3.7	6.89	8.6	0.132	7.7	0.43	2069	66	2097	79	2125	135	97
a45	7801	42	19	0.64	409	0.3601	3.2	6.4	6.7	0.1288	5.9	0.48	1983	55	2032	60	2082	103	95
a46	14299	84	34	0.65	1023	0.3474	3.3	5.55	3.7	0.1159	1.7	0.89	1922	54	1909	32	1894	31	102
a47	2682	32	7	0.57	1523	0.1994	3.1	2.29	5.3	0.0833	4.3	0.58	1172	33	1209	38	1277	85	92
a49	12871	161	34	0.14	1157	0.2179	3.8	2.44	4.4	0.0814	2.1	0.88	1271	44	1256	32	1230	41	103
a52	11259	55	17	0.15	10511	0.3155	3.4	4.65	3.9	0.1068	2	0.86	1768	53	1758	33	1746	37	101
a53	8841	21	11	0.8	373	0.3679	3.8	6.43	5.9	0.1268	4.5	0.64	2020	65	2037	53	2054	79	98
a59	8693	26	13	0.33	192	0.4303	3.1	9.17	7	0.1545	6.3	0.45	2307	61	2355	66	2396	106	96
b03	15170	128	45	0.52	2694	0.3005	3	4.31	3.4	0.104	1.7	0.87	1694	45	1695	29	1696	31	100
b05	19966	125	47	0.26	4931	0.3517	2.8	5.71	3.2	0.1177	1.4	0.9	1943	48	1933	28	1921	25	101
b09	6456	57	21	0.83	2120	0.2863	2.9	3.9	4.2	0.0988	3.1	0.68	1623	41	1614	35	1602	58	101

b10	9196	105	32	0.2	724	0.2953	2.9	4.28	4	0.1052	2.8	0.72	1668	43	1690	33	1718	51	97
b13	9292	100	32	0.22	536	0.3011	2.8	4.45	5.8	0.1072	5.1	0.49	1697	42	1722	49	1752	93	97
b17	1556	24	5	0.41	1881	0.209	3.5	2.37	5.3	0.0824	4	0.66	1224	39	1235	39	1255	78	98
b18	11819	91	31	0.44	9785	0.301	2.8	4.43	3.6	0.1068	2.2	0.79	1696	42	1719	30	1746	40	97
b23	3153	60	16	0.94	1332	0.2207	2.8	2.63	5	0.0864	4.2	0.55	1285	32	1309	37	1348	80	95
b24	17780	162	57	0.17	464	0.3455	3.1	5.74	5.5	0.1204	4.5	0.57	1913	52	1937	48	1962	80	97
b26	7132	44	15	0.31	233	0.2854	3.3	3.94	12.6	0.1002	12.2	0.26	1618	47	1622	108	1628	227	99
b28	23914	286	88	0.17	3169	0.3022	2.8	4.31	3.2	0.1034	1.6	0.87	1702	42	1695	27	1686	29	101
b31	24593	52	34	0.23	612	0.5492	2.9	15.98	3.5	0.2111	2	0.81	2822	66	2876	34	2914	33	97
b32	6960	40	20	0.64	240	0.3905	2.7	7.75	5.5	0.1439	4.8	0.48	2125	48	2202	51	2274	83	93
b37	7005	57	20	0.75	441	0.2662	4.1	3.46	5.2	0.0943	3.2	0.79	1521	56	1518	42	1514	60	100
b39	10047	115	29	0.32	6605	0.2457	2.8	3.11	3.3	0.0919	1.8	0.85	1416	36	1436	26	1465	34	97
b46	24466	111	40	0.43	1261	0.3226	2.9	5.1	3.3	0.1147	1.6	0.88	1802	45	1836	28	1875	28	96
b48	8870	101	20	0.51	5901	0.1949	3	2.11	3.8	0.0784	2.3	0.79	1148	32	1151	27	1158	46	99
b49	4497	26	8	0.41	4588	0.2783	2.8	3.75	4.2	0.0977	3	0.68	1583	40	1582	34	1581	57	100
b51	10404	58	23	0.59	726	0.3632	3.9	6.25	4.8	0.1248	2.8	0.81	1997	67	2012	43	2026	50	99
b54	3107	21	5	0.23	3690	0.2146	3.7	2.48	5.2	0.0838	3.7	0.7	1253	42	1266	38	1287	72	97
b56	3485	8	5	1.09	230	0.428	3.2	8.86	8.3	0.1501	7.7	0.38	2297	61	2323	79	2347	132	98
b57	31873	18	15	1.31	115	0.4832	2.9	11.14	4.4	0.1672	3.4	0.65	2541	61	2535	42	2530	57	100
b60	13069	31	11	0.35	199	0.2748	2.9	3.62	6	0.0955	5.2	0.48	1565	40	1554	49	1538	98	102

[a] within-run background-corrected mean ^{207}Pb signal in counts per second

[b] U and Pb content and Th/U ratio were calculated relative to GJ-1 and are accurate to approximately 10%.

[c] corrected for background, mass bias, laser induced U-Pb fractionation and common Pb (if detectable, see analytical method) using Stacey & Kramers (1975) model Pb composition. 207Pb/235U calculated using 207Pb/206Pb/(238U/206Pb × 1/137.88). Errors are propagated by quadratic addition of within-run errors (1SE) and the reproducibility of GJ-1 (1SD).

[d] Rho is the error correlation defined as err^{206}Pb/^{238}U/err^{207}Pb/^{235}U.

Table S7: Distribution of the zircon U-Pb ages in Devonian sandstone samples

	Sample	n (± conc.)	Paleoz.+ late Neoprot. 700-400 Ma n (%)	Mesoprot. 1599-1000 Ma n (%)	Paleoprot. 2499-1600 Ma n (%)	Arch. >2500 Ma n (%)
early Mid-Dev.	CXI-124	99	1 (1)	50 (51)	29 (29)	16 (16)
early Mid-Dev.	CXI-120	91	1 (1)	36 (40)	40 (44)	9 (10)
early Mid-Dev.	CXI-119	81	2 (2)	29 (36)	39 (48)	6 (7)
early Mid-Dev.	**all**	**271**	**4 (2)**	**115 (42)**	**108 (40)**	**31 (11)**
late Mid-Dev.	**CXI-125**	**85**	**9 (11)**	**23 (27)**	**41 (48)**	**11 (13)**
Late Dev.	**CXI-126**	**50**	**2 (4)**	**17 (34)**	**25 (50)**	**5 (10)**